What Makes the Behavior of a System Predictable?

Can the complex system approach be useful to you?

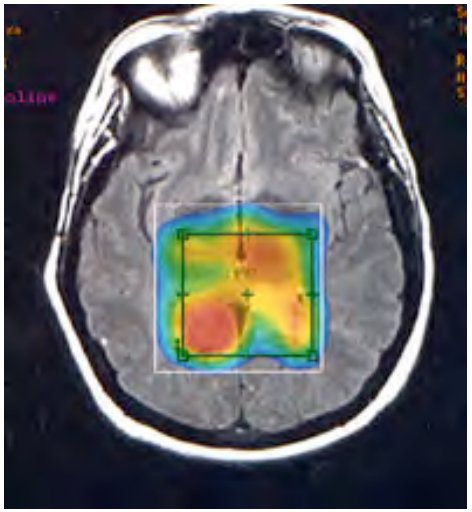

Didier SORNETTE

Department of Management, Technology and Economics, ETH Zurich, Switzerland

Member of the Swiss Finance Institute

co-founder of the Competence Center for Coping with Crises in Socio-Economic Systems, ETH Zurich (http://www.ccss.ethz.ch/)

Professor of Physics associated with the Department of Physics (D-PHYS), ETH Zurich

Professor of Geophysics associated with the Department of Earth Sciences (D-ERWD), ETH Zurich

www.er.ethz.ch

Linear models

- AR, MA, ARMA, ARIMA,...

$$\left(1-\sum_{i=1}^{p}\phi_i L^i\right)(1-L)^d X_t = \left(1+\sum_{i=1}^{q}\theta_i L^i\right)\varepsilon_t$$

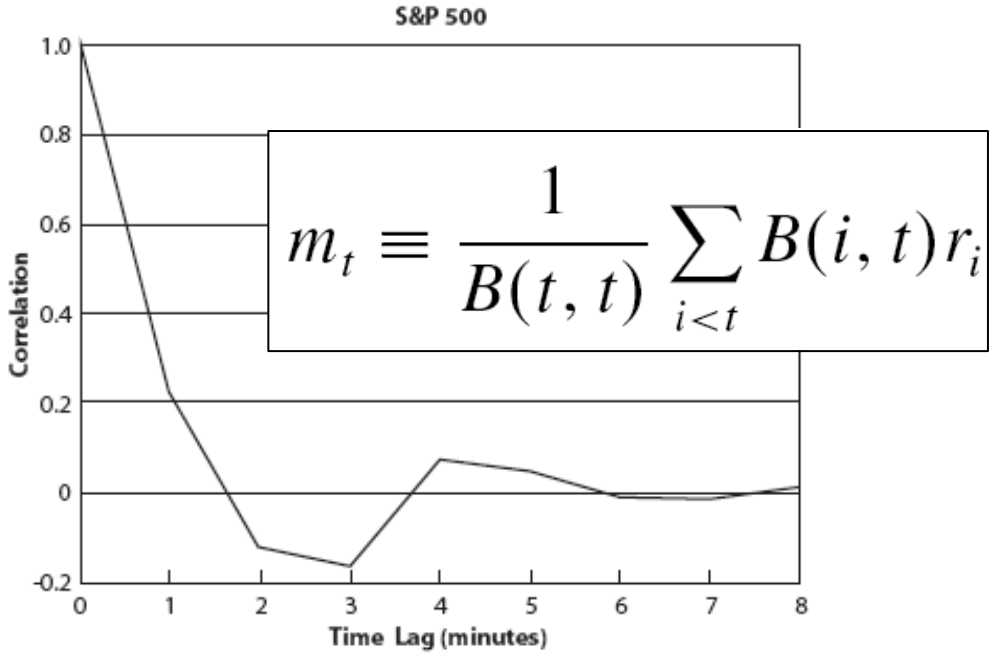

$$m_t \equiv \frac{1}{B(t,t)}\sum_{i<t} B(i,t)\,r_i$$

- linear trends
- linear correlation
- extrapolations work as long as there is not a change of trend, of regime

Low dimensional chaos

- Local vs global prediction methods
- Parameter estimations in the presence of noise
  - leads to inconsistent MLE
  - confluence analysis
- Local vs global prediction

$$s_i = x_i + \eta_i ,$$

$$x_{i+1} = F(x_i, a) \equiv 1 - a x_i^2$$

V. Pisarenko and D. Sornette, On Statistical Methods of Parameter Estimation for Deterministically Chaotic Time-Series, Phys. Rev. E 69, 036122 (2004)

Likelihood contour plot

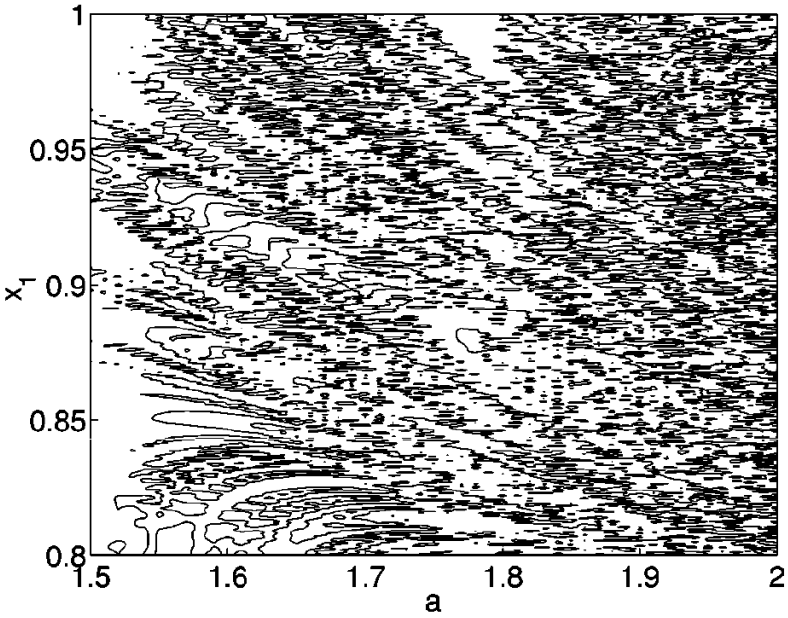

- **Most systems are NOT low dimensional!**
- **Large scale "coherent structures"**

Bilinear stochastic models

$$r(t) = e(t) + be(t-1)e(t-2)$$

e(t) is i.i.d. with std = s

The simplest case of the class of "Volterra discrete series"

$$x(t) = H_1[e(t)] + H_2[e(t)] + H_3[e(t)] + \cdots + H_n[e(t)]$$

$$H_n[e_{t\Sigma}] = \sum_{j_1=0}^{+\infty} \cdots \sum_{j_n=0}^{+\infty} h_n(j_1, \ldots, j_n) e_{t-j_1} \ldots e_{t-j_n}.$$

- Zero linear correlation at all lags
- Non-zero three-point correlation function

$$E[r(t-2)r(t-1)r(t)] = bs^3$$

→ (some) NONLINEAR predictability!

D. Sornette and V.F. Pisarenko, Properties of a simple bilinear stochastic model: estimation and predictability, Physica D 237 (4), 429-445 (2008)

Bilinear stochastic models

$$r(t) = e(t) + be(t-1)e(t-2)$$

e(t) is i.i.d. with std = s

Problems: (i) estimation of b and s; (ii) derive e(t), e(t-1),... from r(t), r(t-1)...

$$e(u) = r(u) + b'e(u-1)e(u-2); \quad u = 1, 2, \ldots,$$

where $b' = -b$.

Impulse response to: $r(u) = \begin{cases} a; & a > 0; u = 1, 2; \\ 0; & u \neq 1, 2, \end{cases}$

$$|e(u)| = |b|^{\Gamma(u)} a^{\Gamma(u)+1} = a(|b|a)^{\Gamma(u)}$$

$$\Gamma(k) = (1/\sqrt{5})[(1+\sqrt{5})/2]^k - (1/\sqrt{5})[(1-\sqrt{5})/2]^k$$

Conclusions: (i) explosive exp(exp) sensitivity on initial conditions for a|b|>1
(ii) the probability for a stable inversion depends on the length of the realization
(not warranted with certainty: strong sample to sample fluctuations)

Hierarchical complexity

- (low-dimensional) chaos
- Spatio-temporal chaos
- Turbulence
- Complex systems

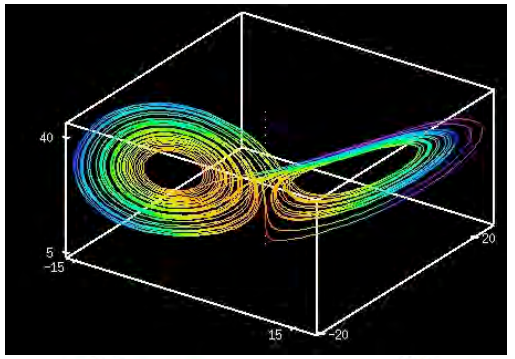

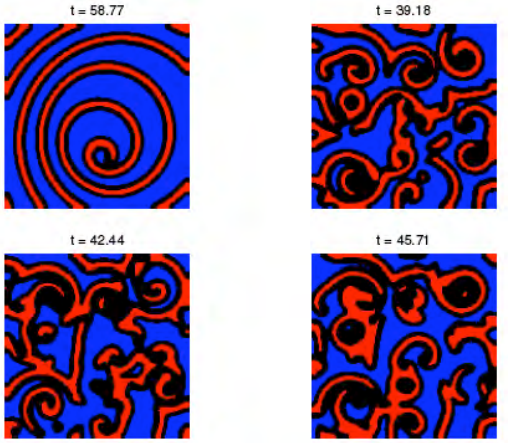

IMPOSSIBILITY THEOREM

Algorithmic complexity theory: most complex systems have been proved to be computationally irreducible, i.e. the only way to decide about their evolution is to actually let them evolve in time.

The future time evolution of most complex systems appears inherently unpredictable.

A new kind of Science?

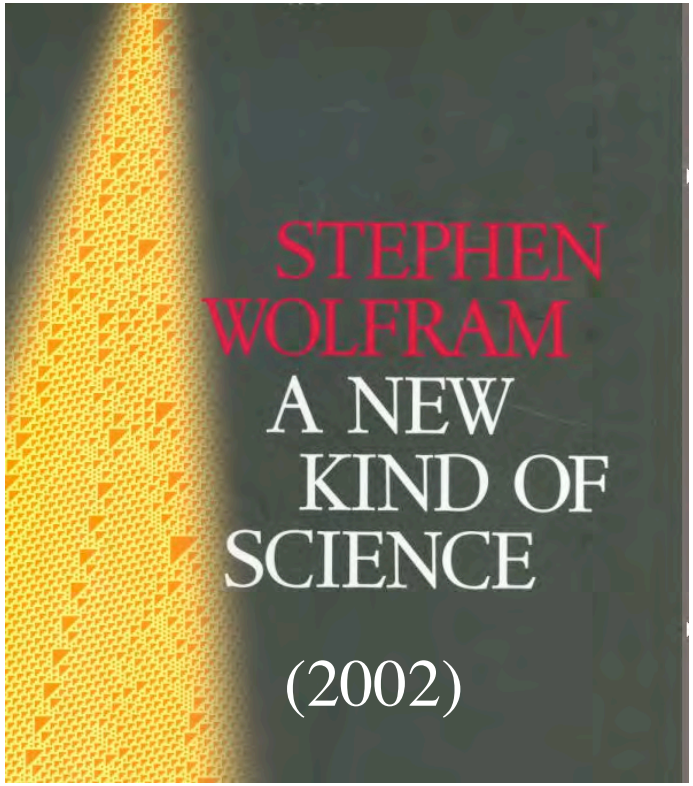

Stephen Wolfram (Mathematica)

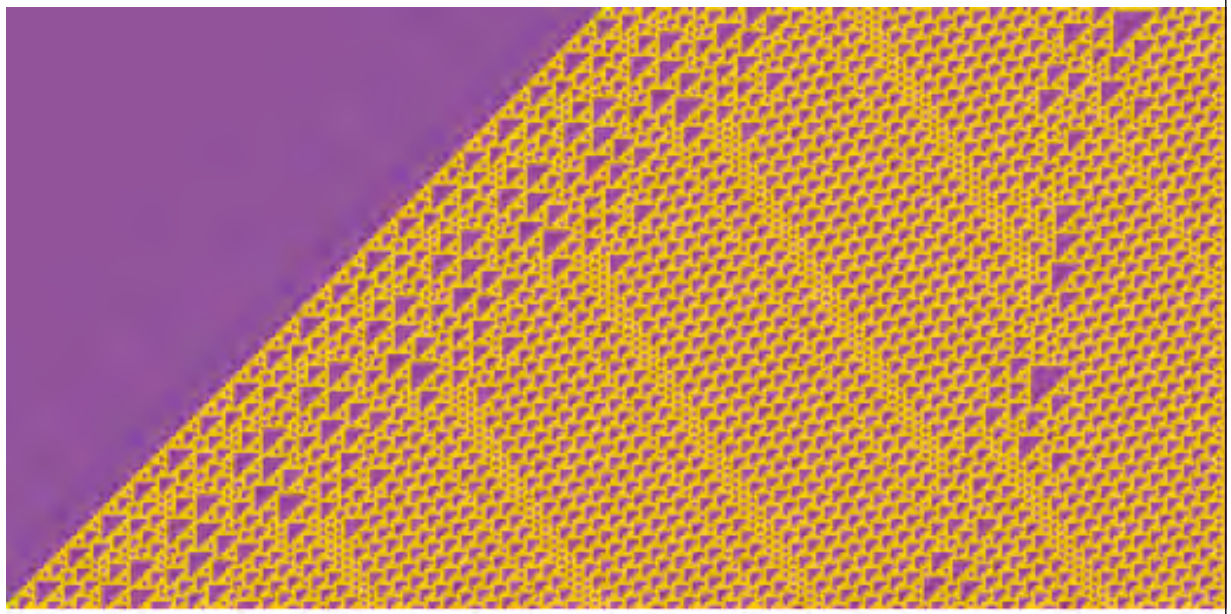

All in one: the simple 'rule 110' can perform the same range of calculations as any physical computer.

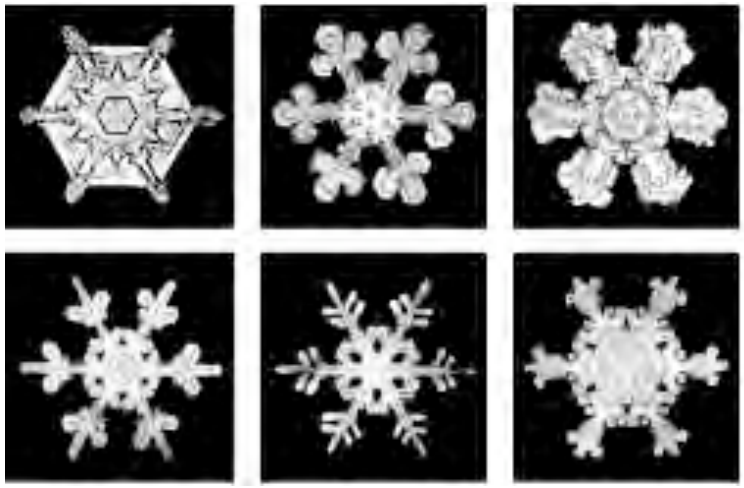

Lesson from bottom-up hierarchical grouping

Computational Irreducibility and the Predictability of Complex Physical Systems

256 nearest neighbor 1D cellular automata (Wolfram)

Class 3 ⟶ Class 1

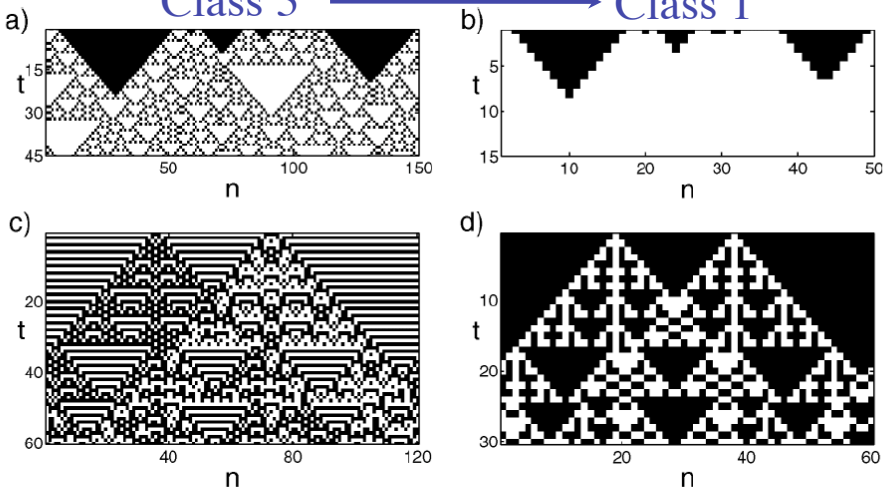

FIG. 1. Examples of coarse-graining transitions. (a) and (b) show coarse-graining rule 146 by rule 128. (a) shows results of running rule 146. The top line is the initial condition and time progress from top to bottom. (b) shows the results of running rule 128 with the coarse-grained initial condition from (a). (c) and (d) show coarse-graining rule 105 by rule 150. (c) shows rule 105 and (d) shows rule 150.

$$C(f_A^{T\cdot t}a(0)) = f_B^t C(a(0)).$$

Namely, running the original CA for Tt time steps and then coarse graining is equivalent to coarse graining the initial condition and then running the modified CA t time steps. The constant T is a time scale associated with the coarse graining.

240 coarse-grainable

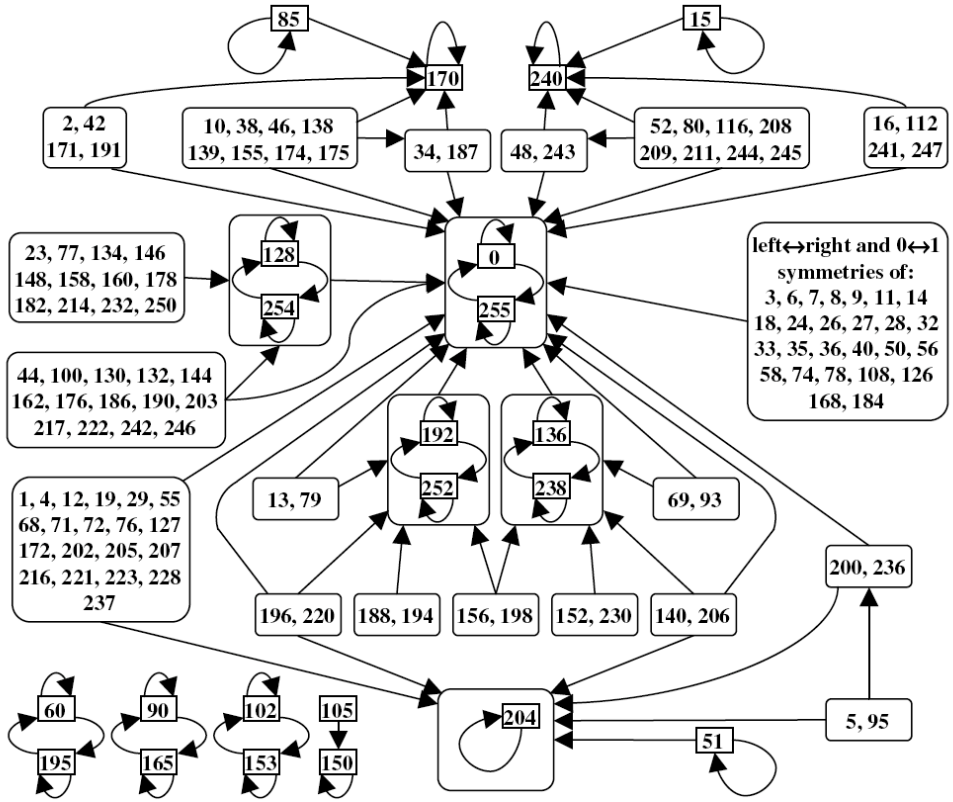

FIG. 2. Coarse-graining transitions within the family of 256 elementary CA. Only transitions with a cell block size $N = 2$, 3, and 4 are shown. An arrow indicates that the origin rules can be coarse grained by the target rules and may correspond to several choices of N and P.

N-block approach with N=2, 3 or 4

Coarse-graining rule 110: CIR => C1

Navot Israeli and Nigel Goldenfeld PhysRevLett.92.074105

Complexity vs simplicity of gas law

- Extraordinary complexity of the 10^{25} trajectories of molecules in this room (maximum complexity and unpredictability)

- Contrast with "ideal gas law" $pV = nRT$

  or even Van der Waals equation

Physics works and is not hampered by computational irreducibility because we only ask for answers at some coarse-grained level.

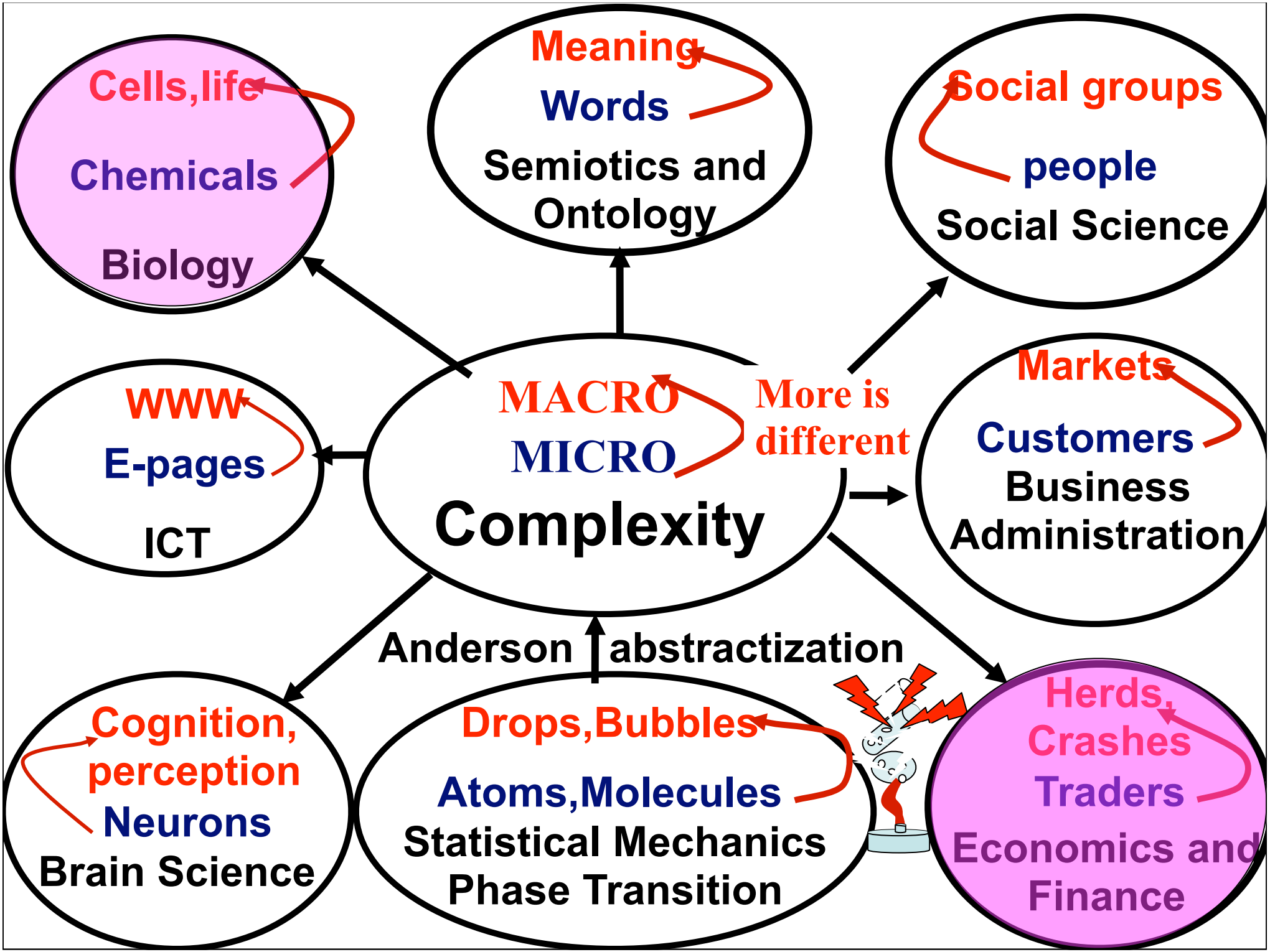
Cells,life
Chemicals
Biology
Meaning
Words
Semiotics and
Ontology
Social groups
people
Social Science
WWW
E-pages
ICT
MACRO
MICRO
More is
different
Complexity
Markets
Customers
Business
Administration
Anderson
abstractization
Cognition,
perception
Neurons
Brain Science
Drops,Bubbles
Atoms,Molecules
Statistical Mechanics
Phase Transition
Herds,
Crashes
Traders
Economics and
Finance

The Black Swan syndrome

vs

Dragons and PREDICTION

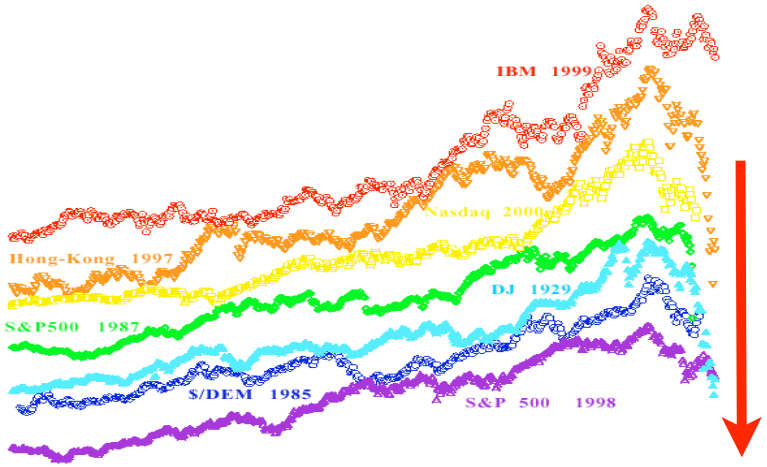

Black Swan Uncertainty

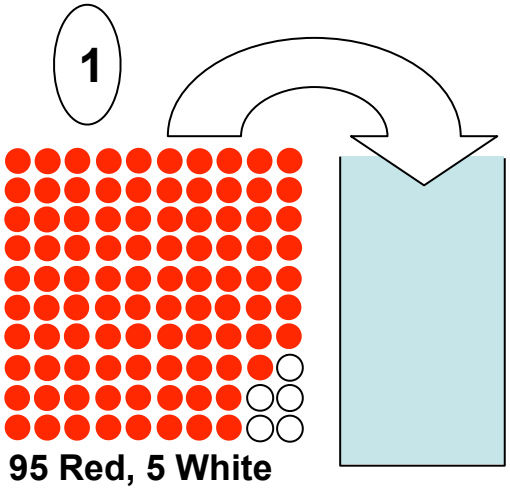

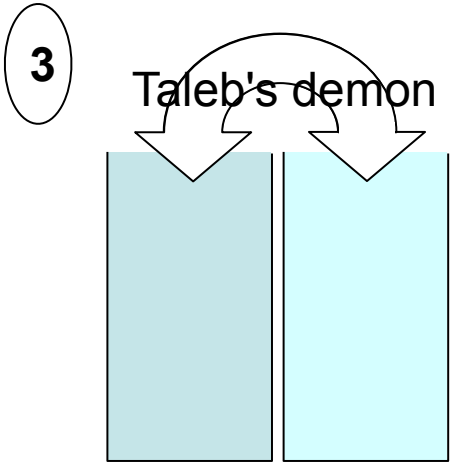

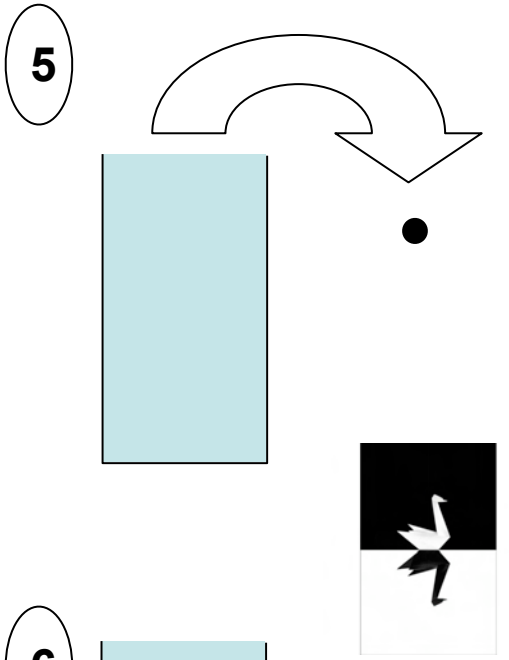

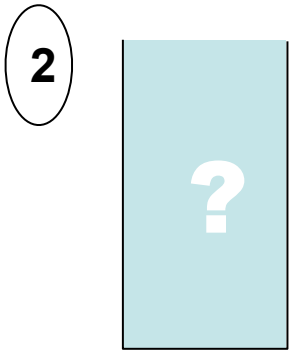

White 5%
Red 95%

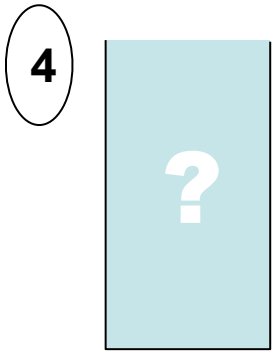

Odds of a white?

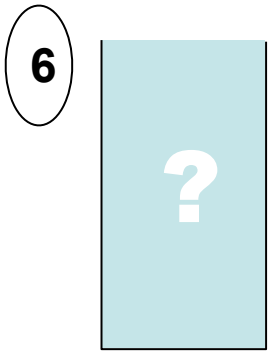

Odds of a black?

The Black Swan: The Impact of the Highly Improbable, by Nassim Nicholas Taleb

courtesy P. Taylor

Self-organized criticality

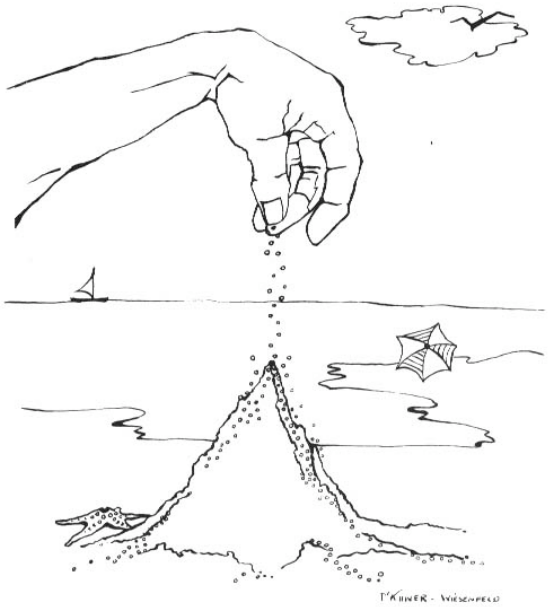

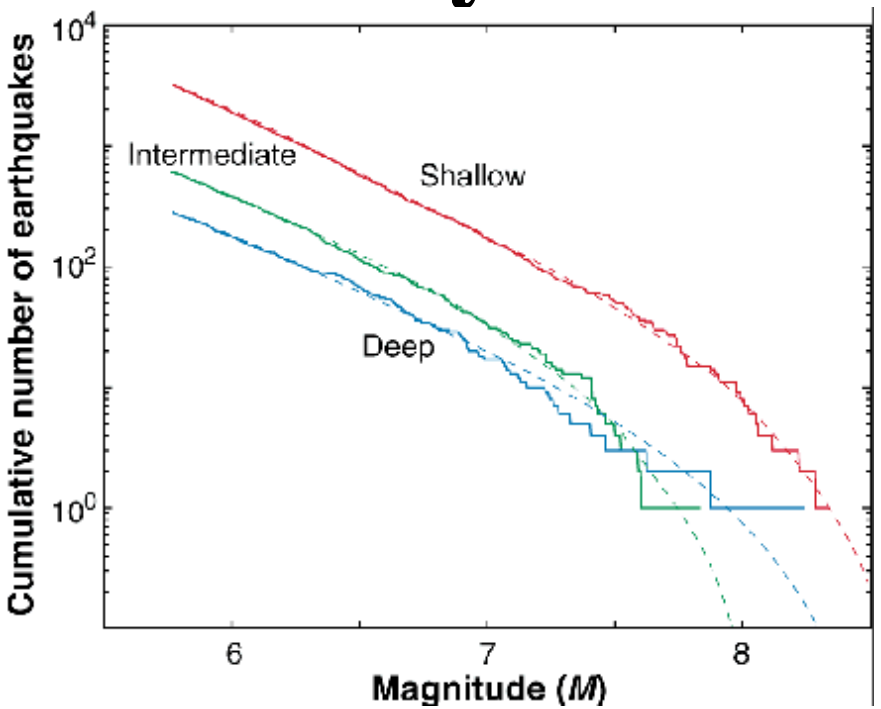

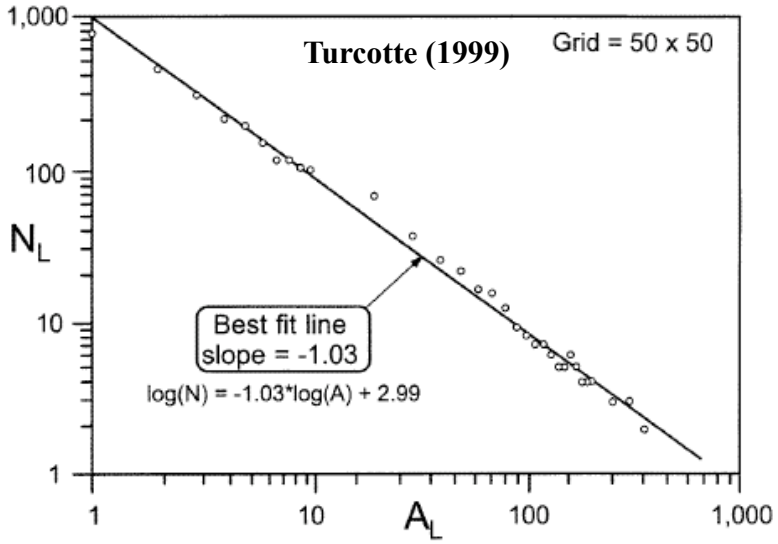

Earthquakes Cannot Be Predicted

Robert J. Geller, David D. Jackson, Yan Y. Kagan, Francesco Mulargia
Science 275, 1616-1617 (1997)

Heavy tails in pdf of earthquakes

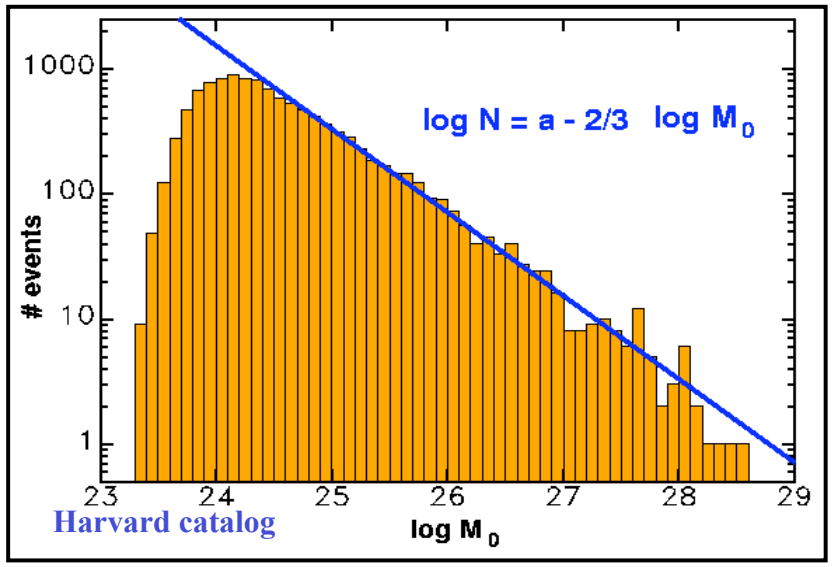

Heavy tails in pdf of seismic rates

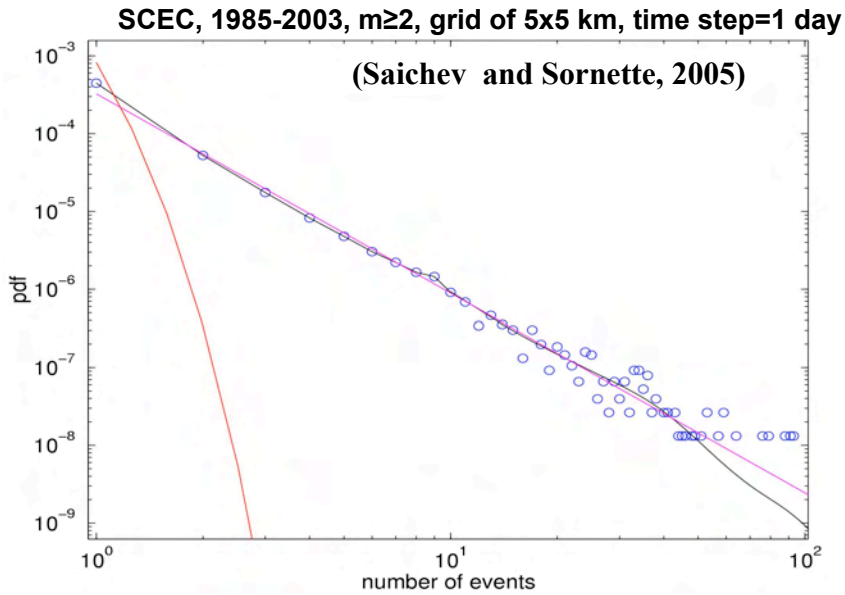

Heavy tails in ruptures

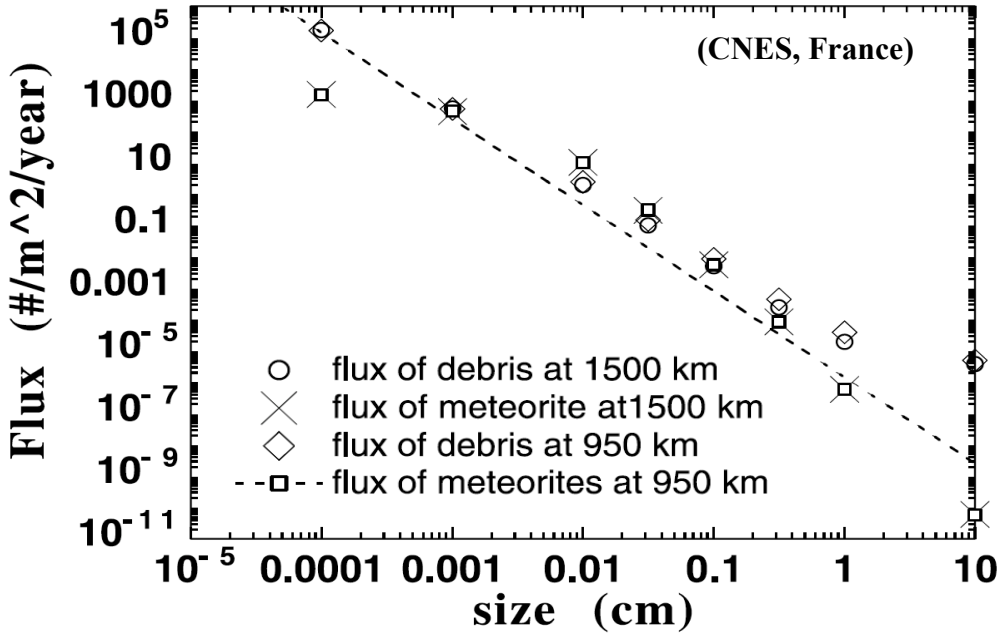

Heavy tails in pdf of rock falls, Landslides, mountain collapses

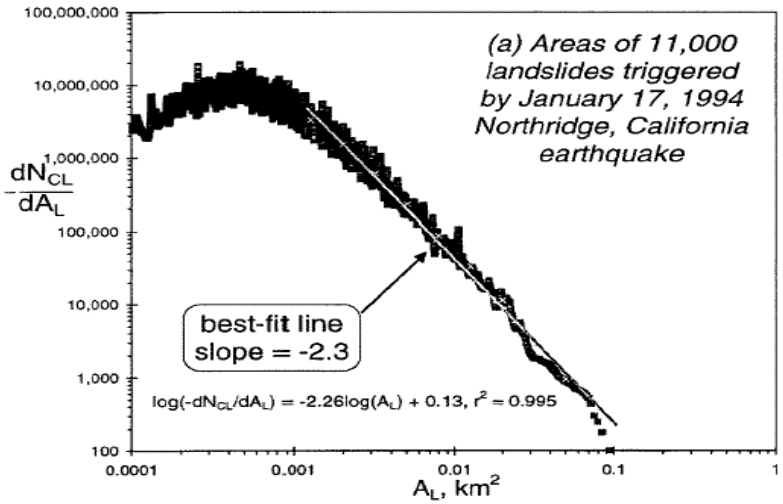

Turcotte (1999)

Heavy tails in pdf of forest fires

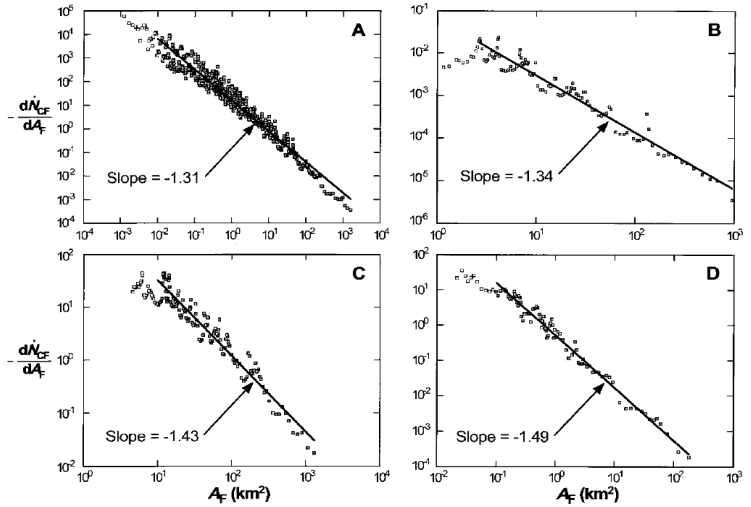

Fig. 2. Noncumulative frequency-area distributions for actual forest fires and wildfires in the United States and Australia: (**A**) 4284 fires on U.S. Fish and Wildlife Service lands (1986–1995) (*9*), (**B**) 120 fires in the western United States (1150–1960) (*10*), (**C**) 164 fires in Alaskan boreal forests (1990–1991) (*11*), and (**D**) 298 fires in the ACT (1926–1991) (*12*). For each data set, the noncumulative number of fires per year ($-d\dot{N}_{CF}/dA_F$) with area (A_F) is given as a function of A_F (*13*). In each case, a reasonably good correlation over many decades of A_F is obtained by using the power-law relation (Eq. 1) with $\alpha = 1.31$ to 1.49; $-\alpha$ is the slope of the best-fit line in log-log space and is shown for each data set.

Malamud et al., Science 281 (1998)

Heavy tails in pdf of Hurricane losses

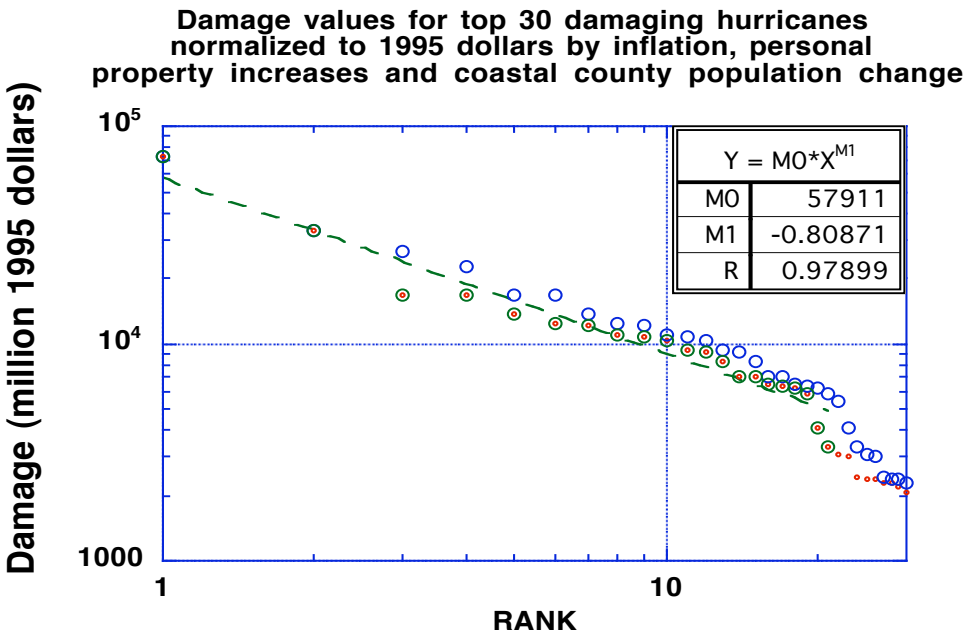

Heavy tails in pdf of Solar flares

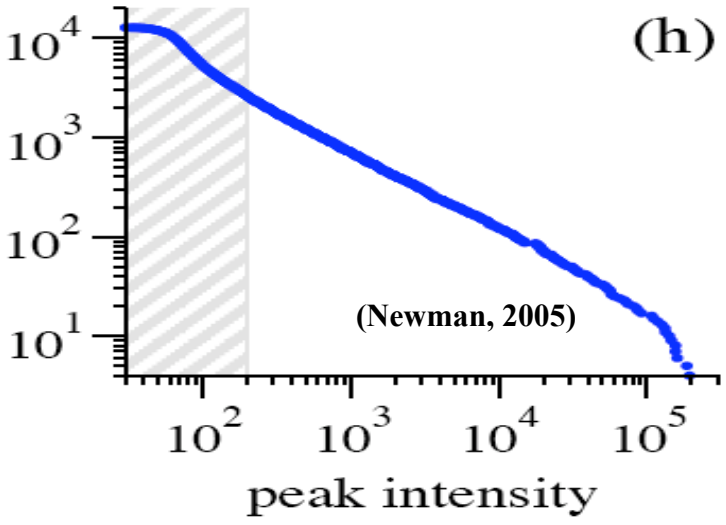

Heavy tails in pdf of rain events

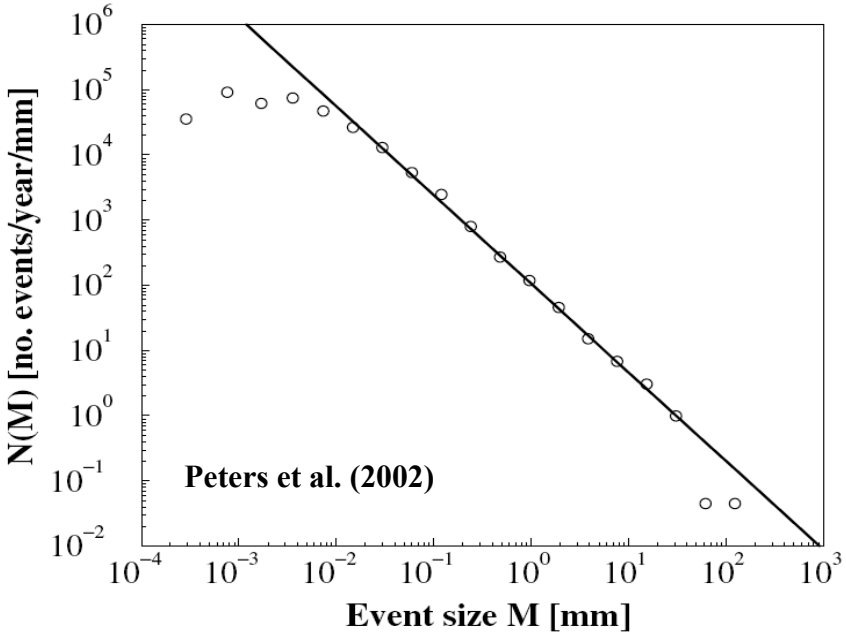

City sizes (Zipf's law)

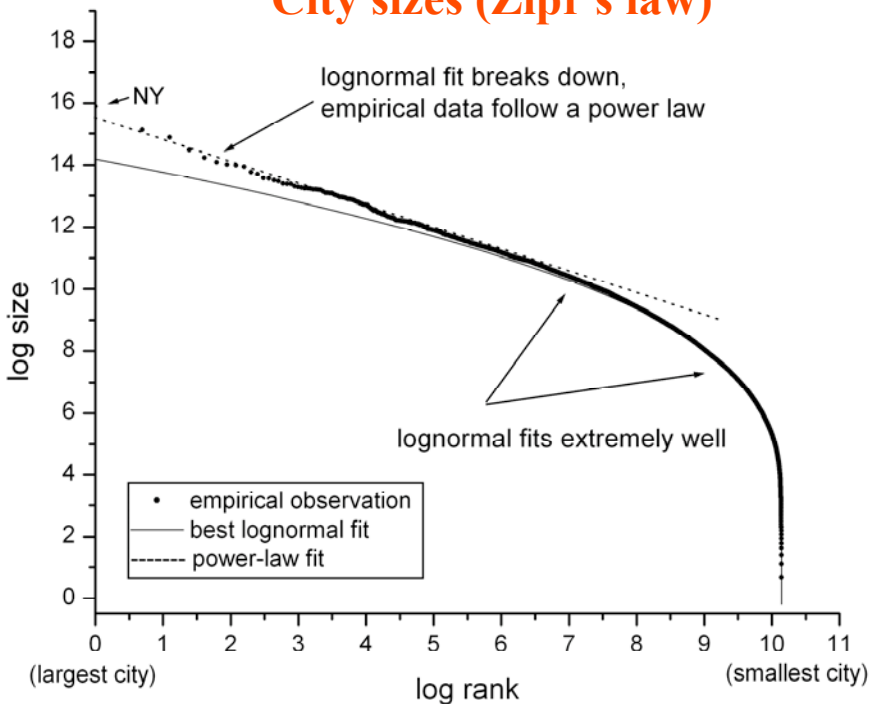

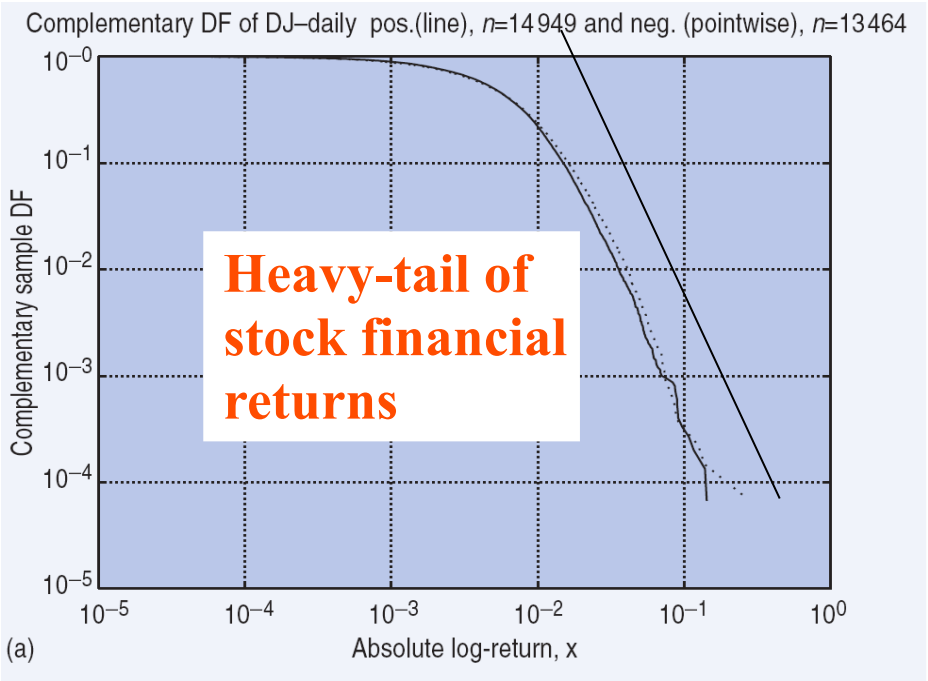

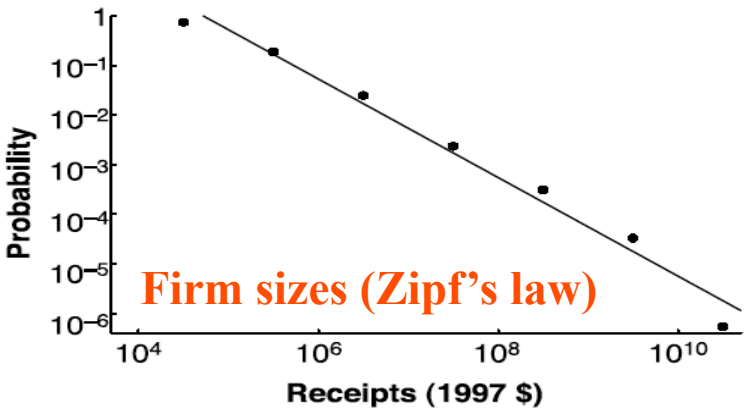

Fig. 2. Tail cumulative distribution function of U.S. firm sizes, by receipts in dollars. Data are for 1997 from the U.S. Census Bureau, tabulated in bins whose width increases in powers of 10. The solid line is the OLS regression line through the data and has slope of 0.994 (SE = 0.064; adjusted R^2 = 0.976).

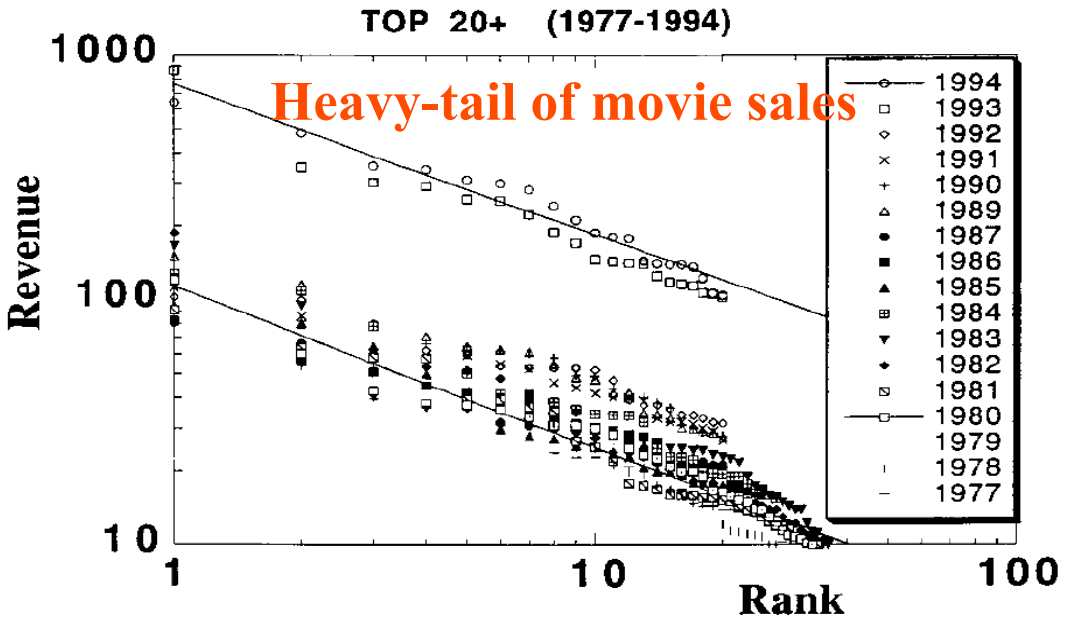

Heavy-tail of pdf of book sales

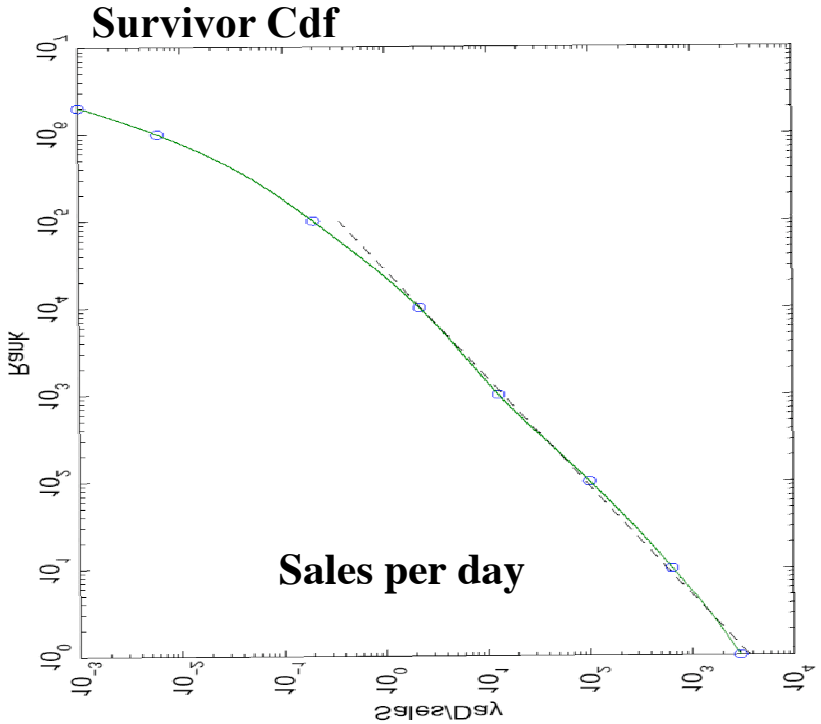

Heavy-tail of pdf of health care costs

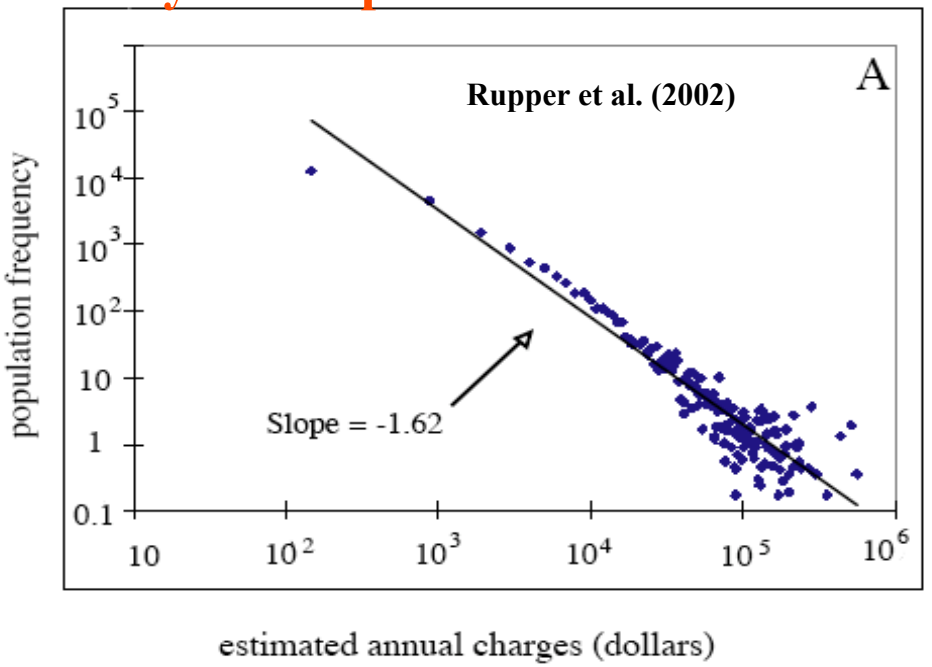

Heavy-tail of pdf of terrorist intensity

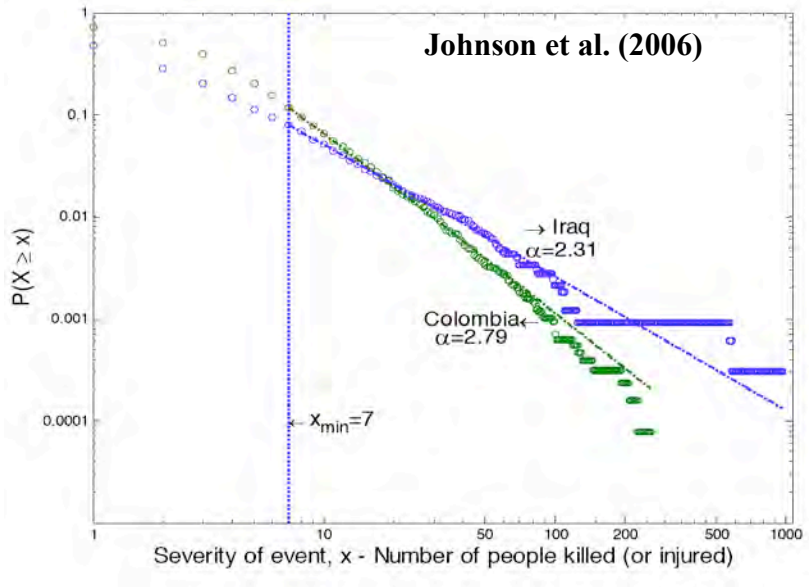

Heavy-tail of pdf of war sizes

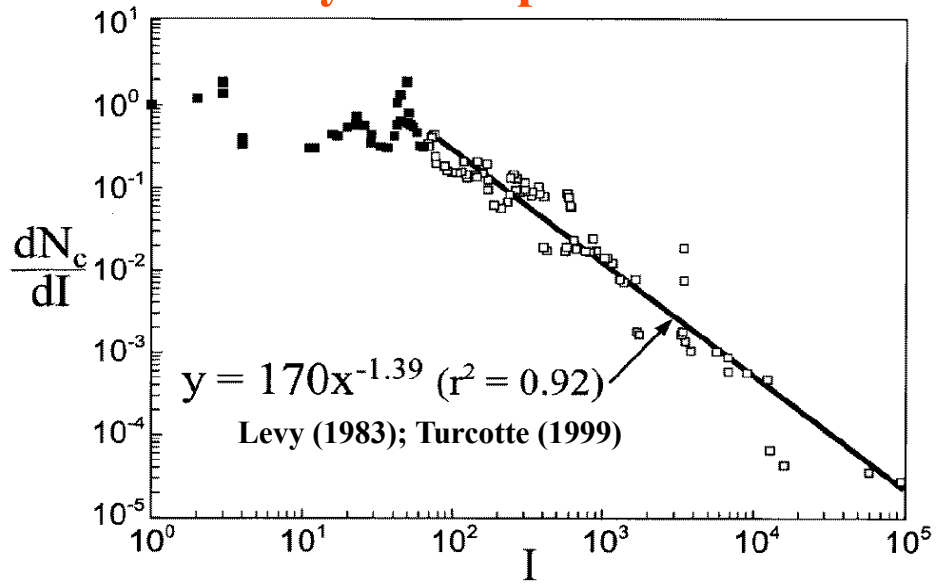

Heavy-tail of cdf of cyber risks

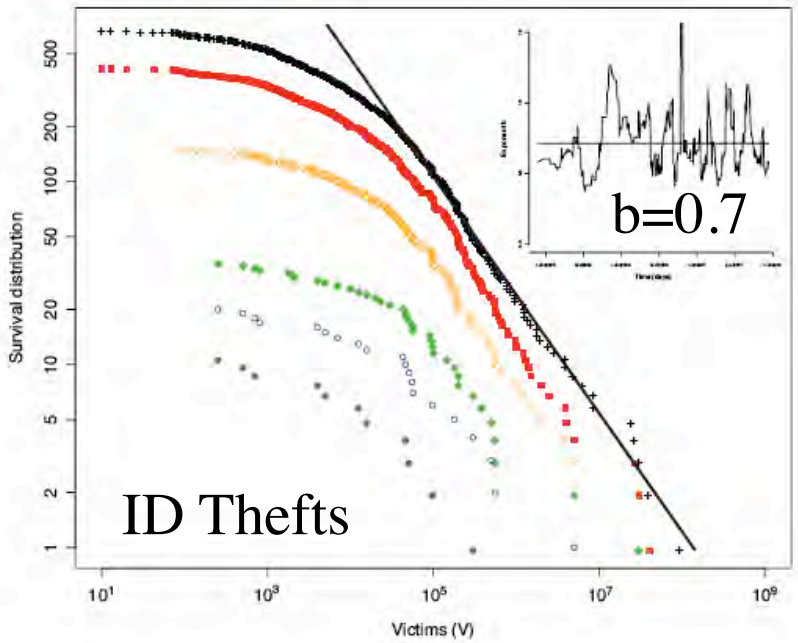

Software vulnerabilities

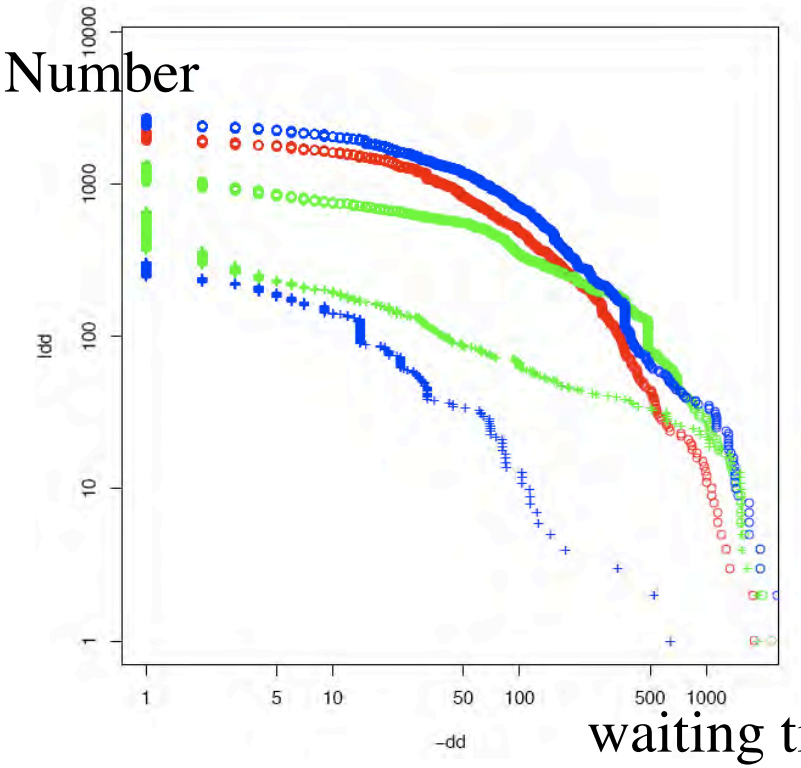

Heavy-tail of YouTube view counts

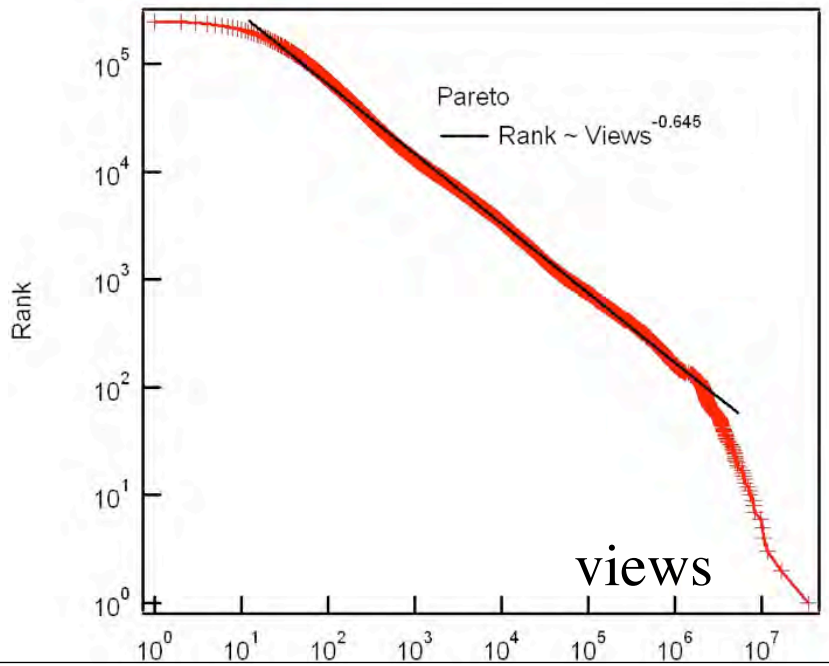

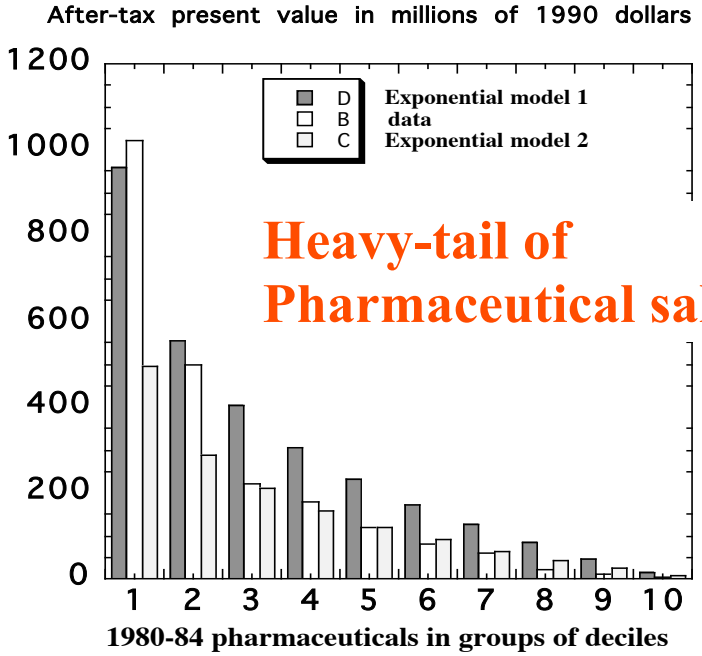

Heavy-tail of Pharmaceutical sales

Dragons and PREDICTION

Beyond power laws: six examples of "Dragons"

Financial economics: Outliers and dragons in the distribution of financial drawdowns.

Population geography: Paris as the dragon-king in the Zipf distribution of French city sizes.

Material science: failure and rupture processes.

Hydrodynamics: Extreme dragon events in the pdf of turbulent velocity fluctuations.

Brain medicine: Epileptic seizures

Geophysics: Gutenberg-Richter law and characteristic earthquakes.

Crashes as "Black swans"?

Traditional emphasis on
Daily returns do not reveal
any anomalous events

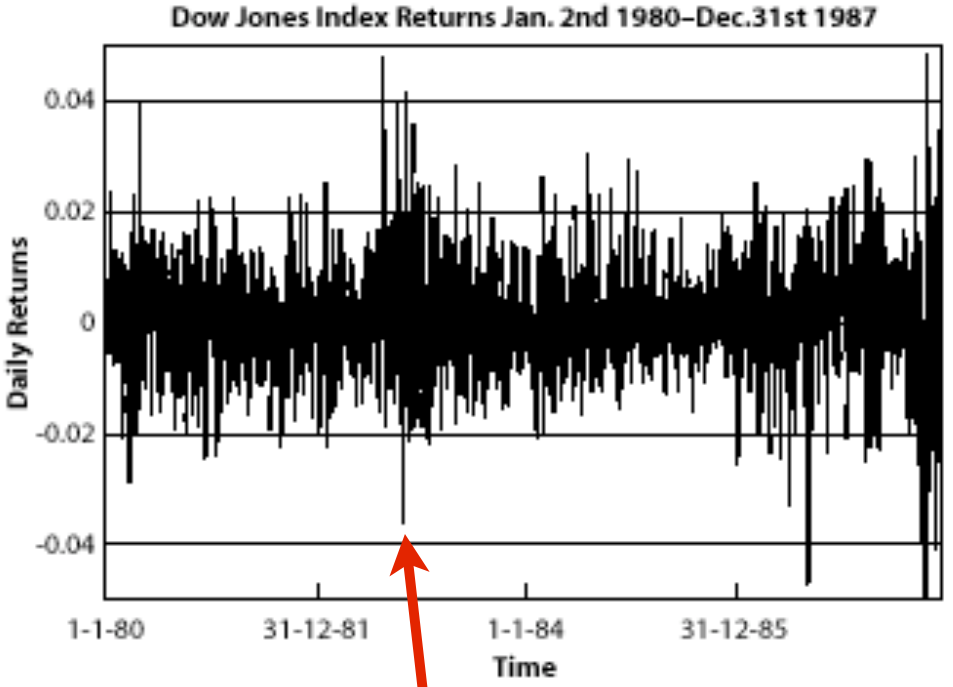

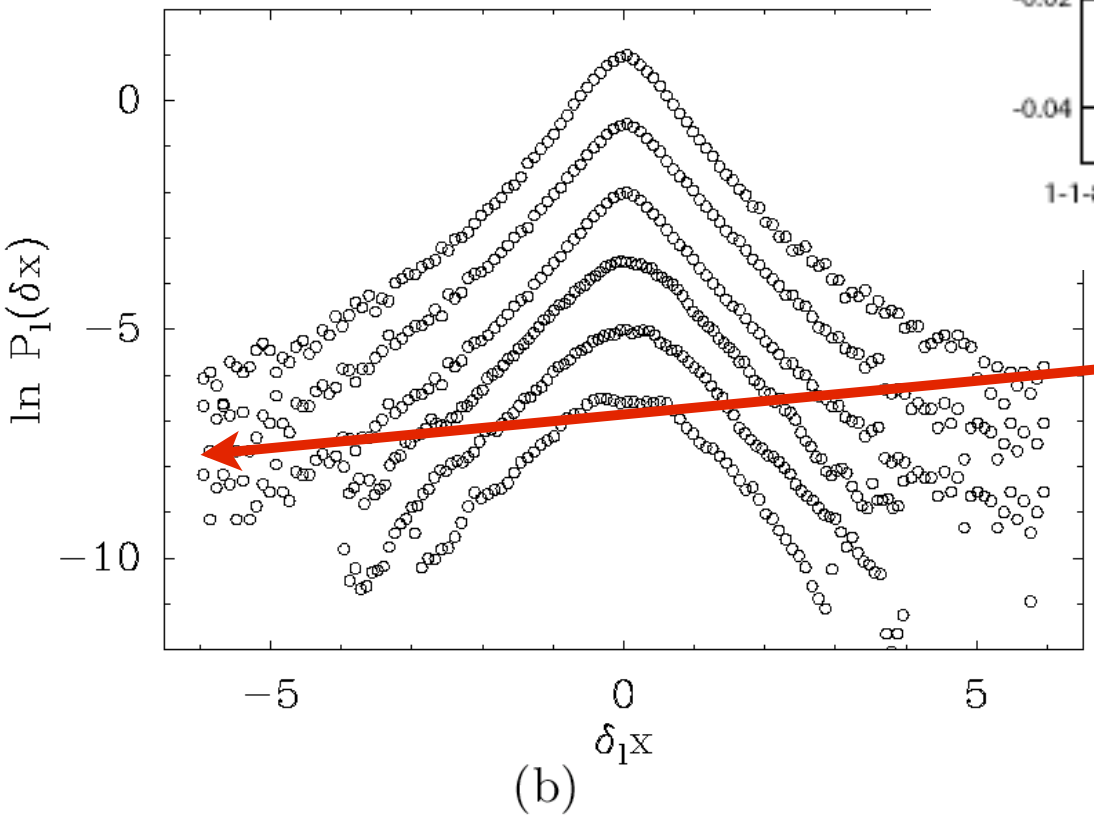

"Black swans"

Better risk measure: drawdowns

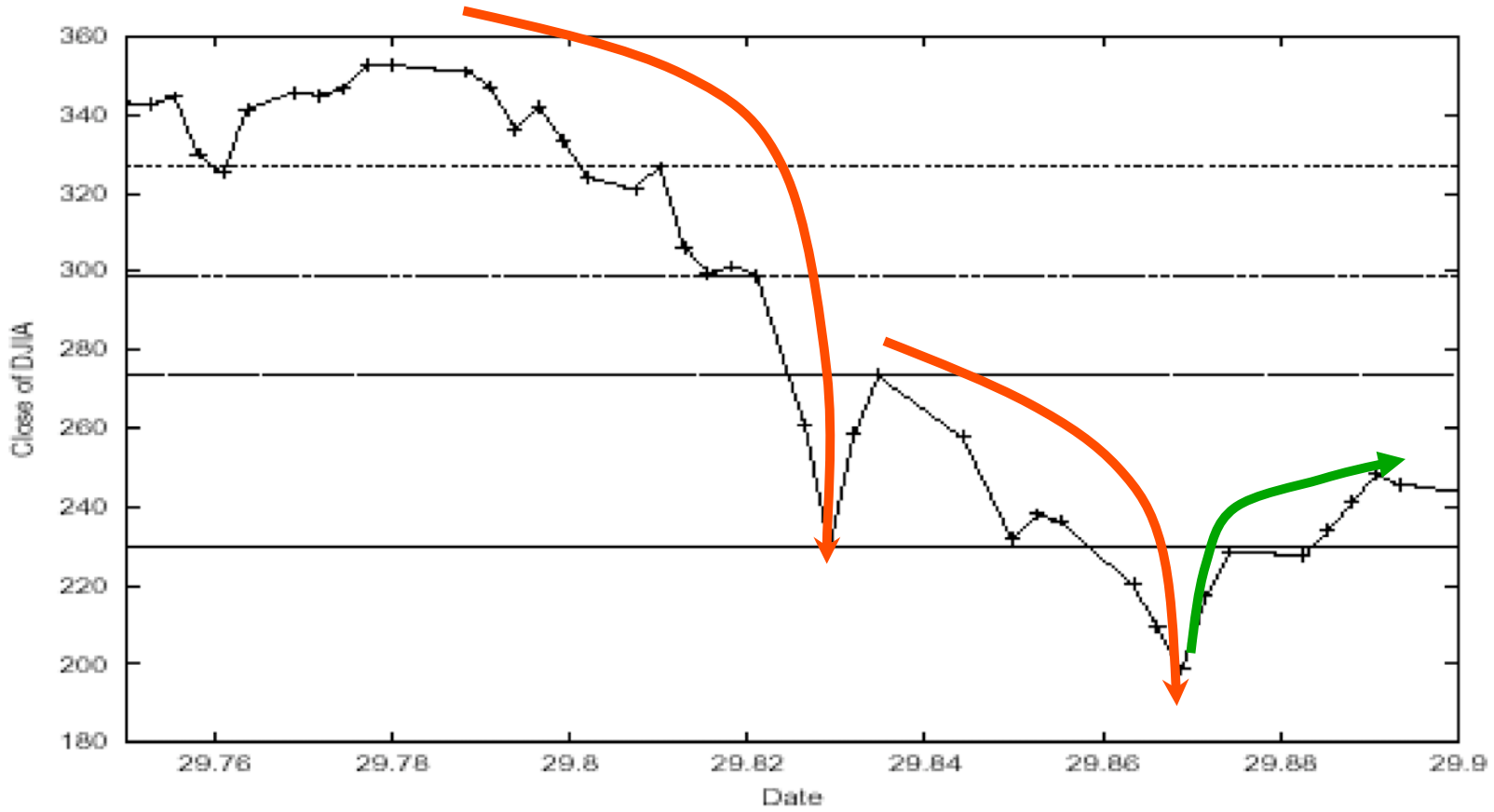

"Dragons" of financial risks

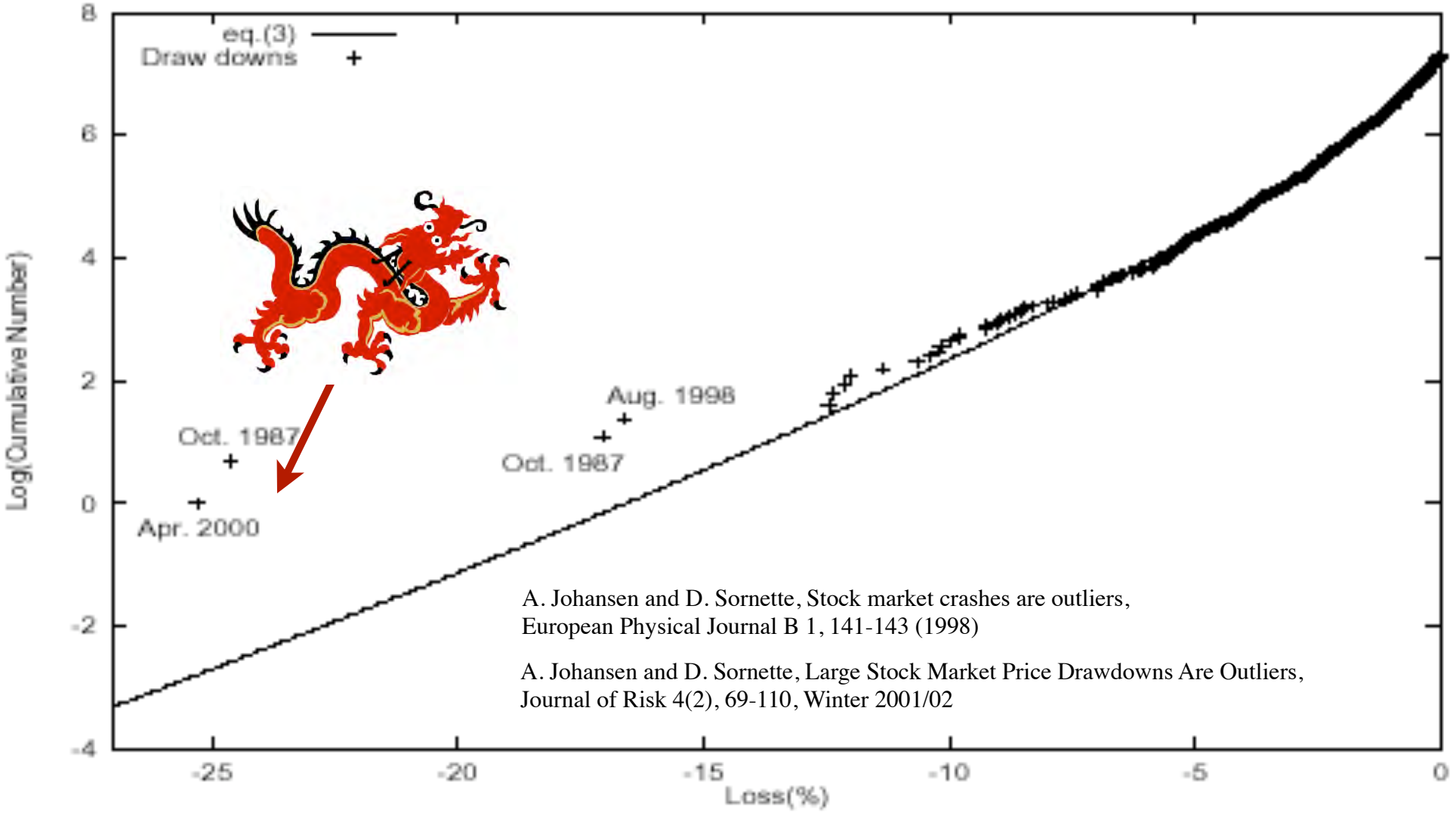

A. Johansen and D. Sornette, Stock market crashes are outliers,
European Physical Journal B 1, 141-143 (1998)

A. Johansen and D. Sornette, Large Stock Market Price Drawdowns Are Outliers,
Journal of Risk 4(2), 69-110, Winter 2001/02

$$N(DD) = A \exp\left(-\left(|DD|/\chi\right)^{z}\right).$$

"Dragons" of financial risks

(require special mechanism and may be more predictable)

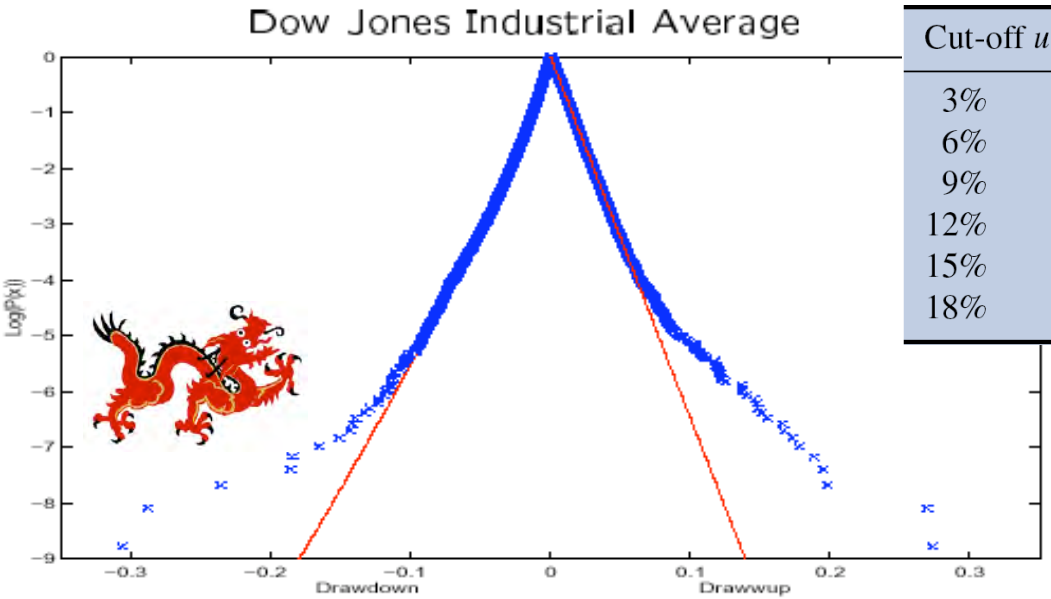

Cut-off u	Quantile	z	$\ln(L_0)$	$\ln(L_1)$	T	Proba
3%	87%	0.916, 0.940	4890.36	4891.16	1.6	20.5%
6%	97%	0.875, 0.915	4944.36	4947.06	5.4	2.0%
9%	99.0%	0.869, 0.918	4900.75	4903.66	5.8	1.6%
12%	99.7%	0.851, 0.904	4872.47	4877.46	10.0	0.16%
15%	99.7%	0.843, 0.898	4854.97	4860.77	11.6	0.07%
18%	99.9%	0.836, 0.890	4845.16	4851.94	13.6	0.02%

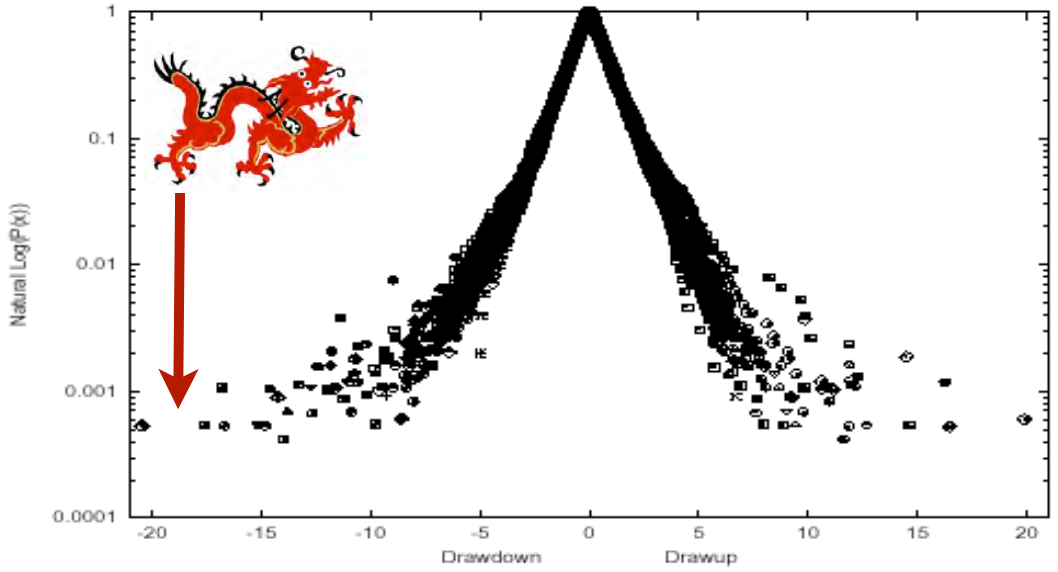

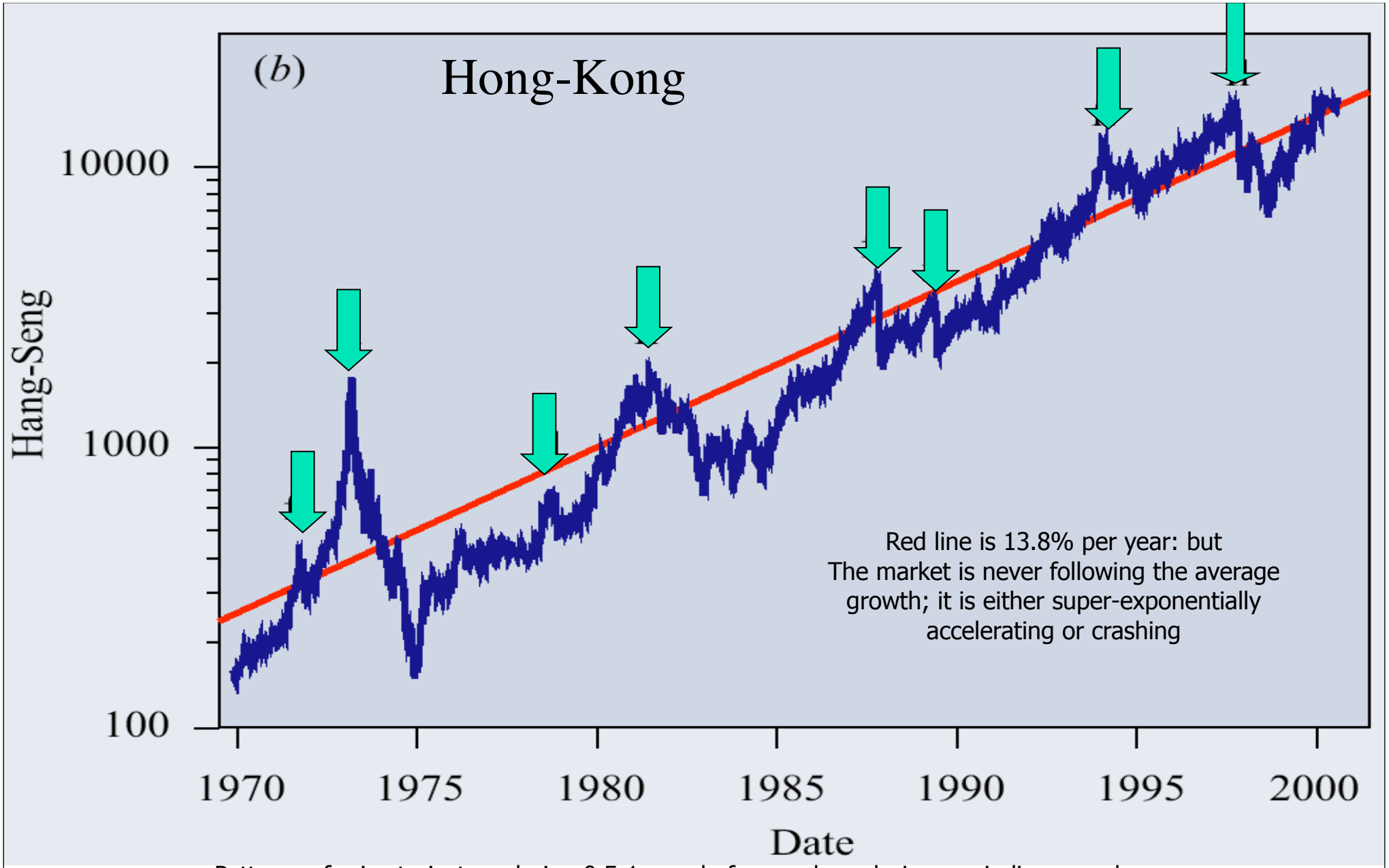

Patterns of price trajectory during 0.5-1 year before each peak: Log-periodic power law

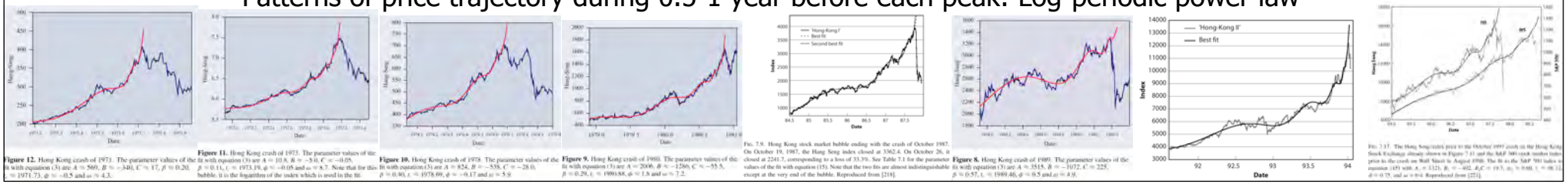

Beyond power laws: six examples of "Dragons"

Financial economics: Outliers and dragons in the distribution of financial drawdowns.

Population geography: Paris as the dragon-king in the Zipf distribution of French city sizes.

Material science: failure and rupture processes.

Hydrodynamics: Extreme dragon events in the pdf of turbulent velocity fluctuations.

Brain medicine: Epileptic seizures

Geophysics: Gutenberg-Richter law and characteristic earthquakes.

Paris as a king-dragon

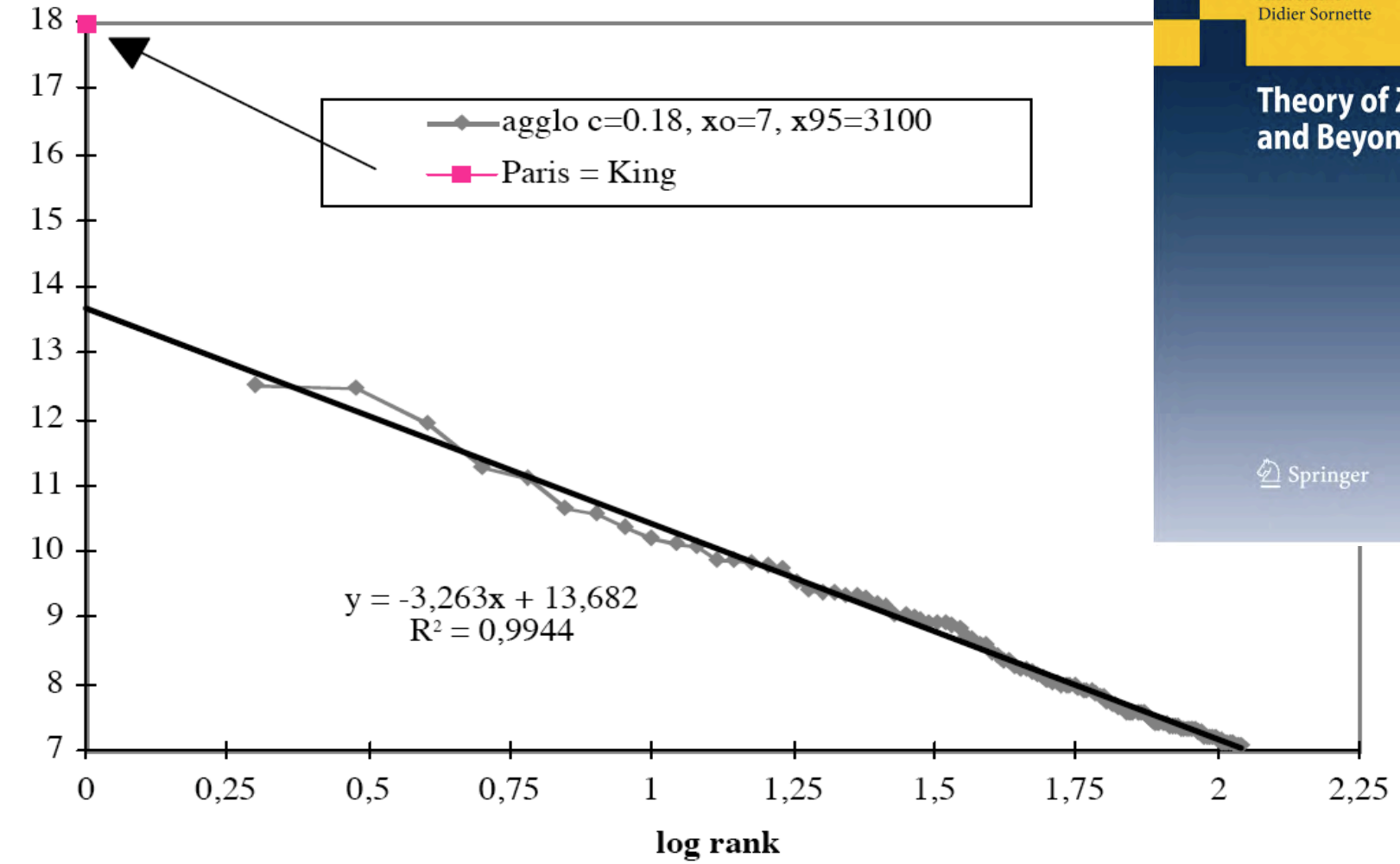

Fig. 7. French agglomerations: stretched exponential and "King effect".

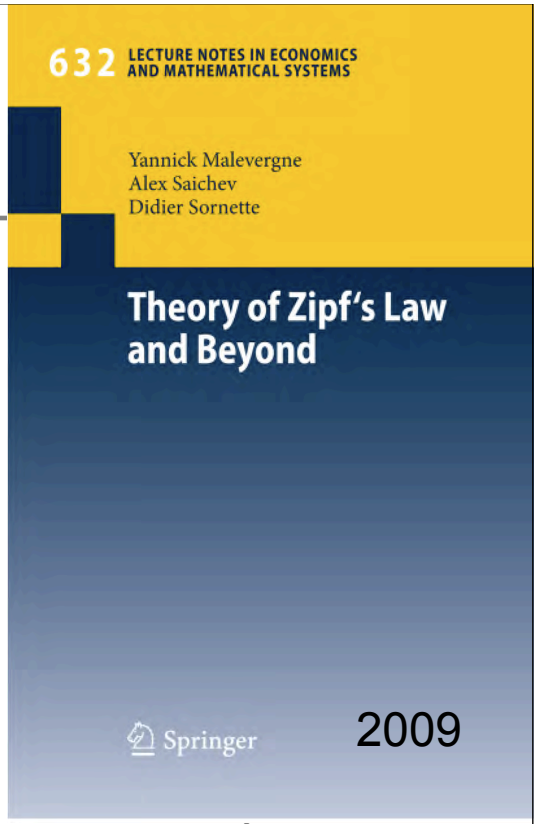

Jean Laherrere and Didier Sornette, Stretched exponential distributions in Nature and Economy: ``Fat tails" with characteristic scales, European Physical Journal B 2, 525-539 (1998)

Beyond power laws: six examples of "Dragons"

Financial economics: Outliers and dragons in the distribution of financial drawdowns.

Population geography: Paris as the dragon-king in the Zipf distribution of French city sizes.

Material science: failure and rupture processes.

Hydrodynamics: Extreme dragon events in the pdf of turbulent velocity fluctuations.

Brain medicine: Epileptic seizures

Geophysics: Gutenberg-Richter law and characteristic earthquakes.

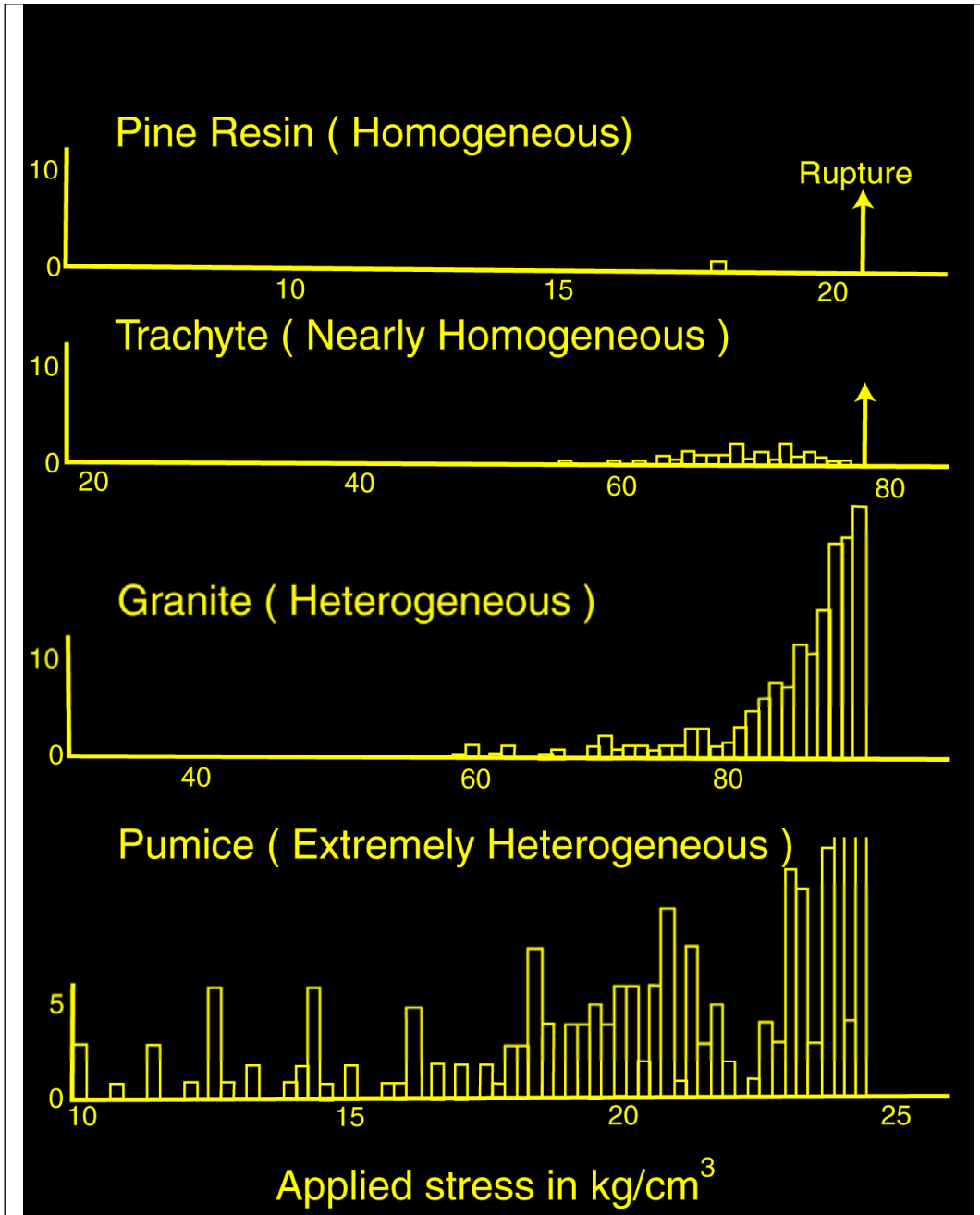

Fig. 4. Frequency of elastic shocks under increasing stresses in materials with different heterogeneity. From Mogi [1962]

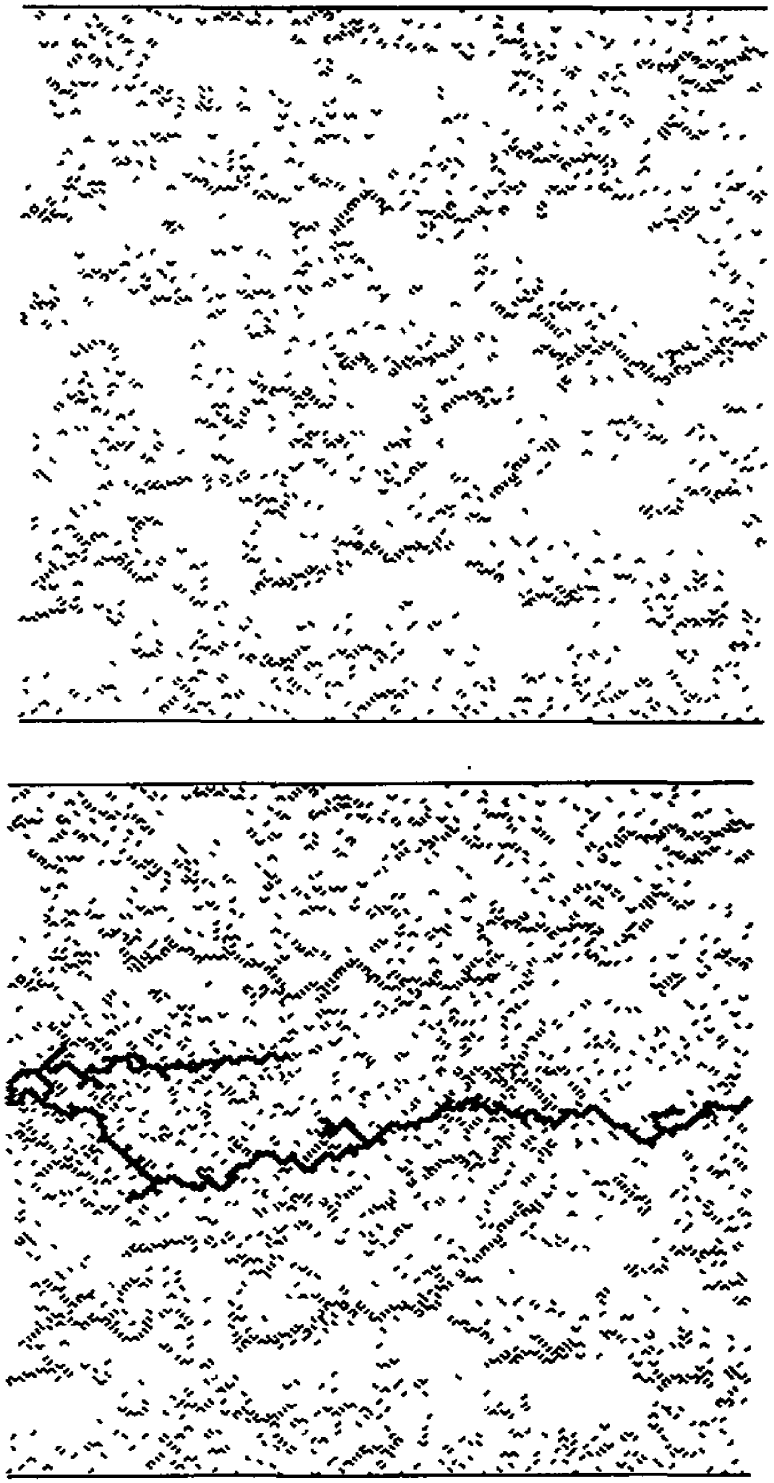

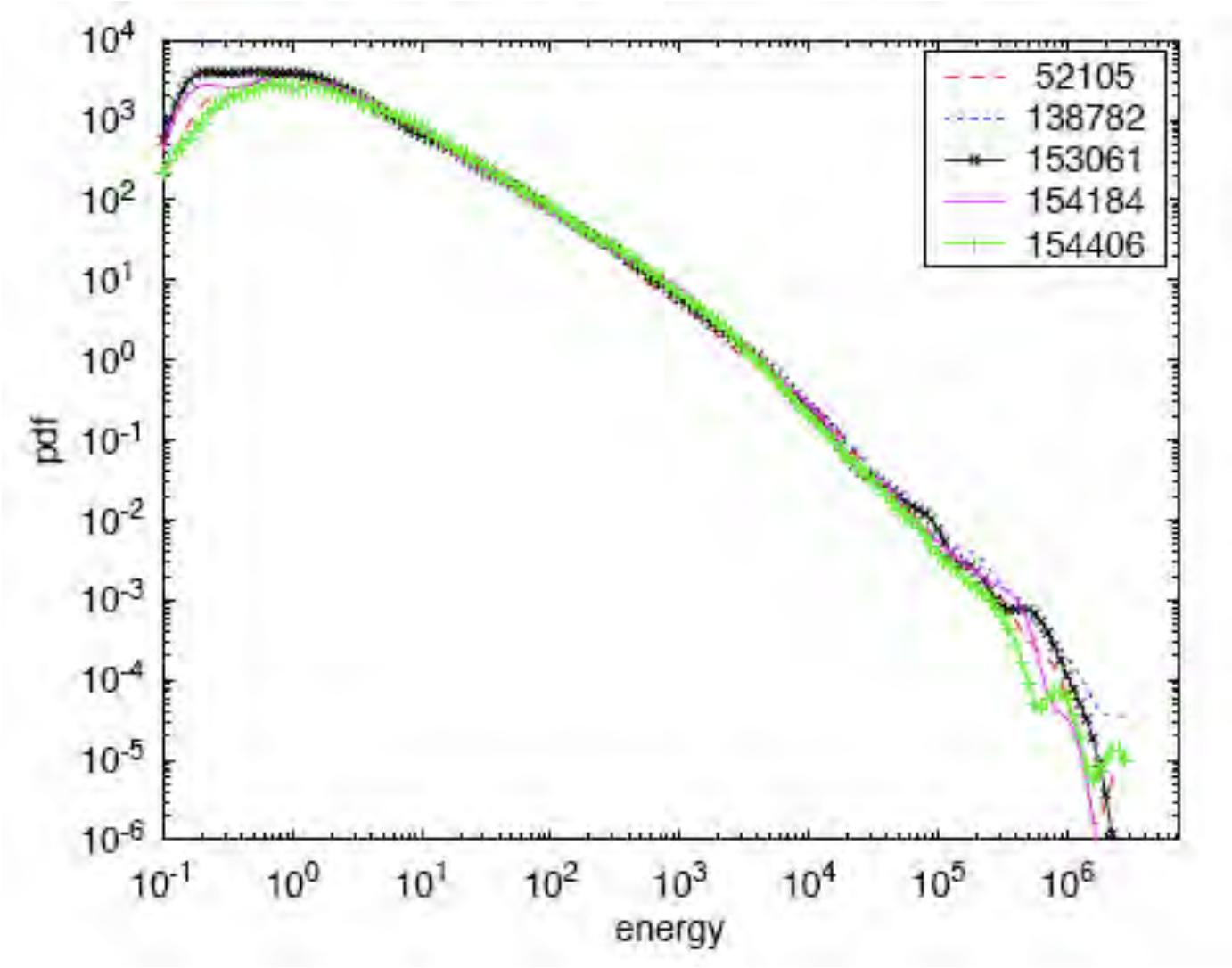

• • •

Energy distribution for the [+-62] specimen #4 at different times, for 5 time windows with 3400 events each. The average time (in seconds) of events in each window is given in the caption.

H. Nechad, A. Helmstetter, R. El Guerjouma and D. Sornette, Andrade and Critical Time-to-Failure Laws in Fiber-Matrix Composites: Experiments and Model, Journal of Mechanics and Physics of Solids (JMPS) 53, 1099-1127 (2005)

Beyond power laws: six examples of "Dragons"

Financial economics: Outliers and dragons in the distribution of financial drawdowns.

Population geography: Paris as the dragon-king in the Zipf distribution of French city sizes.

Material science: failure and rupture processes.

Hydrodynamics: Extreme dragon events in the pdf of turbulent velocity fluctuations.

Brain medicine: Epileptic seizures

Geophysics: Gutenberg-Richter law and characteristic earthquakes.

Mathematical Geophysics Conference

Extreme Earth Events

Villefranche-sur-Mer, 18-23 June 2000

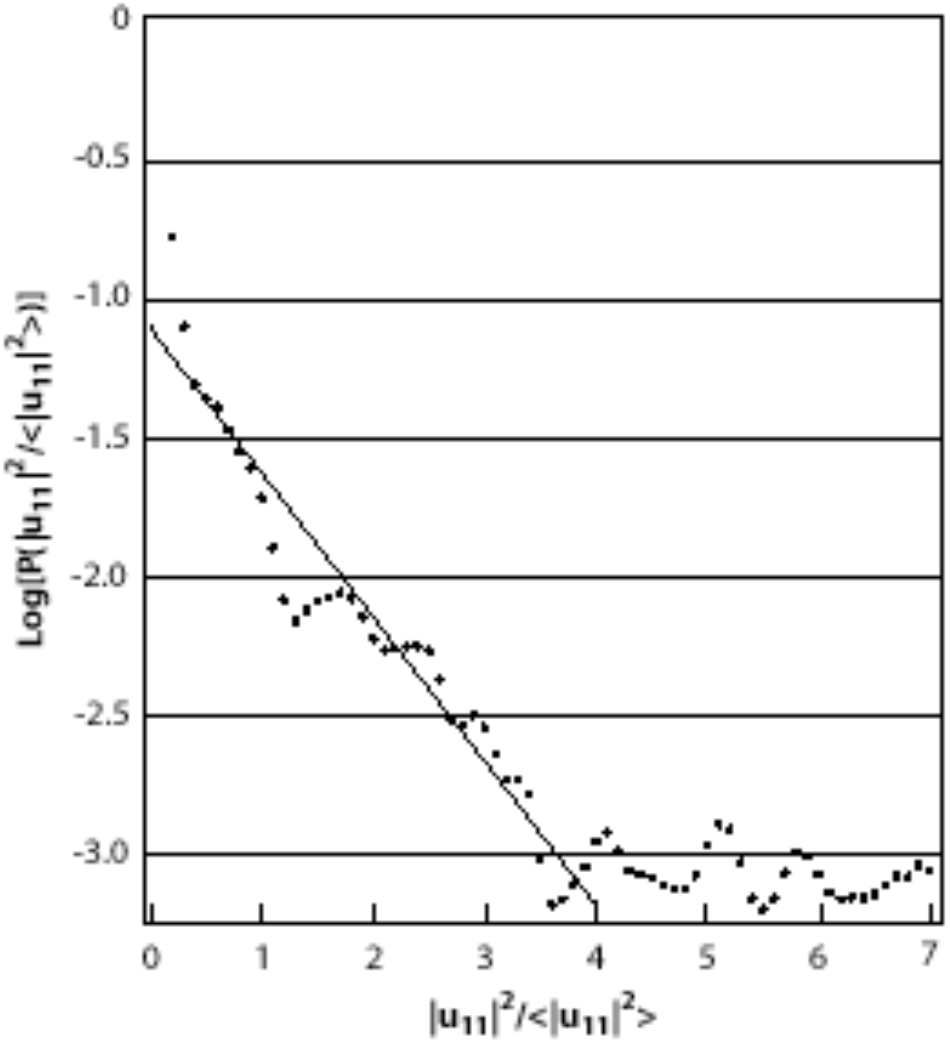

L'vov, V.S., Pomyalov, A. and Procaccia, I. (2001) Outliers, Extreme Events and Multiscaling, Physical Review E 6305 (5), 6118, U158-U166.

FIG. 3.2. Apparent probability distribution function of the square of the fluid velocity, normalized to its time average, in the eleventh shell of the toy model of hydrodynamic turbulence discussed in the text. The vertical axis is in logarithmic scale such that the straight line, which helps the eye, qualifies as an apparent exponential distribution. Note the appearance of extremely sparse and large bursts of velocities at the extreme right above the extrapolation of the straight line. Reproduced from [252].

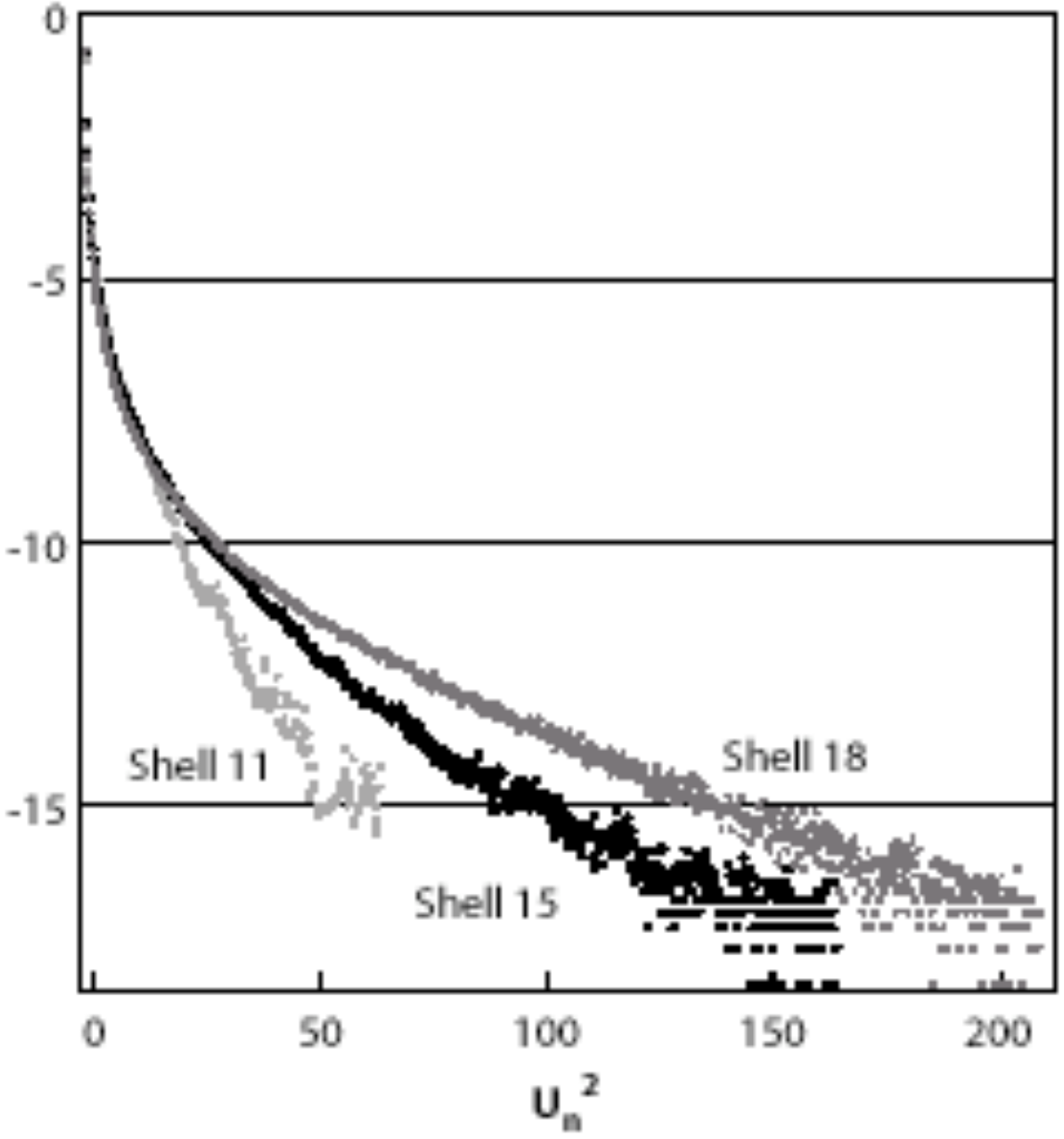

Pdf of the square of the Velocity as in the previous figure but for a much longer time series, so that the tail of the distributions for large Fluctuations is much better constrained. The hypothesis that there are no outliers is tested here by collapsing the distributions for the three shown layers. While this is a success for small fluctuations, the tails of the distributions for large events are very different, indicating that extreme fluctuations belong to a different class of their own and hence are outliers.

L'vov, V.S., Pomyalov, A. and Procaccia, I. (2001) Outliers, Extreme Events and Multiscaling, Physical Review E 6305 (5), 6118, U158-U166.

Beyond power laws: six examples of "Dragons"

Financial economics: Outliers and dragons in the distribution of financial drawdowns.

Population geography: Paris as the dragon-king in the Zipf distribution of French city sizes.

Material science: failure and rupture processes.

Hydrodynamics: Extreme dragon events in the pdf of turbulent velocity fluctuations.

Brain medicine: Epileptic seizures

Geophysics: Gutenberg-Richter law and characteristic earthquakes.

Epileptic Seizures – Quakes of the Brain?

with Ivan Osorio
KUMC & FHS
Mark G. Frei - FHS
John Milton -The Claremont Colleges

(arxiv.org/abs/0712.3929)

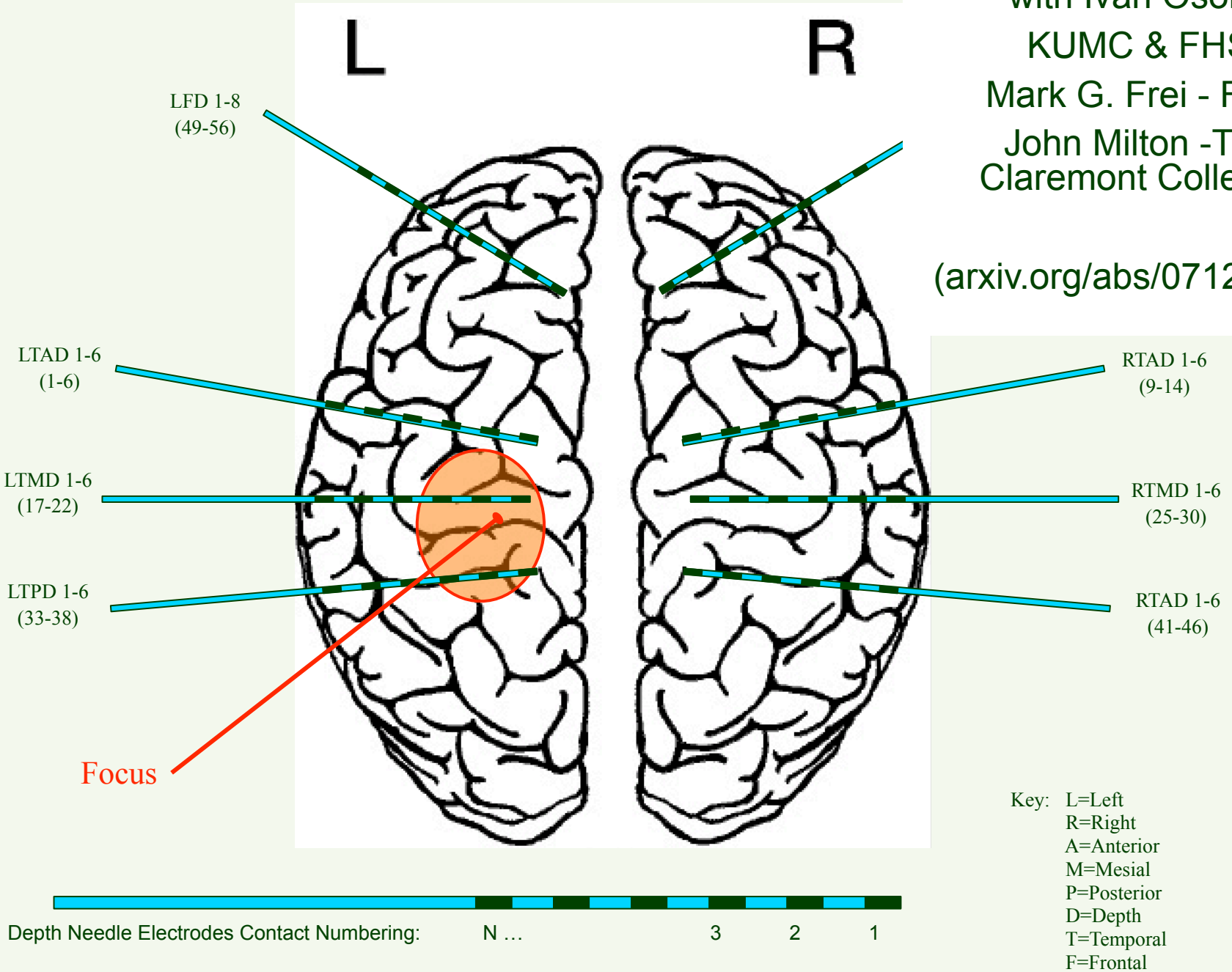

Key: L=Left
R=Right
A=Anterior
M=Mesial
P=Posterior
D=Depth
T=Temporal
F=Frontal

Bursts and Seizures

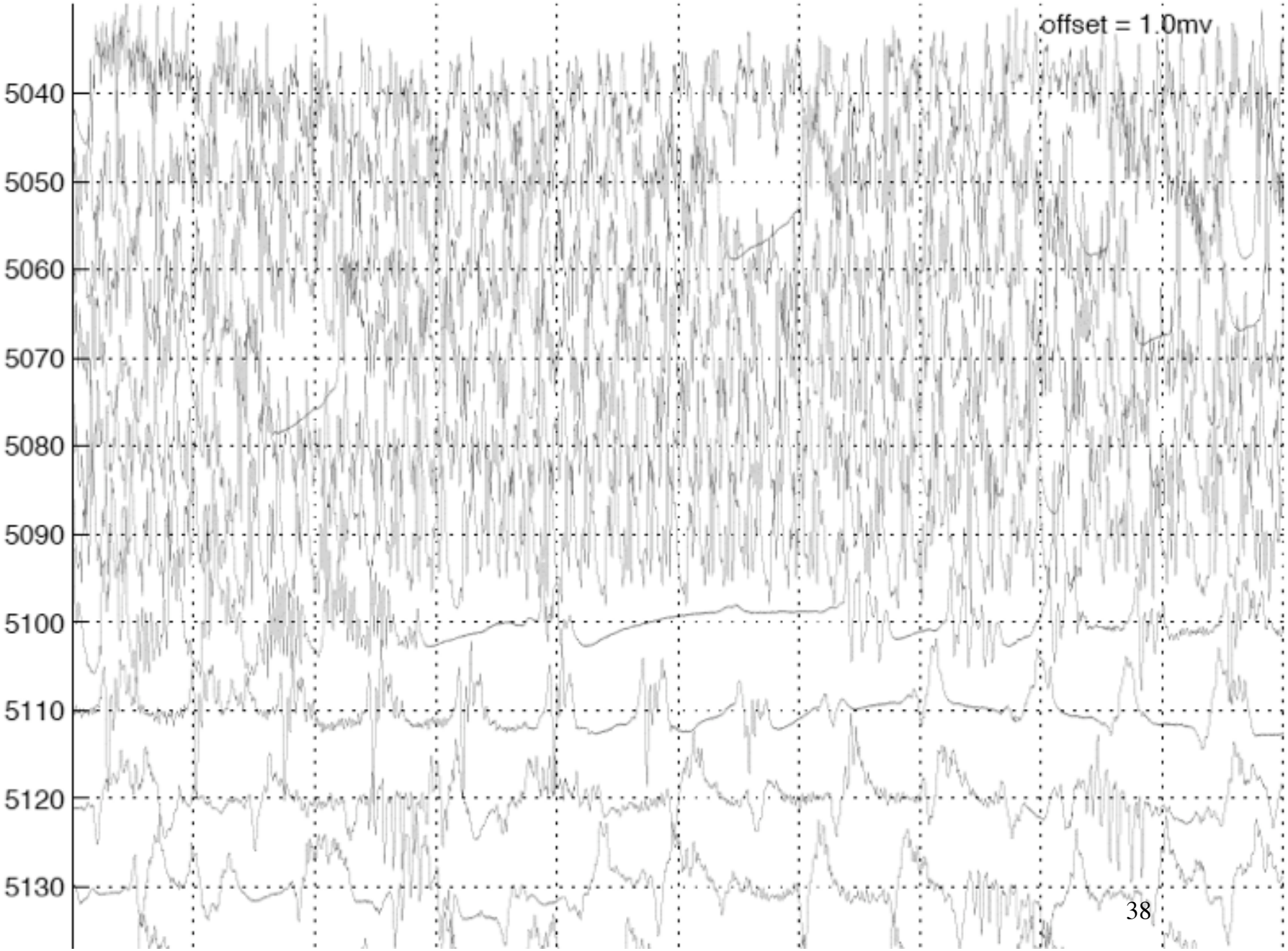

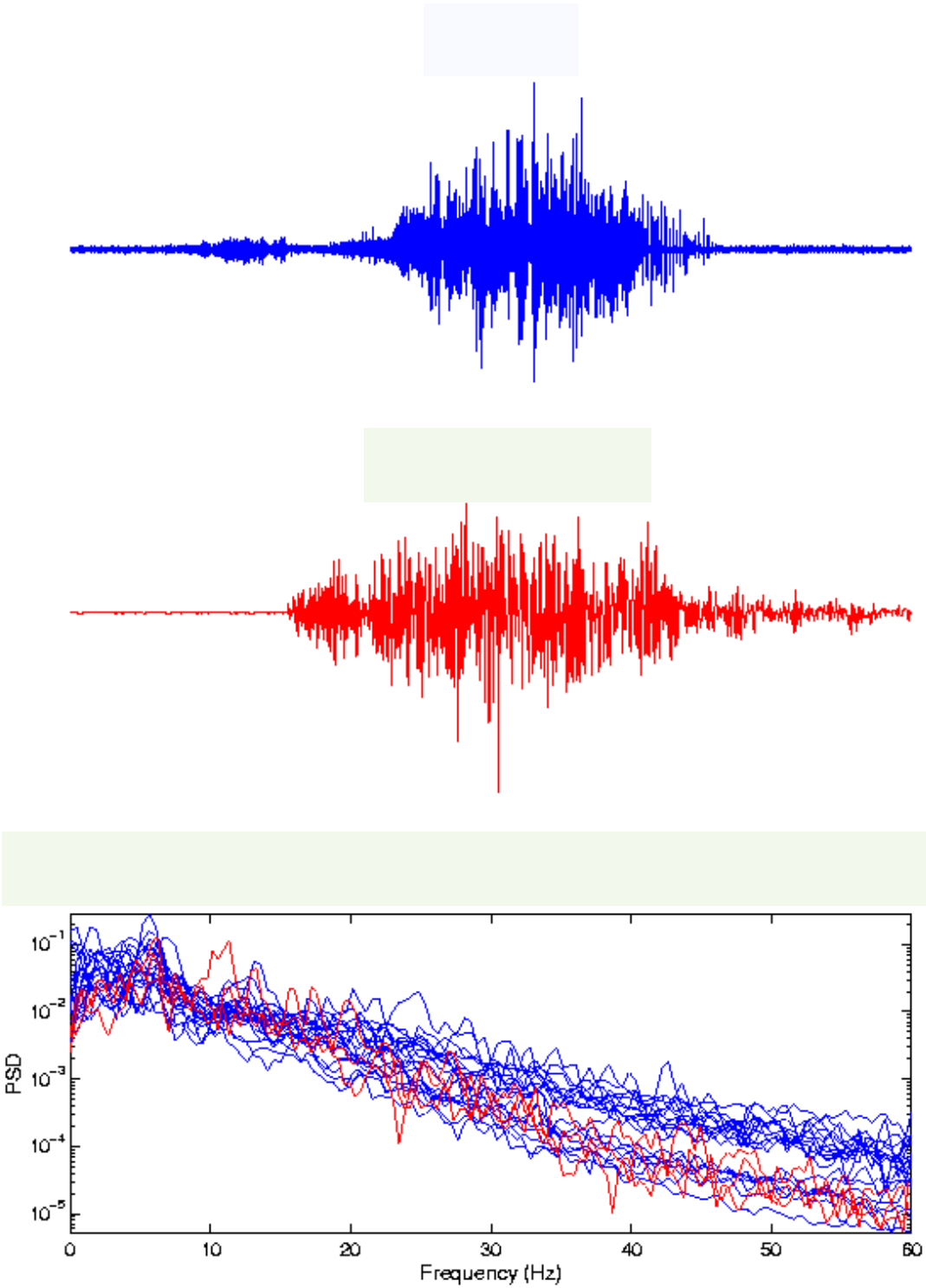
PSD
Frequency (Hz)
0
10
20
30
40
50
60

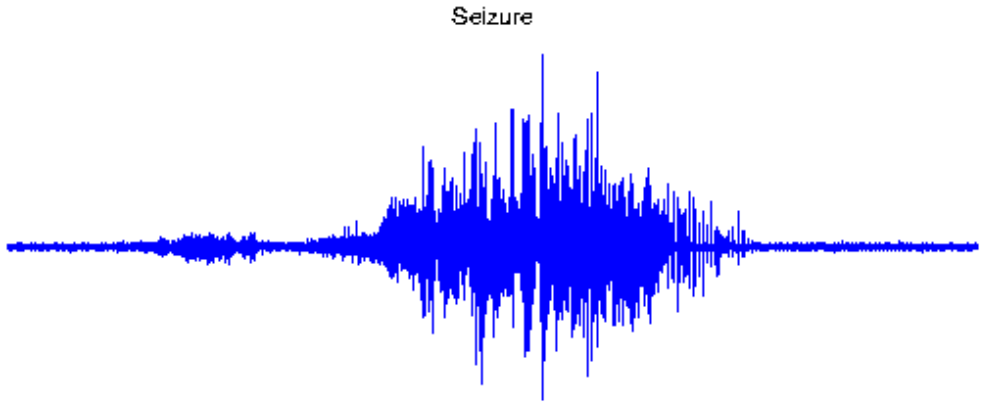
Seizure

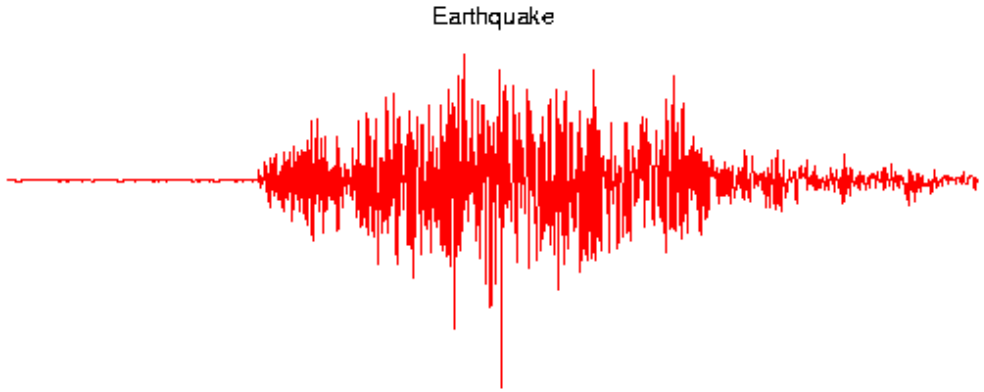
Earthquake

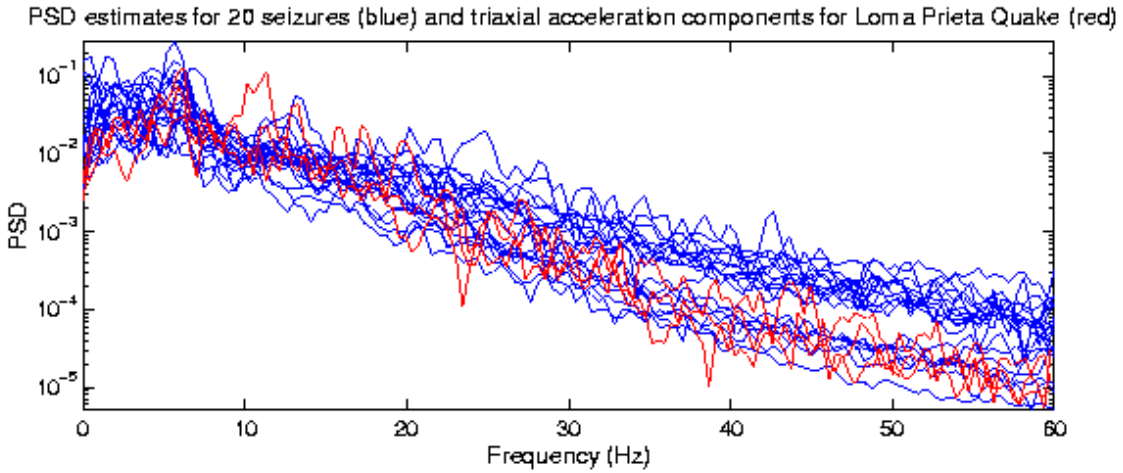
PSD estimates for 20 seizures (blue) and triaxial acceleration components for Loma Prieta Quake (red)
PSD
Frequency (Hz)
10^{-1}
10^{-2}
10^{-3}
10^{-4}
10^{-5}
0
10
20
30
40
50
60

Gutenberg-Richter distribution of sizes

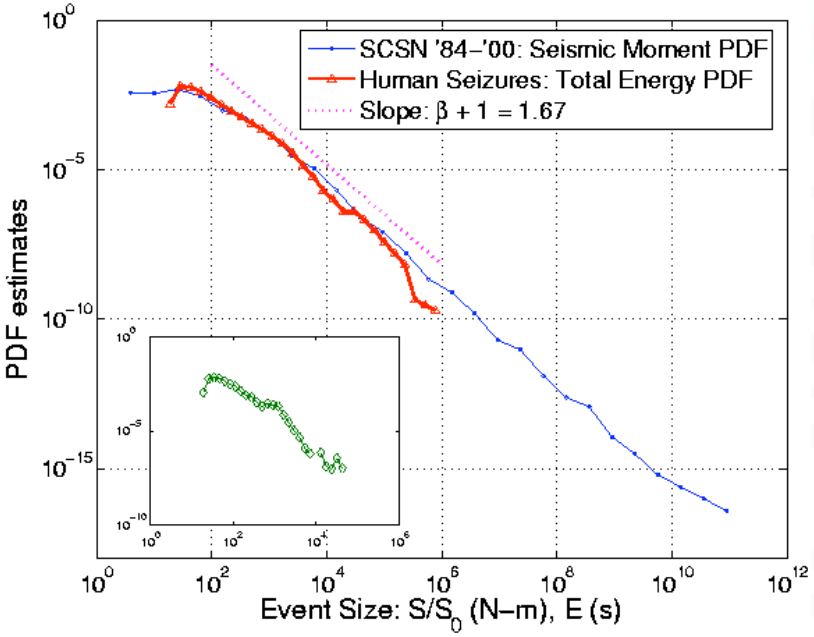

Omori law: Direct and Inverse

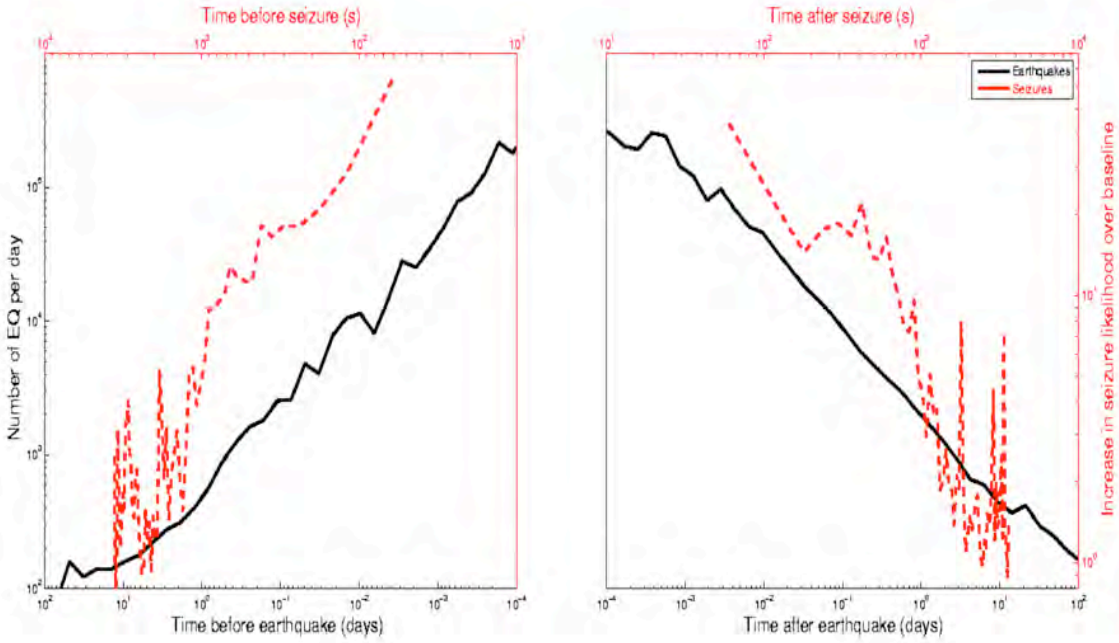

pdf of inter-event waiting times

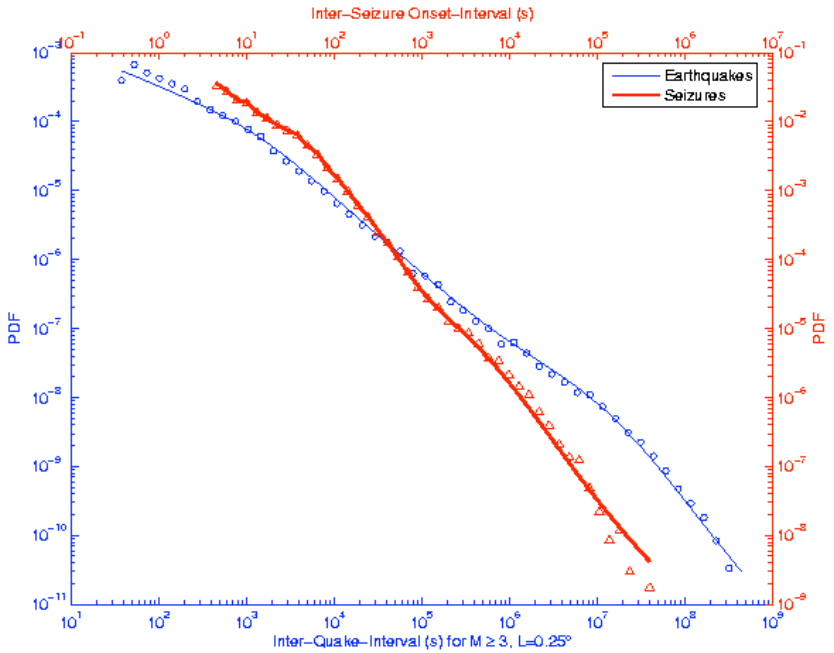

The longer it has been since the last event, the longer it will be since the next one!

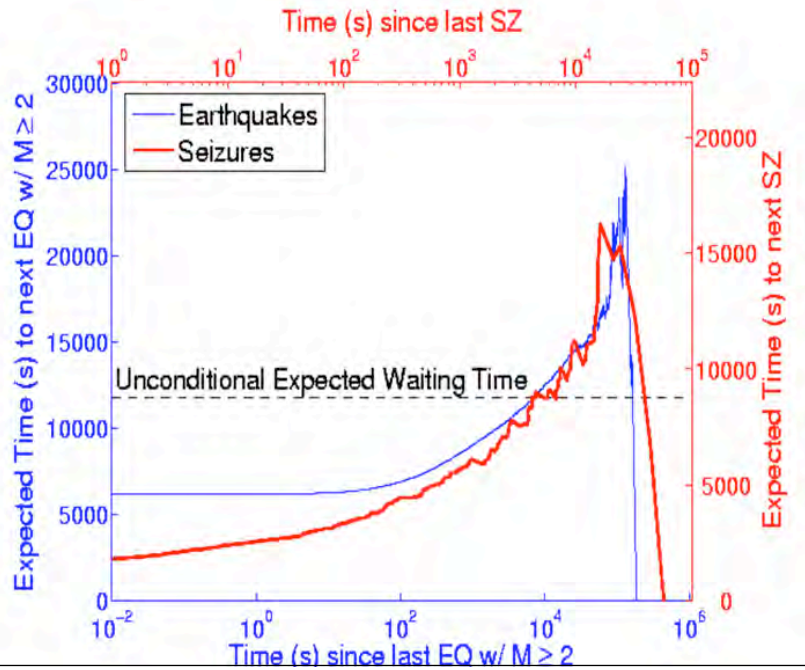

19 rats treated intravenously (2) with the convulsant 3-mercapto-proprionic acid (3-MPA)

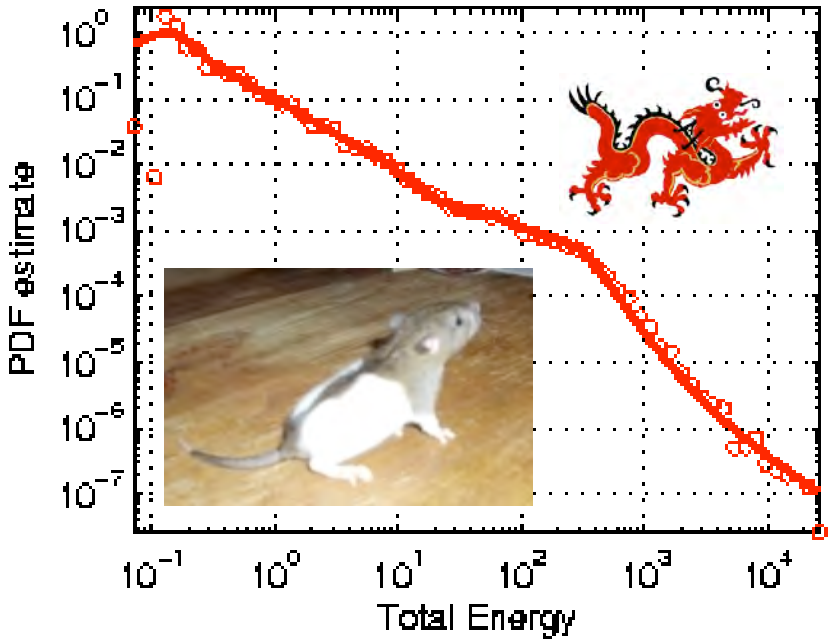

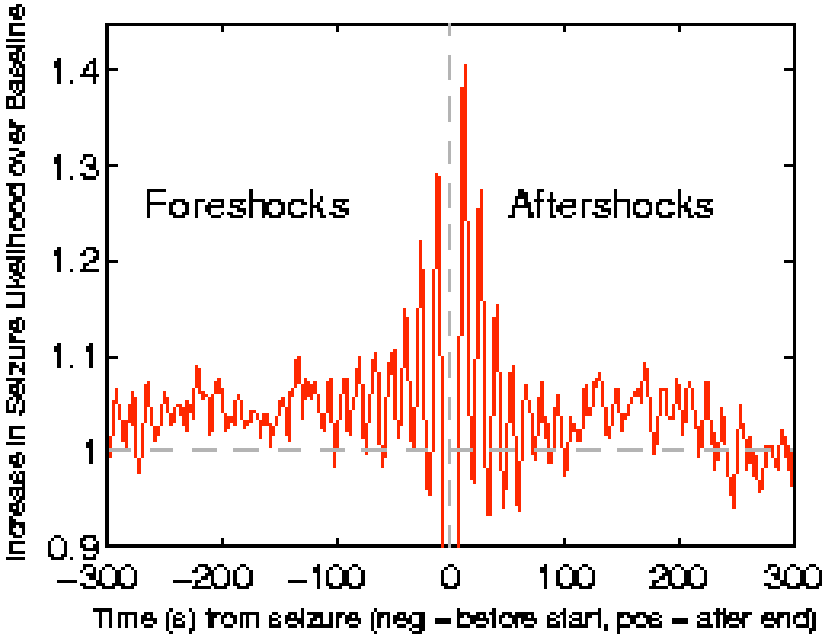

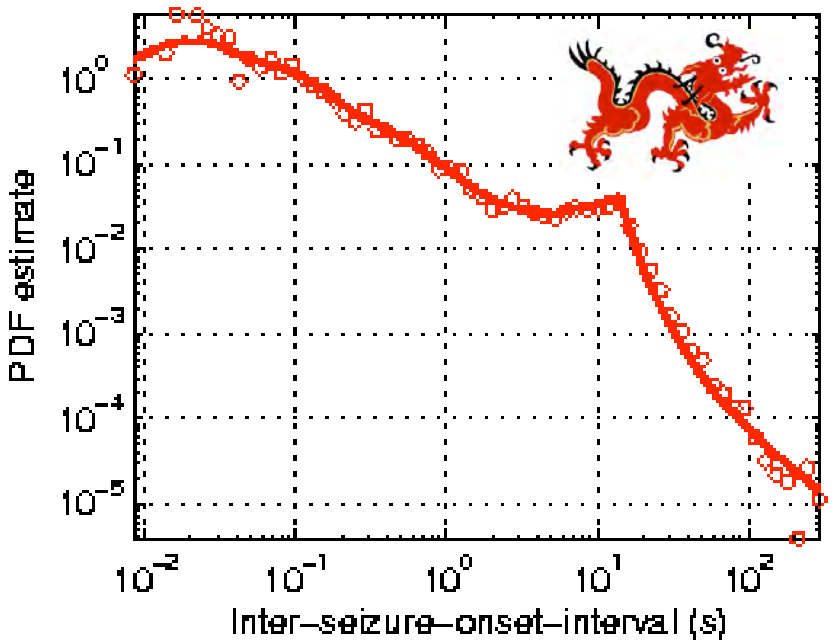

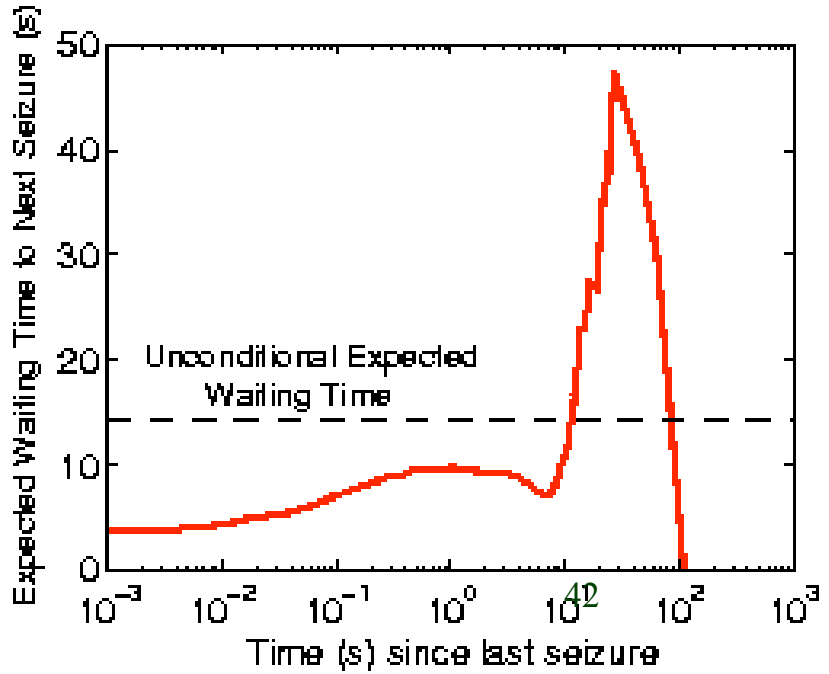

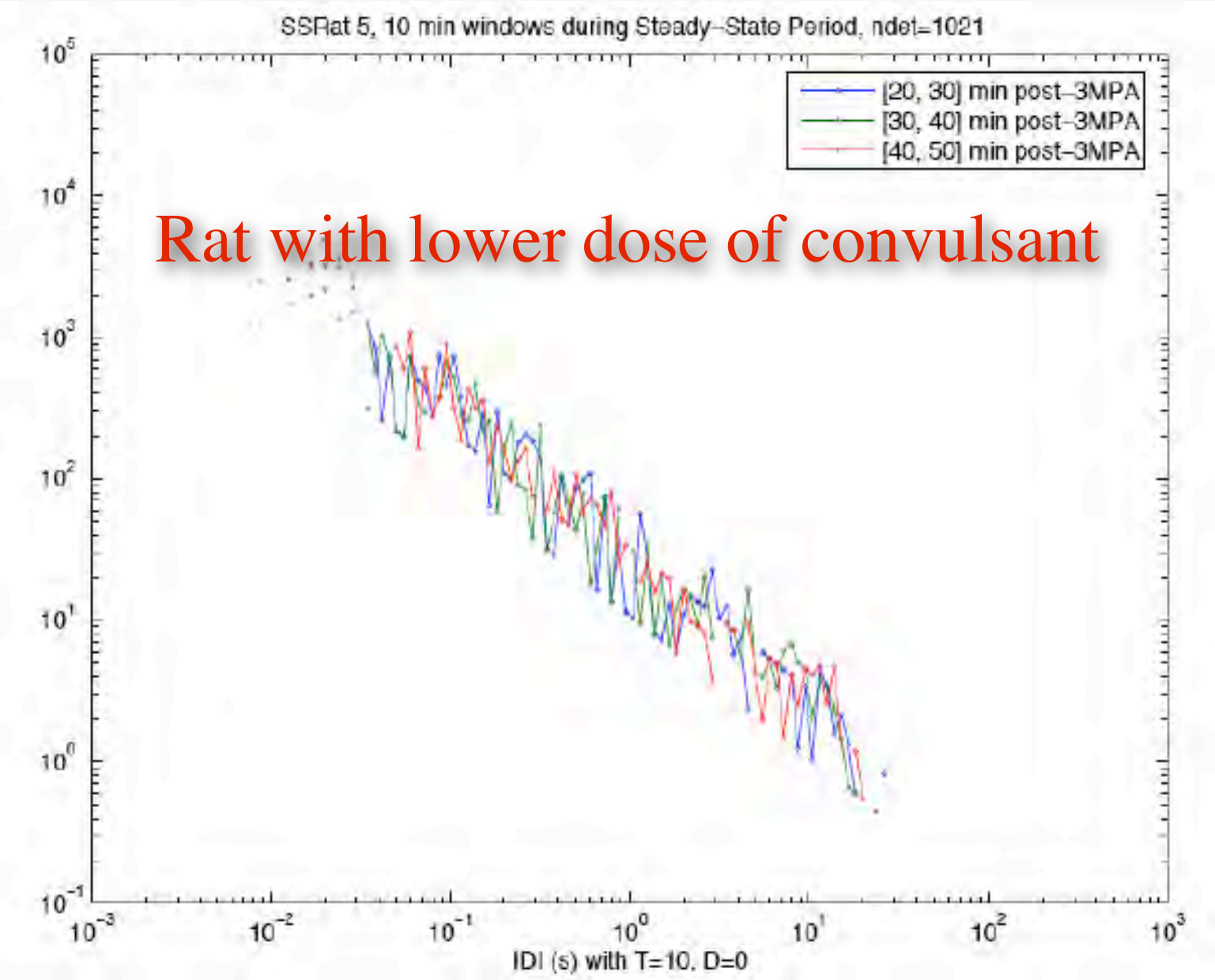

Distribution of inter-seizure time intervals for rat 5, demonstrating a pure power law, which is characteristic of the SOC state. This scale-free distribution should be contrasted with the pdf's obtained for the other rats, which are marked by a strong shoulder associated with a characteristic time scale, which reveals the periodic regime.

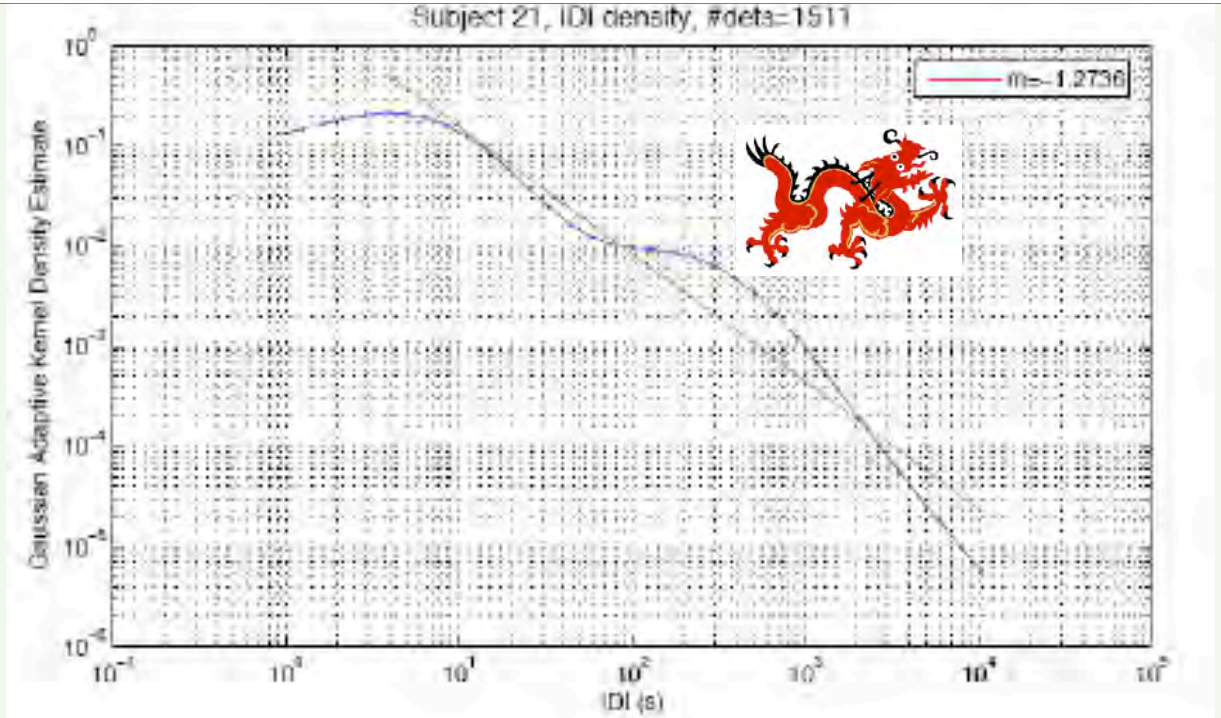

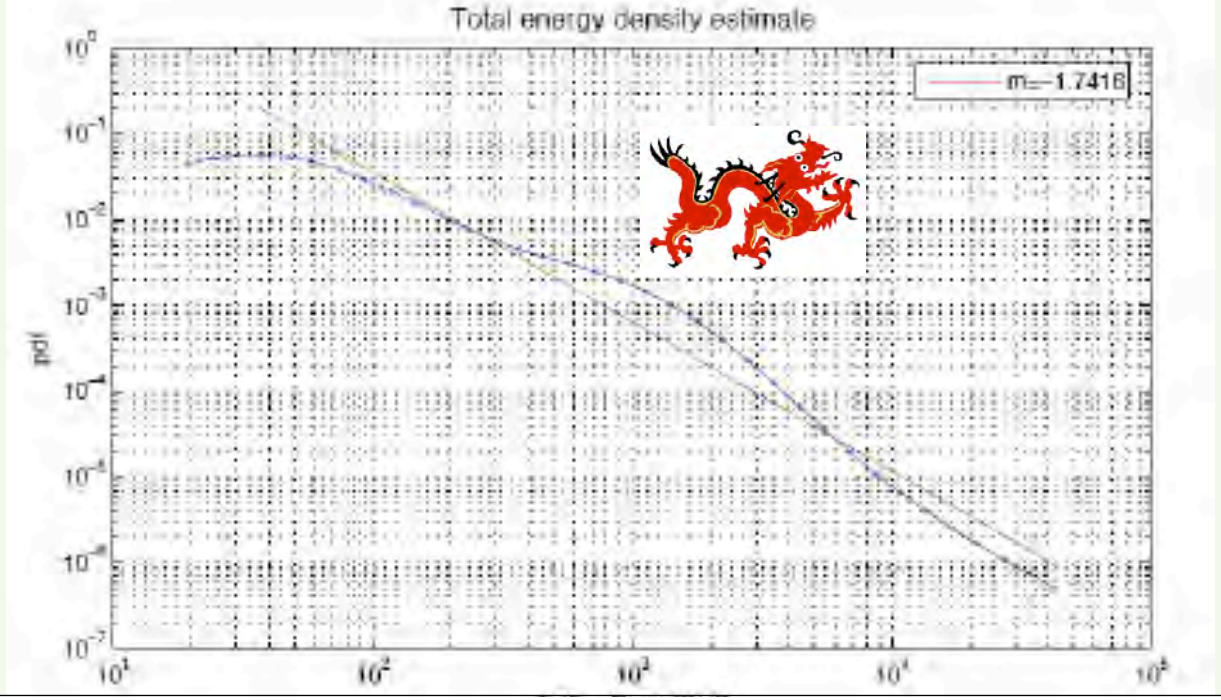

Some humans are like rats with large doses of convulsant

The pdf's of the seizure energies and of the inter-seizure waiting times for subject 21.

Note the shoulder in each distribution, demonstrating the presence of a characteristic size and time scale, qualifying the periodic regime.

Beyond power laws: six examples of "Dragons"

Financial economics: Outliers and dragons in the distribution of financial drawdowns.

Population geography: Paris as the dragon-king in the Zipf distribution of French city sizes.

Material science: failure and rupture processes.

Hydrodynamics: Extreme dragon events in the pdf of turbulent velocity fluctuations.

Brain medicine: Epileptic seizures

Geophysics: Gutenberg-Richter law and characteristic earthquakes.

Complex magnitude distributions

Characteristic earthquakes?

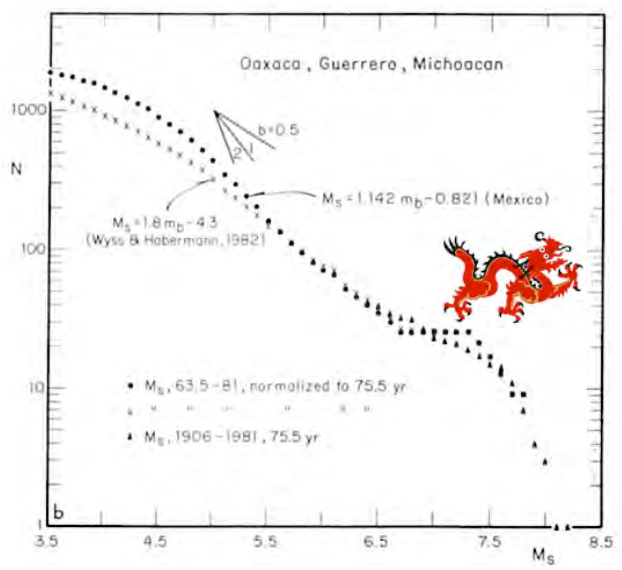

Singh, et. al., 1983, BSSA 73, 1779-1796

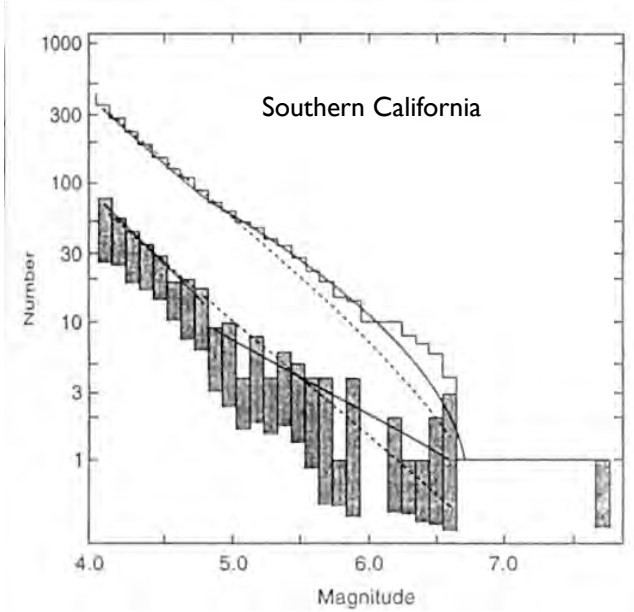

Knopoff, 2000, PNAS 97, 11880-11884

Main, 1995, BSSA 85, 1299-1308

Wesnousky, 1996, BSSA 86, 286-291

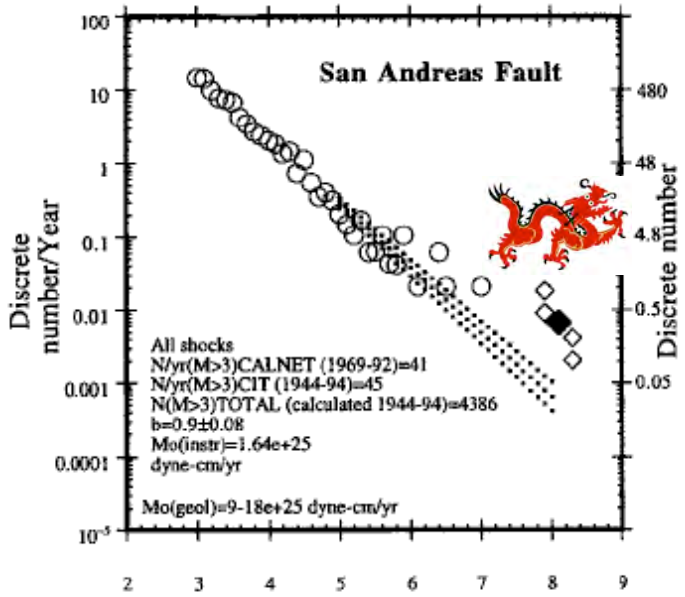

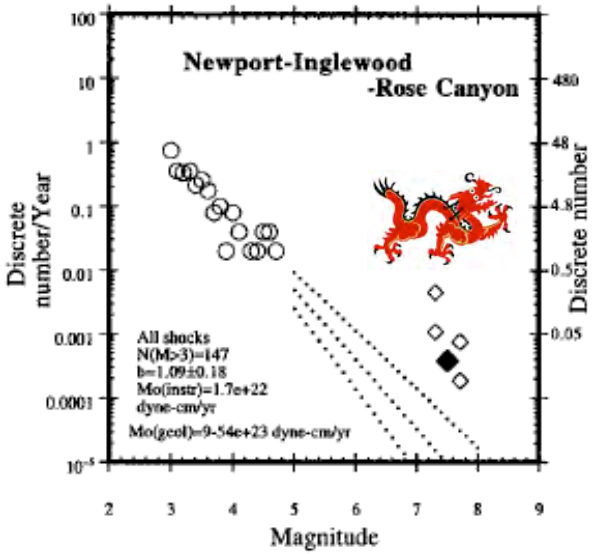

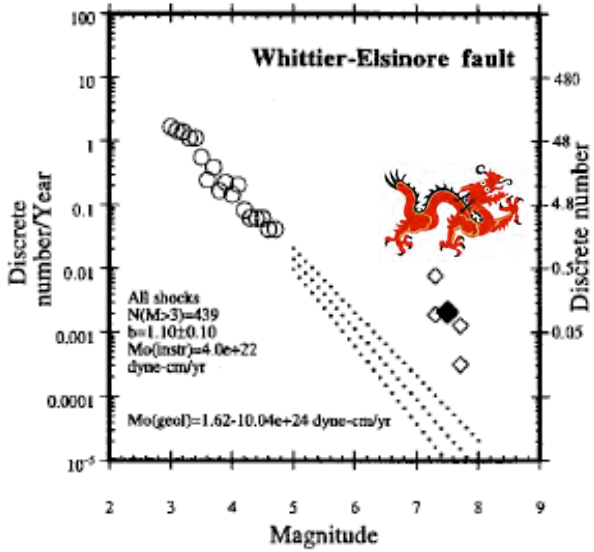

Complex Systems approach to Prediction

-positive feedbacks

-non sustainable regimes

-rupture

Thomas Robert Malthus (1766–1834)

1798

autocatalitic proliferation: $\frac{dx}{dt} = a \cdot x$

with *a* =birth rate - death rate

exponential solution: $X(t) = X(0)e^{a\,t}$

contemporary estimations= doubling of the population every 30yrs

Pierre François Verhulst (1804-1849)

way out exponential explosion:

$dX/dt = a\,X - c\,X^2$ **1838**

Solution: exponential ==========→saturation at X= a / c

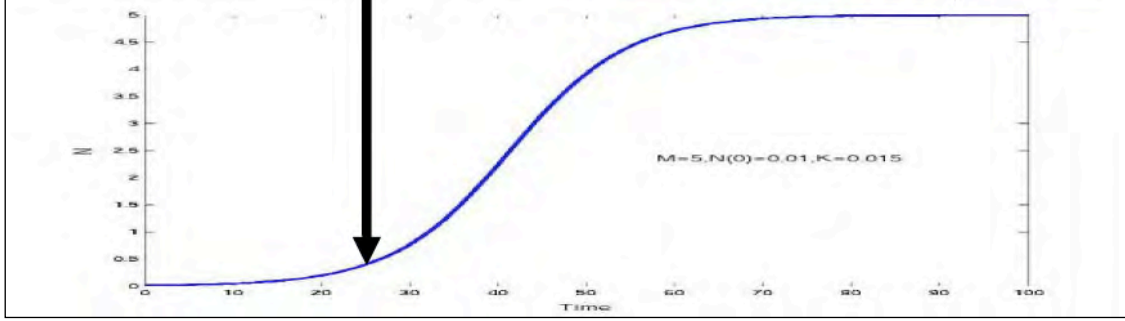

For humans data at the time could not discriminate between:
1. exponential growth of Malthus
2. logistic growth of Verhulst

But data fit on animal population: sheep in Tasmania

- exponential in the first 20 years after their introduction and completely saturated after about half a century. ==> Verhulst

Symbiosis between human population growth and artifacts

Diminishing returns
to
Increasing returns

- **Human propagation follows**

$$\text{rate of change of population} = R(t) \times \text{population}$$

- **Assume increase in technology follows**

$$\text{rate of change of technology} = C \times \text{population}$$

- **Assume also**

$$R(t) = K \times \text{technology}$$

- **Implies double geometric growth**

$$\text{population} = \frac{A}{(t_c - t)}$$

$A = \text{const.}$

$t =$ time

$t_c =$ critical time

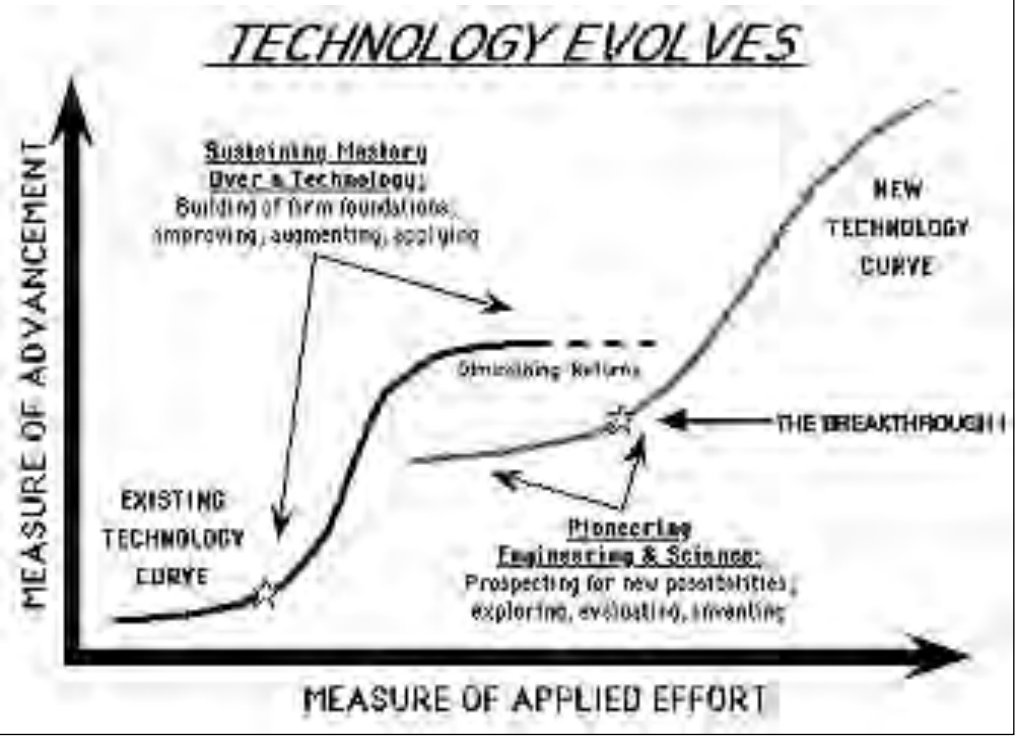

Positive feedback in action

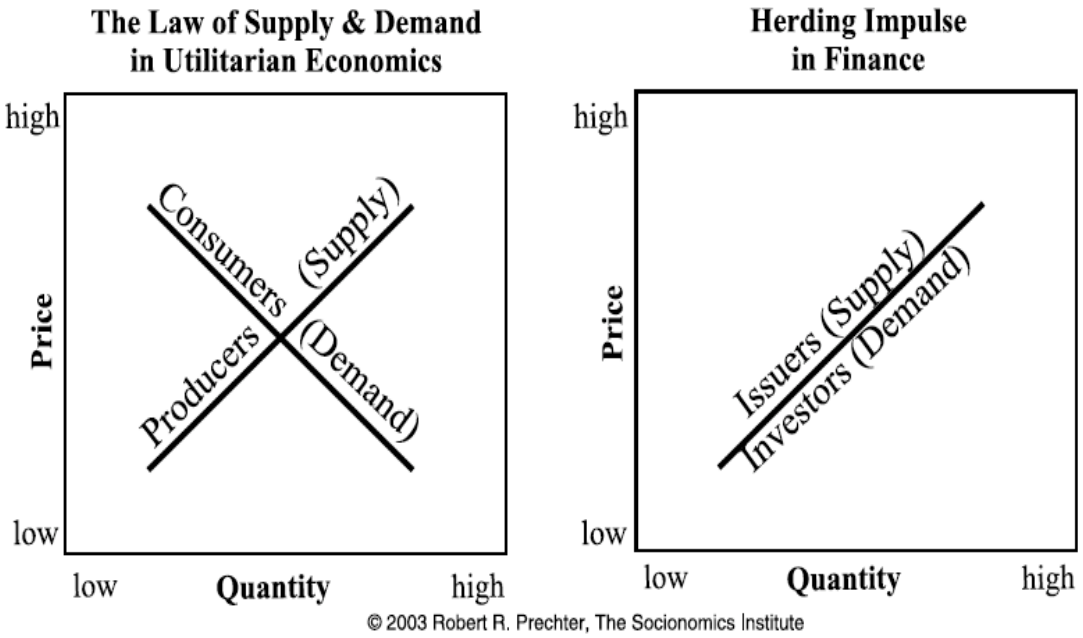

Positive feedbacks

$$\frac{dp}{dt} = cp^d$$

$$p(t) = \left(\frac{c}{m}\right)^{-m} (t_c - t)^{-m}$$

$m = 1/(d-1) > 0$ and $t_c = t_0 + mp_0^{1-d}/c.$

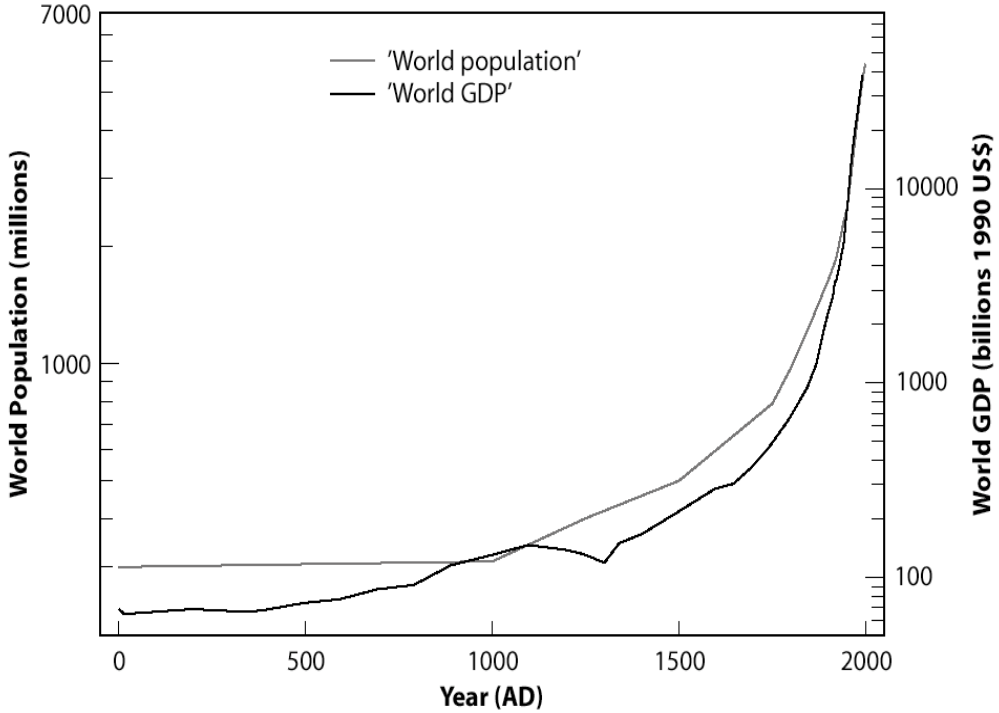

Faster than exponential
transient unsustainable growth

Positive feedback in action

↓

Finite-time Singularity

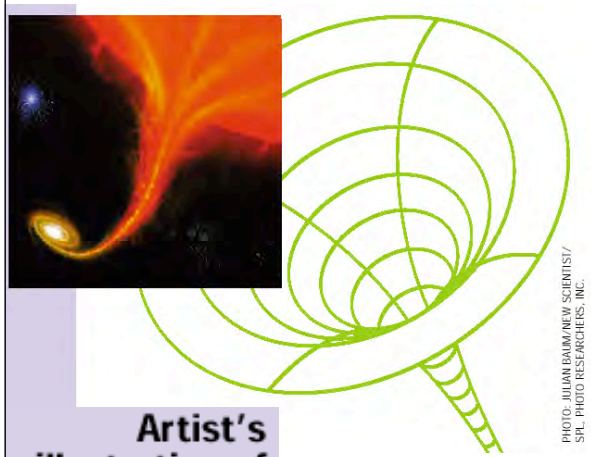

PHOTO: JULIAN BAUM/NEW SCIENTIST/ SPL, PHOTO RESEARCHERS, INC.

Artist's illustration of matter from a red giant star being pulled toward a black hole.

- Planet formation in solar system by run-away accretion of planetesimals
- PDE's: Euler equations of inviscid fluids and relationship with turbulence
- PDE's of General Relativity coupled to a mass field leading to the formation of black holes
- Zakharov-equation of beam-driven Langmuir turbulence in plasma
- rupture and material failure
- Earthquakes (ex: slip-velocity Ruina-Dieterich friction law and accelerating creep)
- Models of micro-organisms chemotaxis, aggregating to form fruiting bodies
- Surface instability spikes (Mullins-Sekerka), jets from a singular surface, fluid drop snap-off
- Euler's disk (rotating coin)
- Stock market crashes...

Simplest Example of a "More is Different" Transition

Water level vs. temperature

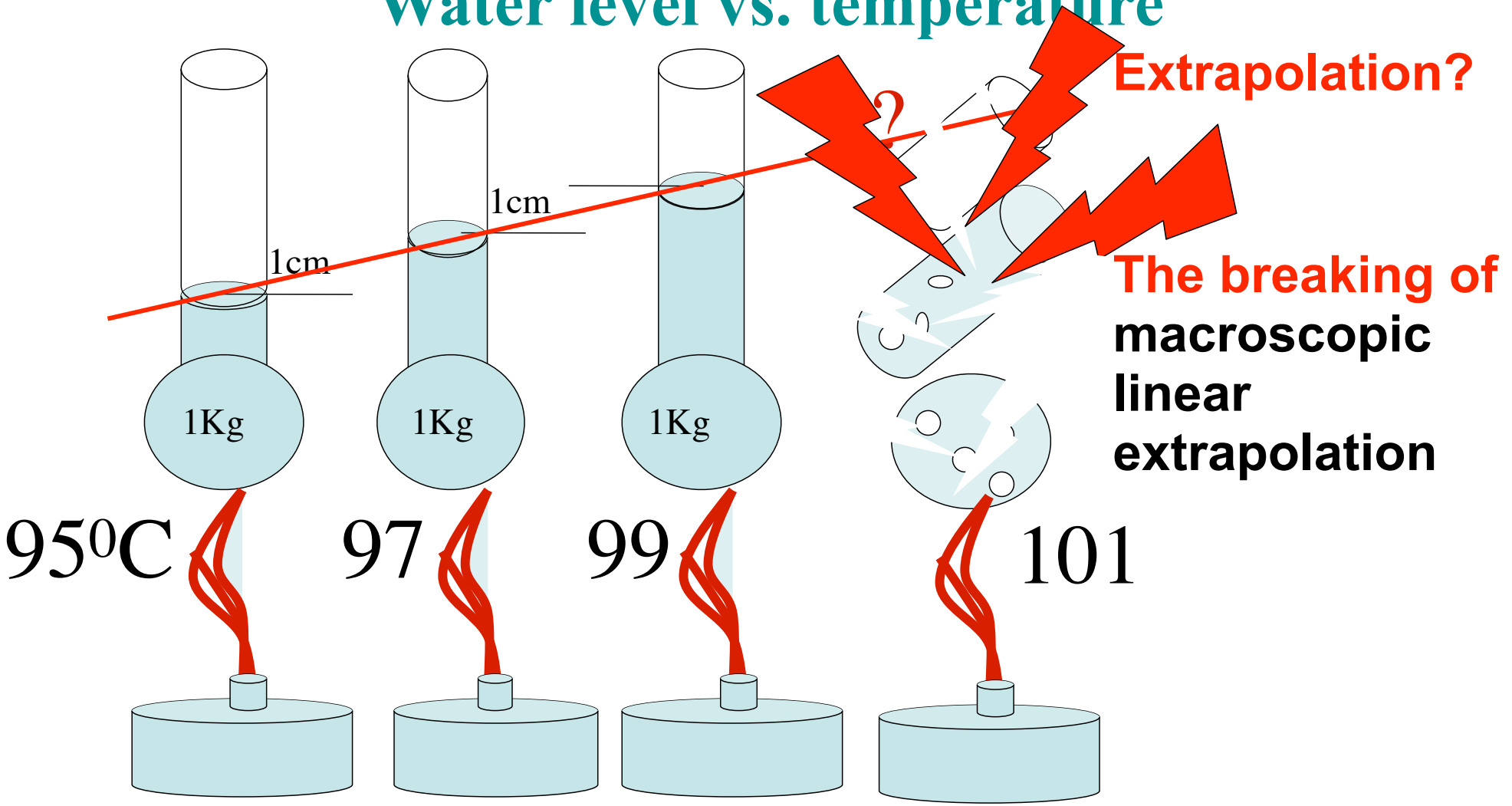

BOILING PHASE TRANSITION

More is different: a single molecule does not boil at 100C⁰

Fundamental reduction theorem

Generically, close to a regime transition, a system bifurcates through the variation of a SINGLE effective "control" parameter

Bifurcation: Qualitative change in behavior as parameter is (slowly) varied

Bifurcation surface: B

Strategy 1: understand from proximity to a reference point as a function of a small parameter

Strategy 2: a few universal "normal forms"

Space of all dynamical systems: $\mathcal{M}$

a particular dynamical system: $M \in \mathcal{M}$

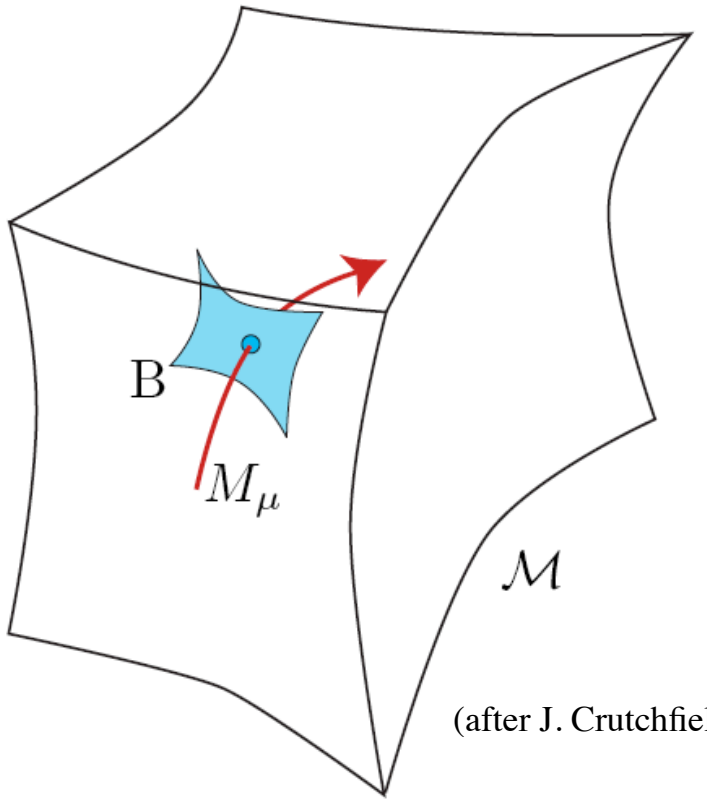

(after J. Crutchfield)

BIFURCATIONS, PHASE TRANSITIONS, CATASTROPHES, TIPPING POINTS...

Phase Transitions

Haken 1983 *Synergetics: An Introduction* Springer-Verlag
Kelso 1995 *Dynamic Patterns* MIT Press

Tap the left index finger in-phase with the tick of the metronome.

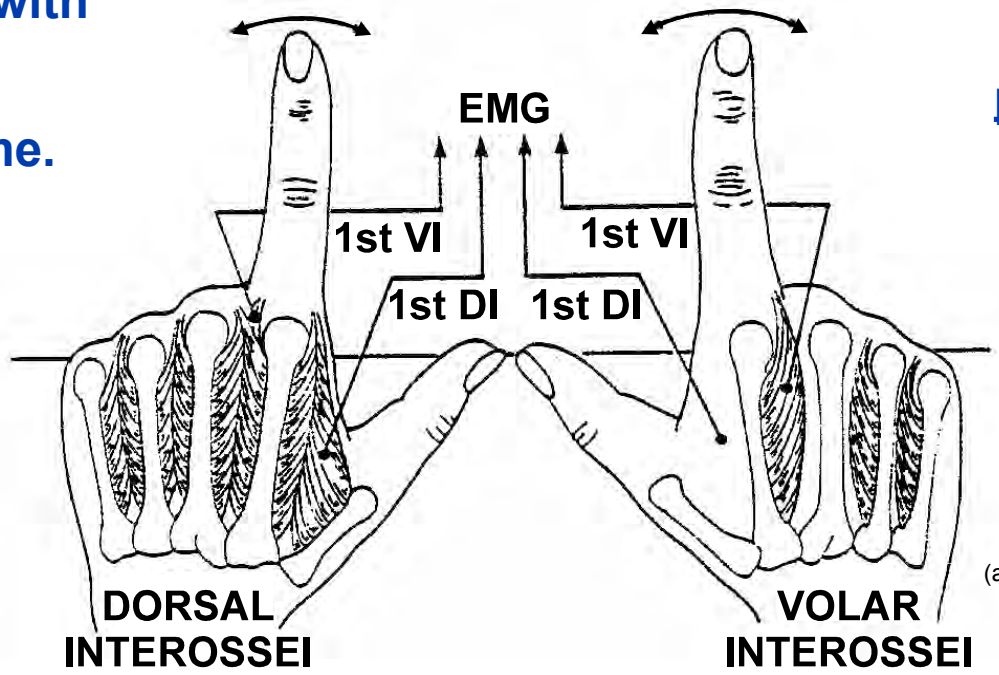

(after Liebovitch)

Try to tap the right index finger out-of-phase with the tick of the metronome.

Phase Transitions

Haken 1983 *Synergetics: An Introduction* Springer-Verlag
Kelso 1995 *Dynamic Patterns* MIT Press

As the frequency of the metronome increases, the right finger shifts from out-of-phase to in-phase motion.

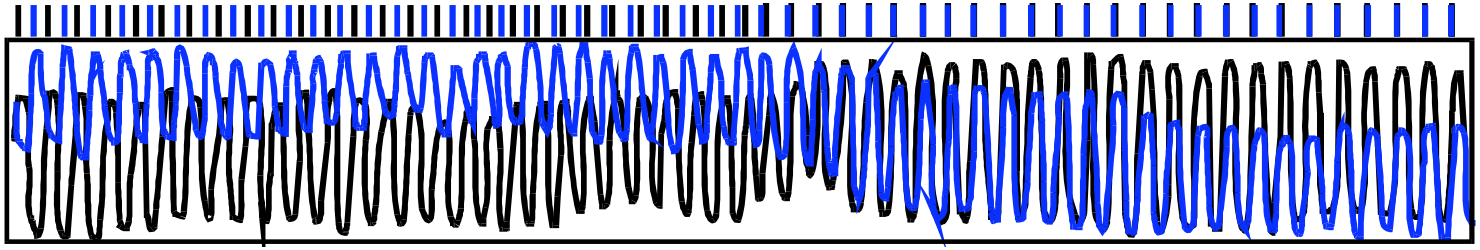

Position of Right Index Finger
Position of Left Index Finger

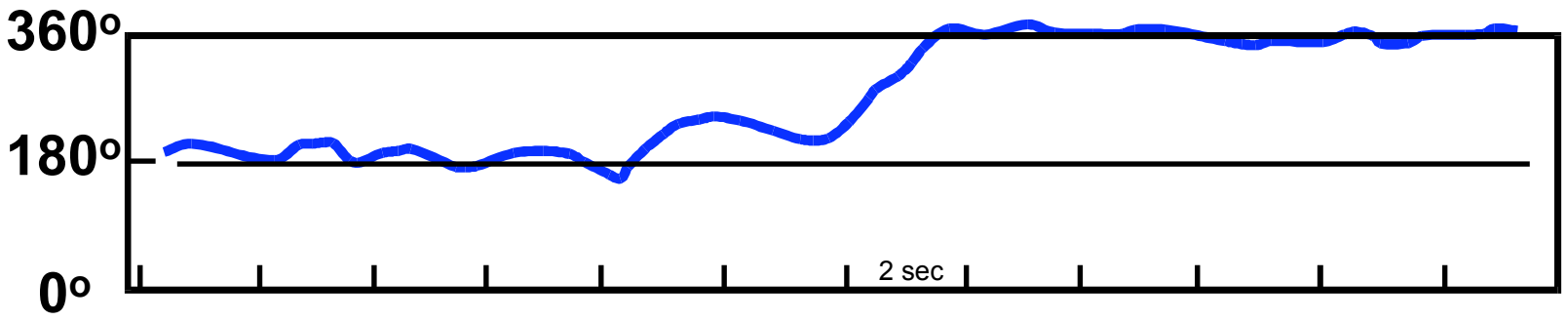

(after Liebovitch)

Phase Transition

Haken 1983 *Synergetics: An Introduction*
Springer-Verlag
Kelso 1995 *Dynamic Patterns* MIT Press

This bifurcation can be explained as a change in a potential energy function similar to the change which occurs in a physical phase transition.

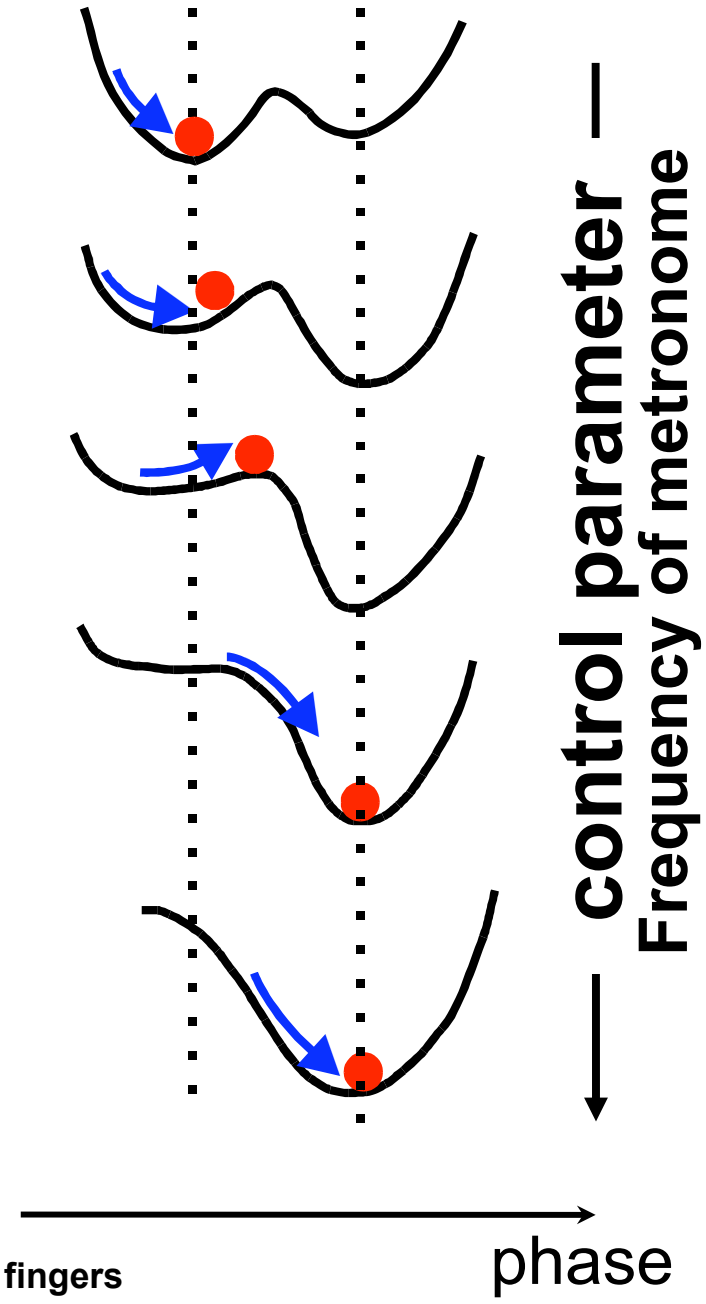

Order parameter: difference in phase between right and left fingers

(after Liebovitch)

$$s_i(t-1) = \mathrm{sign}\left(K \sum_{j \in N_i} s_j + \varepsilon_i \right)$$

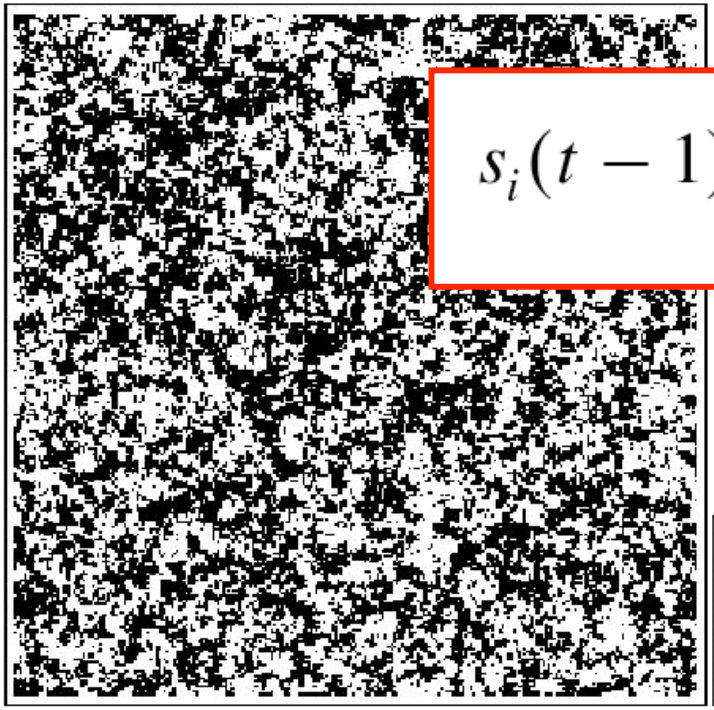

Disorder : K small

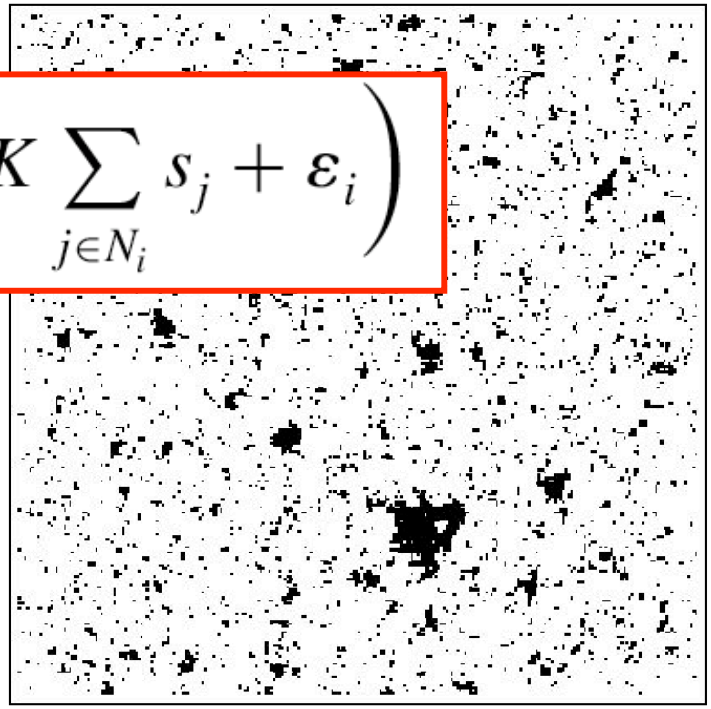

Order
K large

Renormalization group:
Organization of the description scale by scale

Critical:
K=critical value

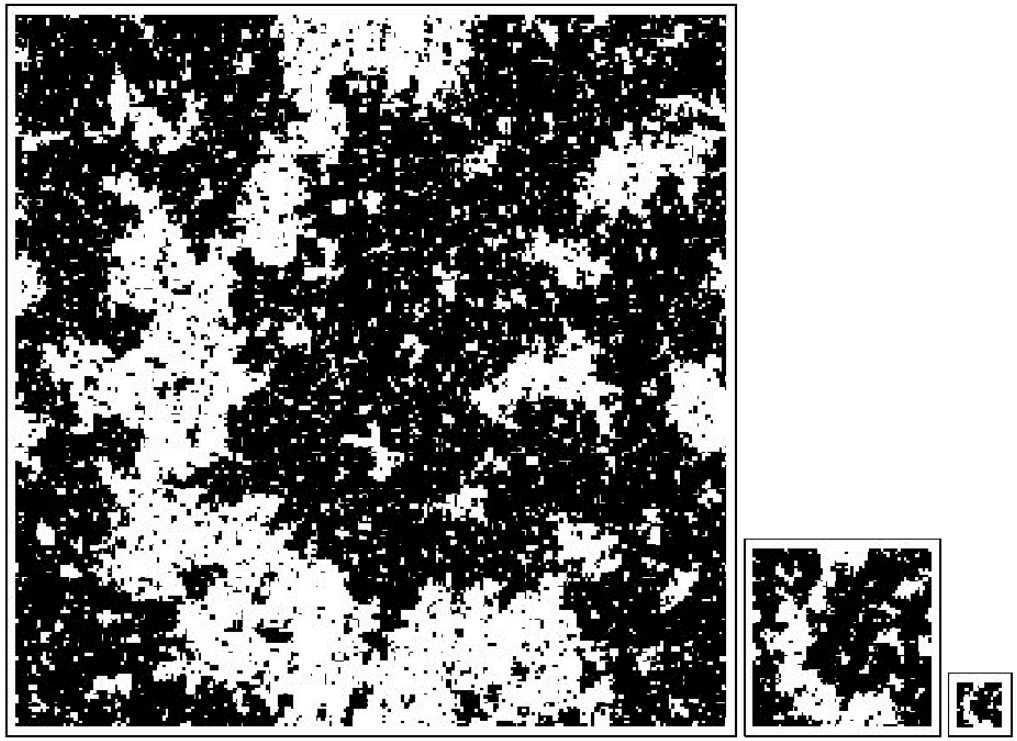

Tipping Pointedly Colder and Hotter

For much of Earth history, the climate has been considerably warmer than it is today. But 33.7 million years ago, at the Eocene-Oligocene boundary, the world became trapped in the glacial state that continues to this day.

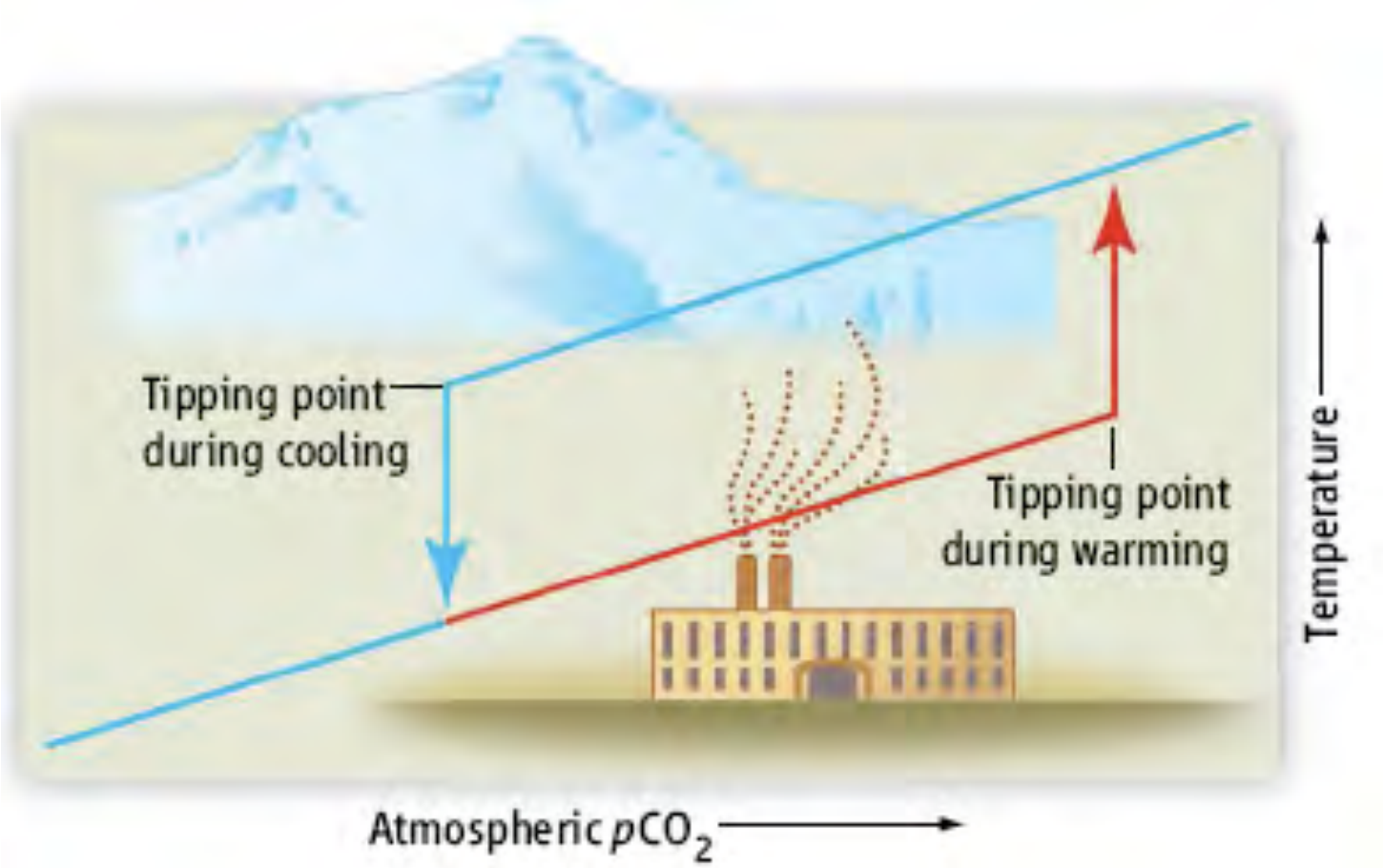

Data from multiple ocean basins elucidate an ancient climate transition from greenhouse to icehouse.

Lee R. Kump SCIENCE VOL 323 27 FEBRUARY 2009

SYNCHRONISATION AND COLLECTIVE EFFECTS IN EXTENDED STOCHASTIC SYSTEMS

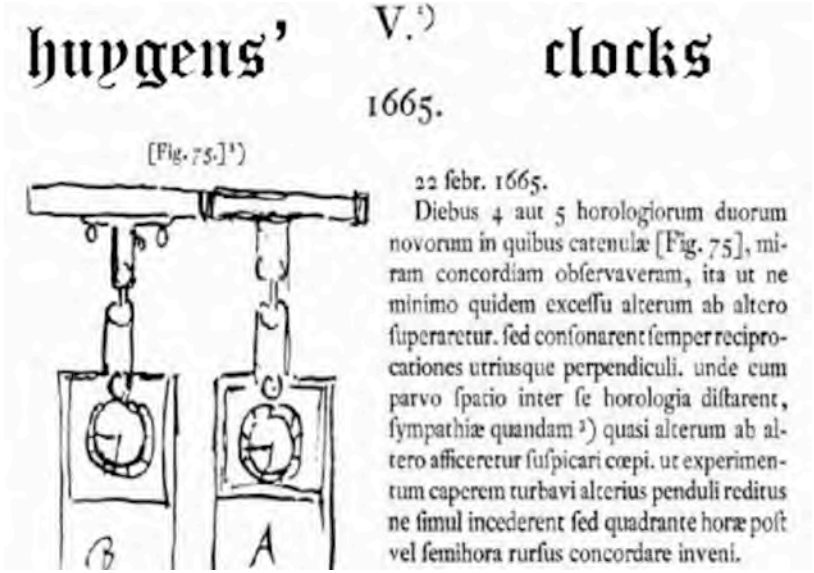

huygens' V.[5] clocks

1665.

[Fig. 75.][1])

22 febr. 1665.

Diebus 4 aut 5 horologiorum duorum novorum in quibus catenulæ [Fig. 75], miram concordiam obſervaveram, ita ut ne minimo quidem exceſſu alterum ab altero ſuperaretur. ſed conſonarent ſemper reciprocationes utriusque perpendiculi. unde cum parvo ſpatio inter ſe horologia diſtarent, ſympathiæ quandam [2]) quasi alterum ab altero afficeretur ſuſpicari cœpi. ut experimentum caperem turbavi alterius penduli reditus ne ſimul incederent ſed quadrante horæ poſt vel ſemihora rurſus concordare inveni.

Fireflies

Earthquake-fault model

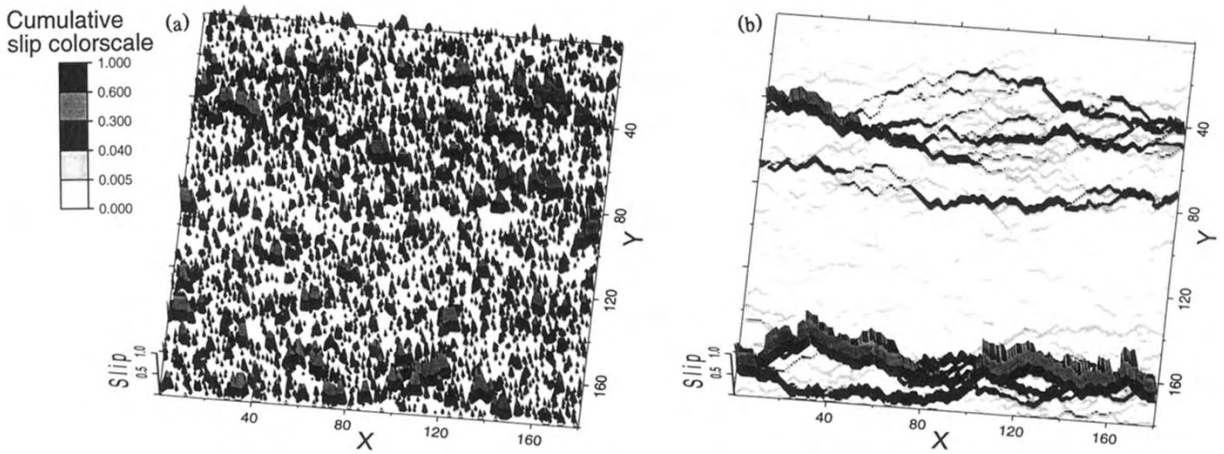

FIG. 1. Evolution of the cumulative earthquake slip, represented along the vertical axis in the white to black color code shown above the picture, at two different times: (a) early time and (b) long time, in a system of size $L=90$ by $L=90$, where $\Delta\sigma=1.9$ and $\beta=0.1$.

Miltenberger et al. (1993)

Generic phase diagram

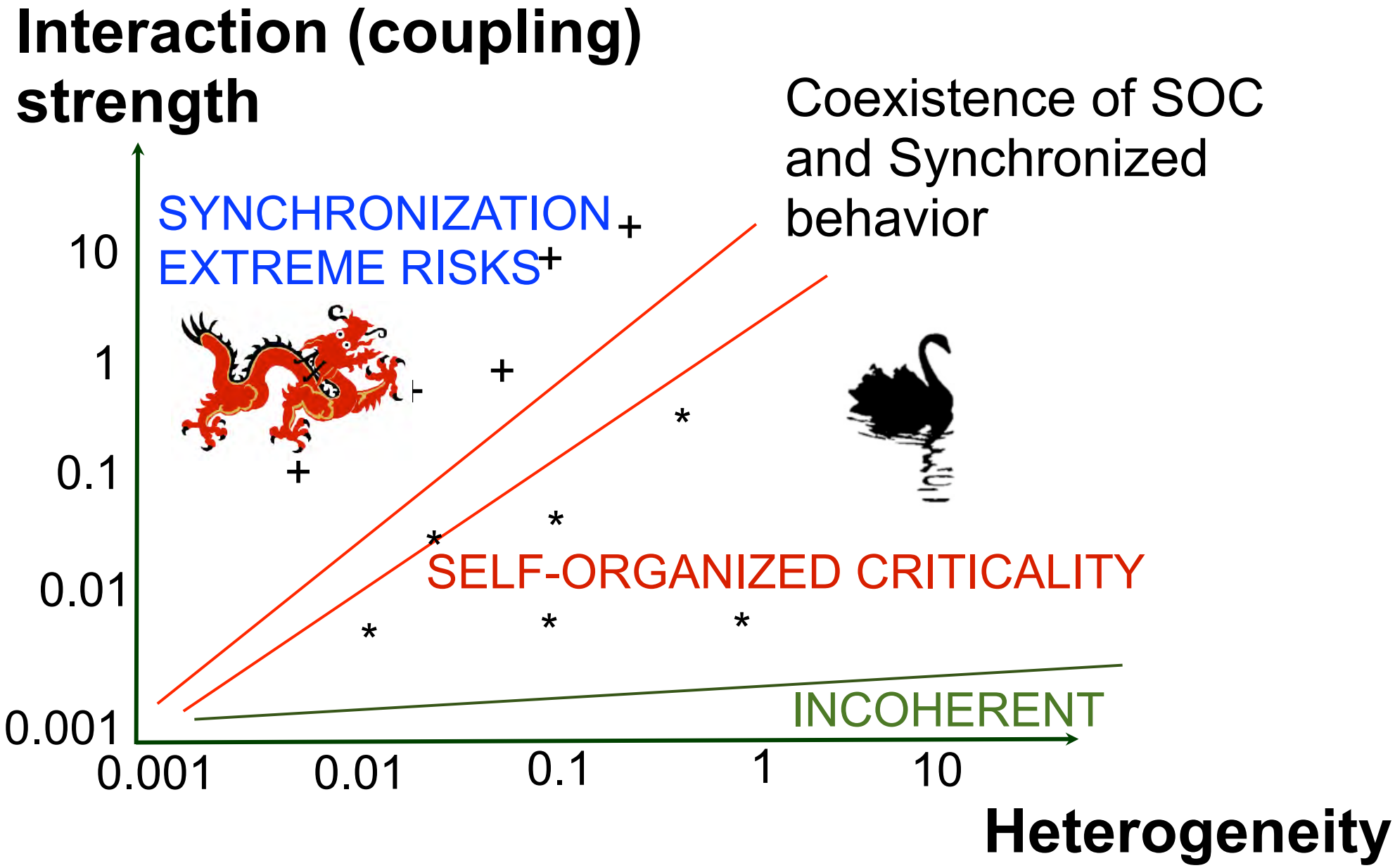

Landau-Ginzburg Theory of Self-Organized Criticality

Dynamics of an order parameter (OP) and of the corresponding *control* parameter (CP): within the sandpile picture, $\frac{\partial h}{\partial x}$ is the slope of the sandpile, h being the local height, and S is the state variable distinguishing between static grains ($S = 0$) and rolling grains ($S \neq 0$).

L. Gil and D. Sornette "Landau-Ginzburg theory of self-organized criticality", Phys. Rev.Lett. 76, 3991-3994 (1996)

Normal form of sub-critical bifurcation

$$\frac{\partial S}{\partial t} = \chi \left\{ \mu S + 2\beta S^3 - S^5 \right\} \qquad (1)$$

where

$$\mu = \left[\left(\frac{\partial h}{\partial x} \right)^2 - \left(\frac{\partial h}{\partial x}|_c \right)^2 \right] \qquad (2)$$

and $\beta > 0$ (subcritical condition).

$$F\left(S, \frac{\partial h}{\partial x} \right) = -\alpha \frac{\partial h}{\partial x} S^2, \qquad \alpha > 0$$

Diffusion equation

$$\frac{\partial h}{\partial t} = -\frac{\partial F\left(S, \frac{\partial h}{\partial x}\right)}{\partial x} + \Phi \qquad (3)$$

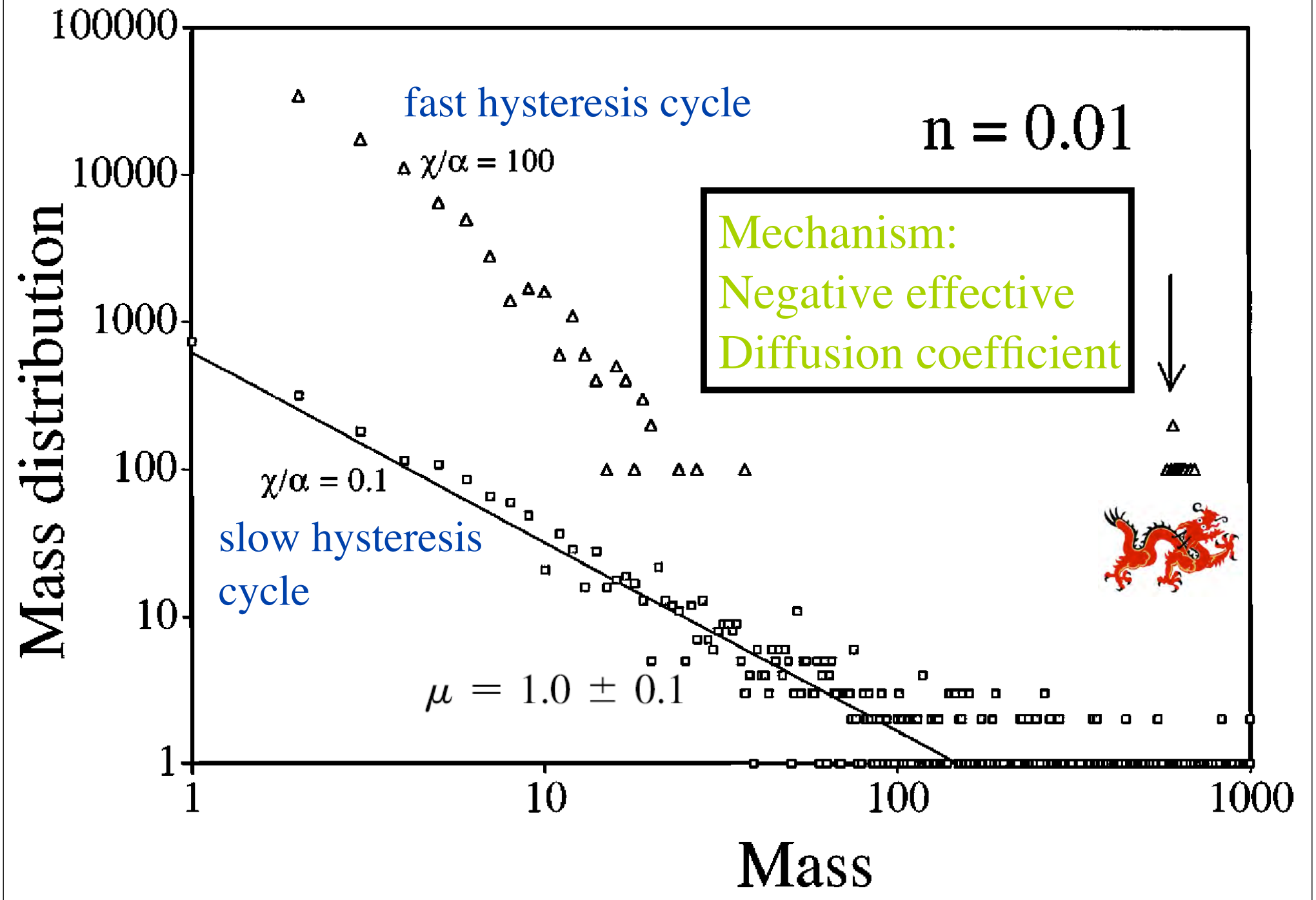

System sizes range from $L/a = 64$ to 2048.

$$P(M)dM \simeq M^{-(1+\mu)}dM,$$

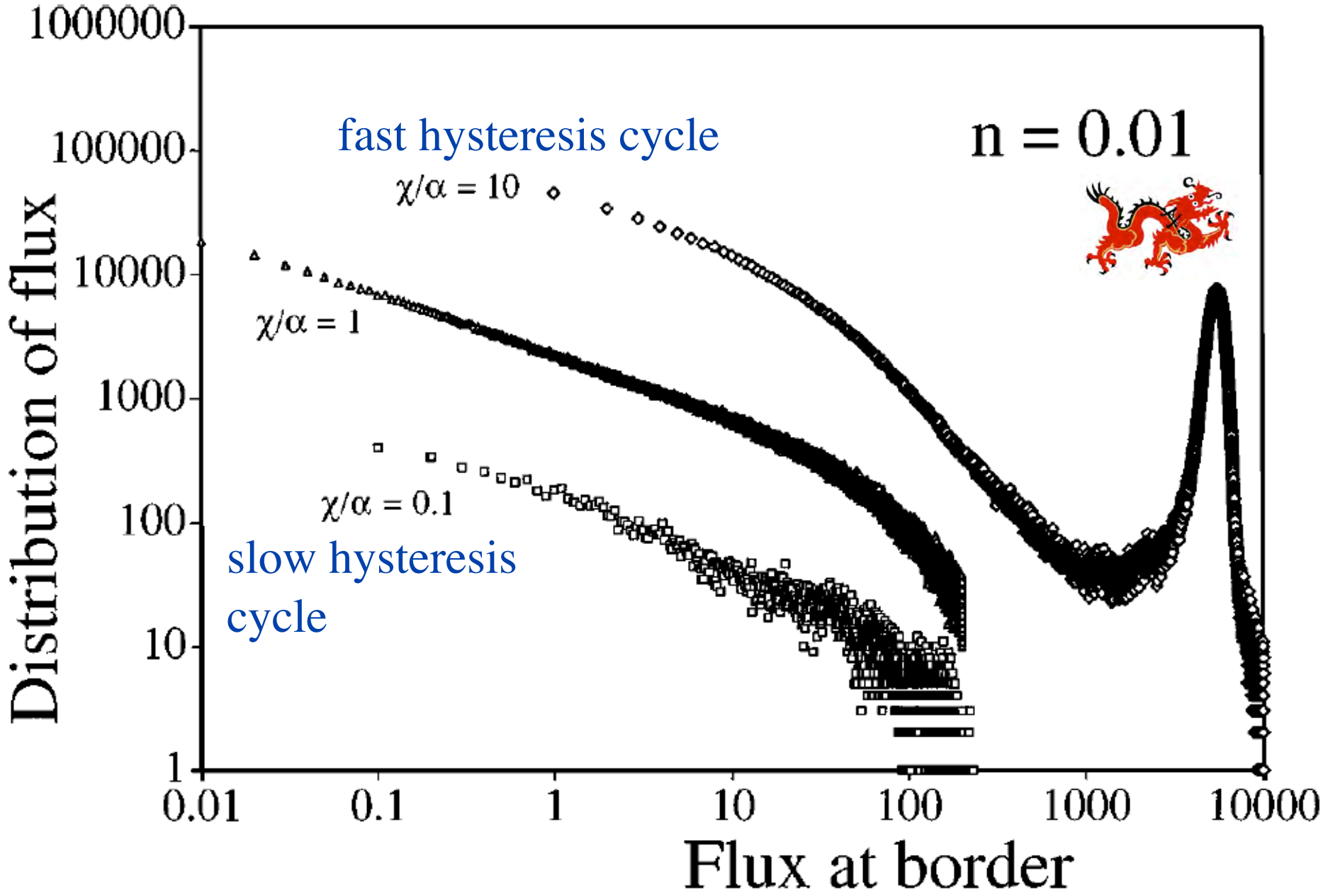

FIG. 3. Distribution $P(J)$ of flux amplitudes at the right border, in the same conditions as for Fig. 1.

Generic phase diagram => pdf (I)

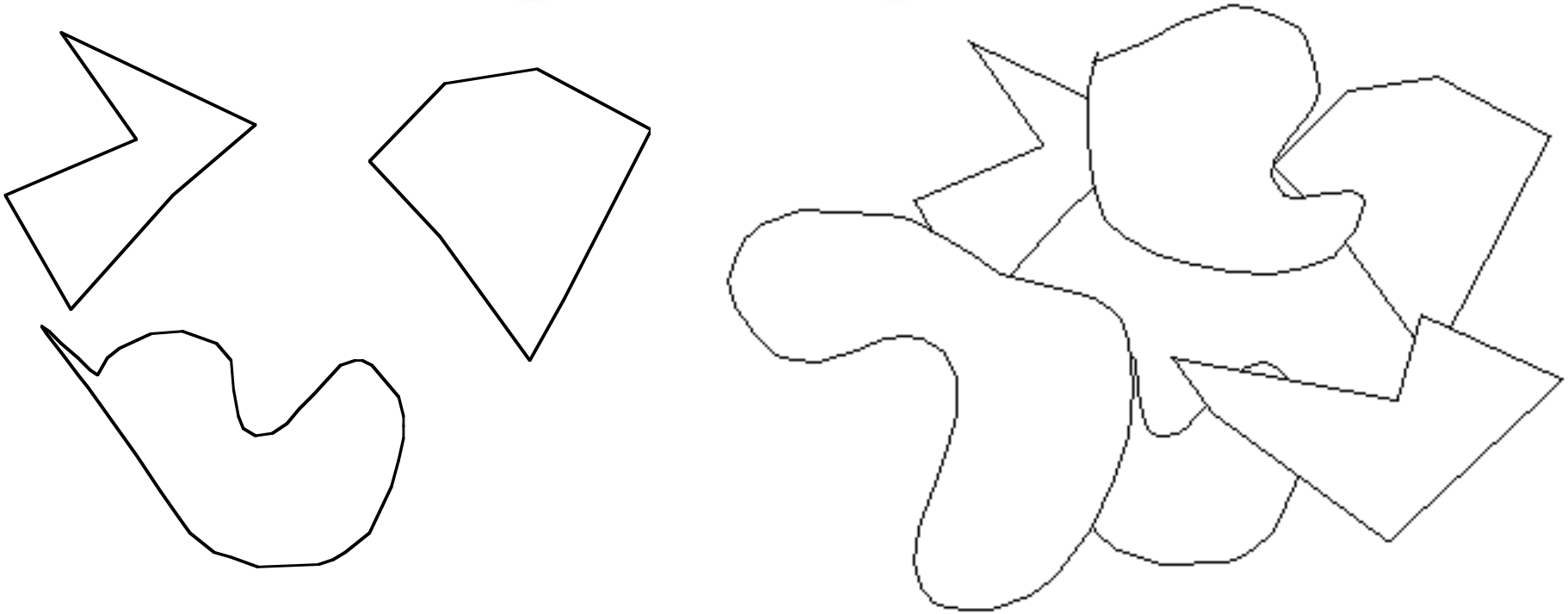

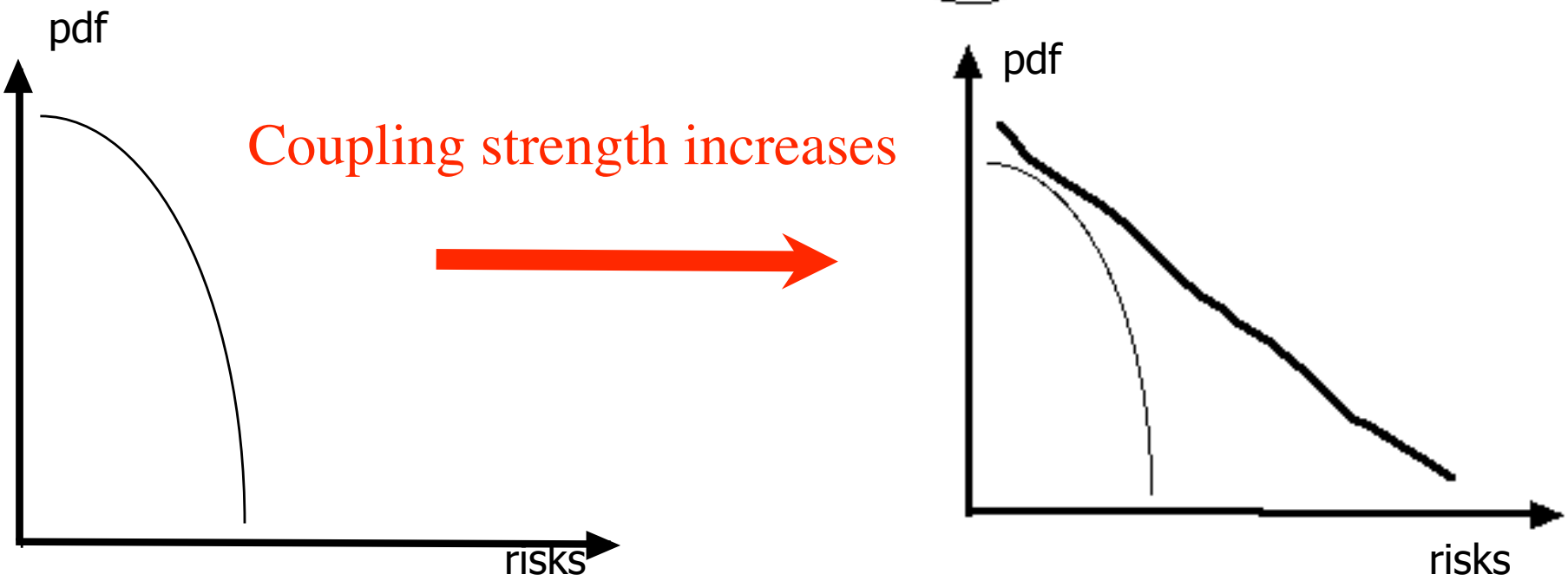

Generic phase diagram => pdf (II)

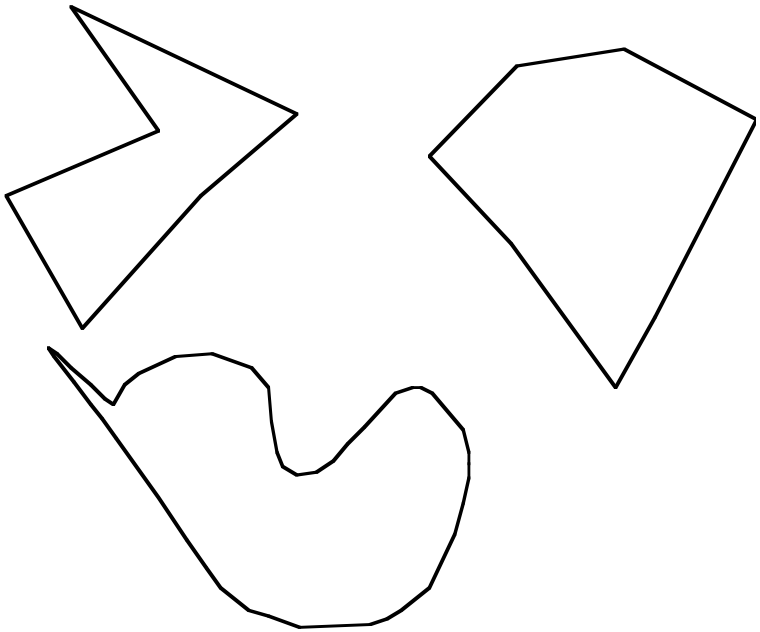

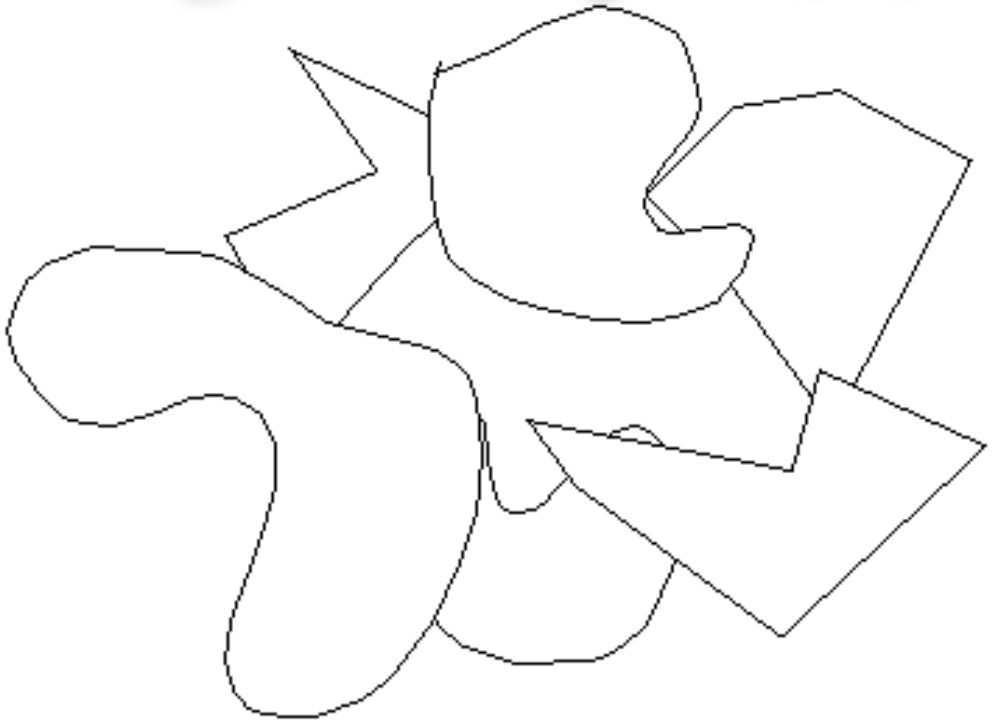

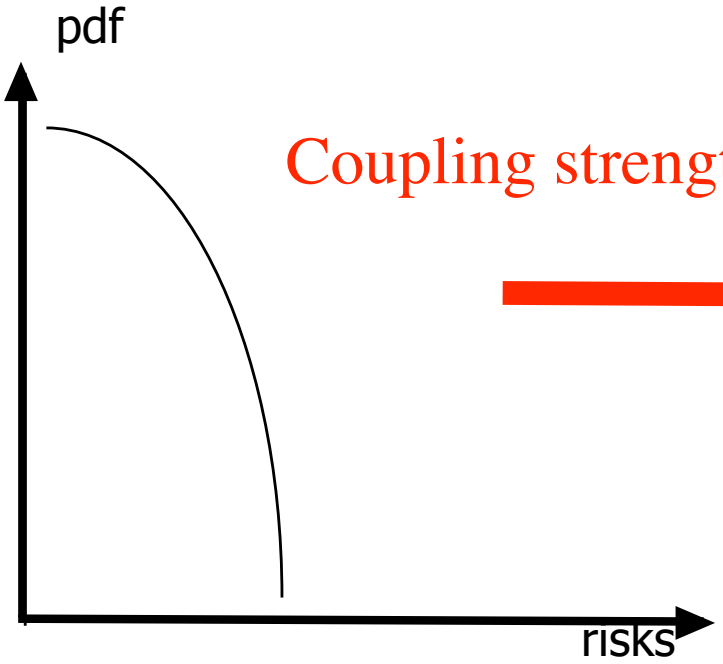

Coupling strength increases

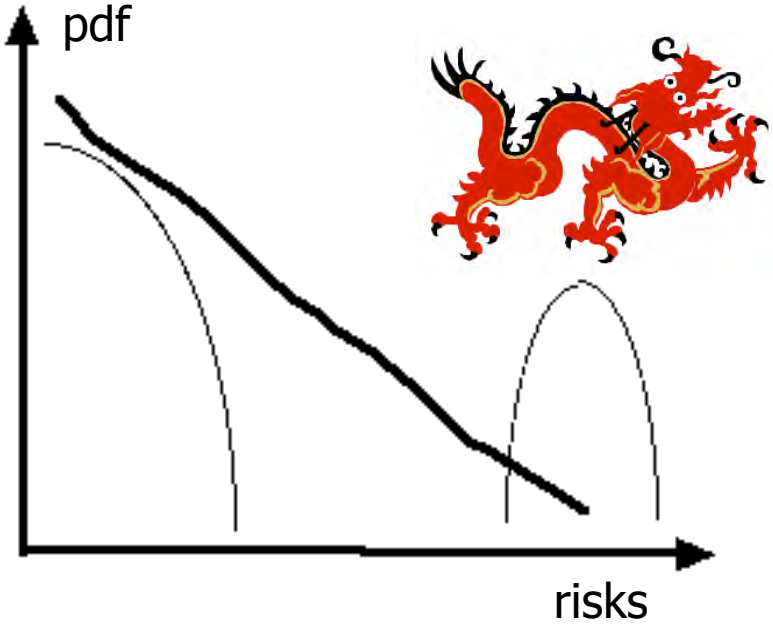

Illustration: THE GREAT MODERATION

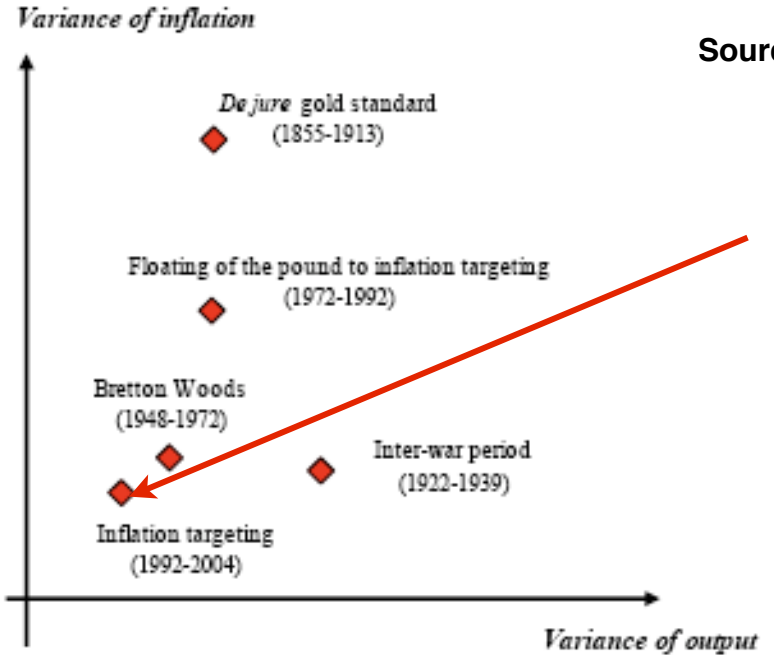

Source: SIR JOHN GIEVE, Deputy Governor, Bank of England, Feb 2009

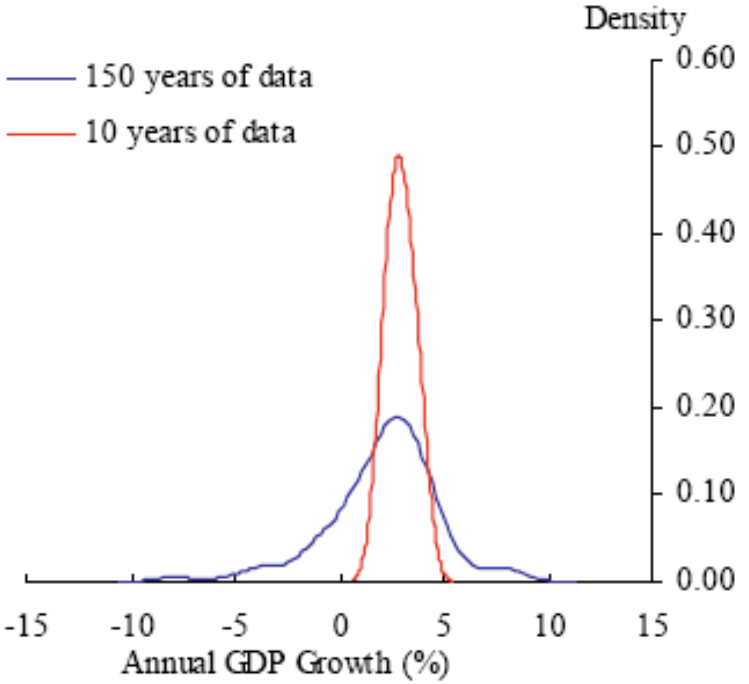

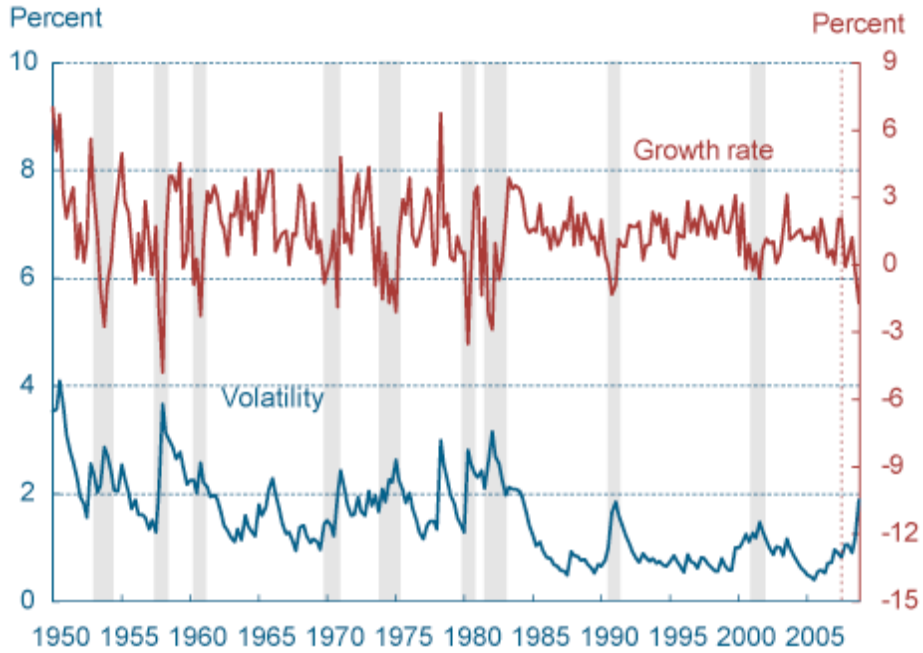

Notes: Shaded bars indicate recessions. The dashed red line indicates the onset of the current recession. Volatility is computed using deviations of the GDP growth rate from a constant mean and a GARCH (1,1) with a 0.729 first-order serial correlation.
Sources: Bureau of Economic Analysis; authors' calculations.

http://www.clevelandfed.org/research/trends/2009/0309/03ecoact.cfm

Illustration: The 2007-???? crisis

Illustration: The 2007-???? crisis

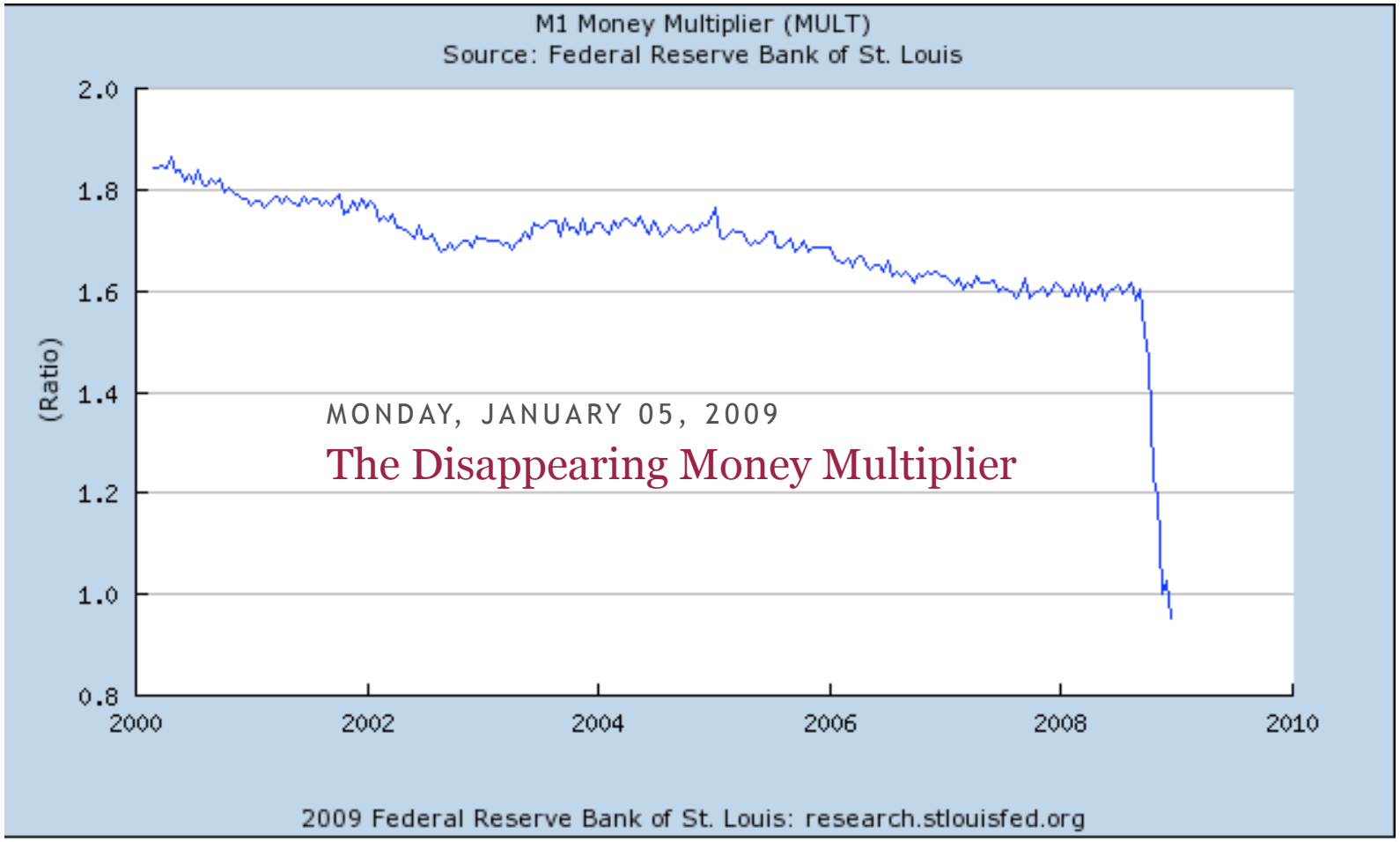

Econ prof Bill Seyfried of Rollins College:
The M1 money multiplier just slipped below 1. So each $1 increase in reserves (monetary base) results in the money supply increasing by $0.95 (OK, so banks have substantially increased their holding of excess reserves while the M1 money supply hasn't changed by much).

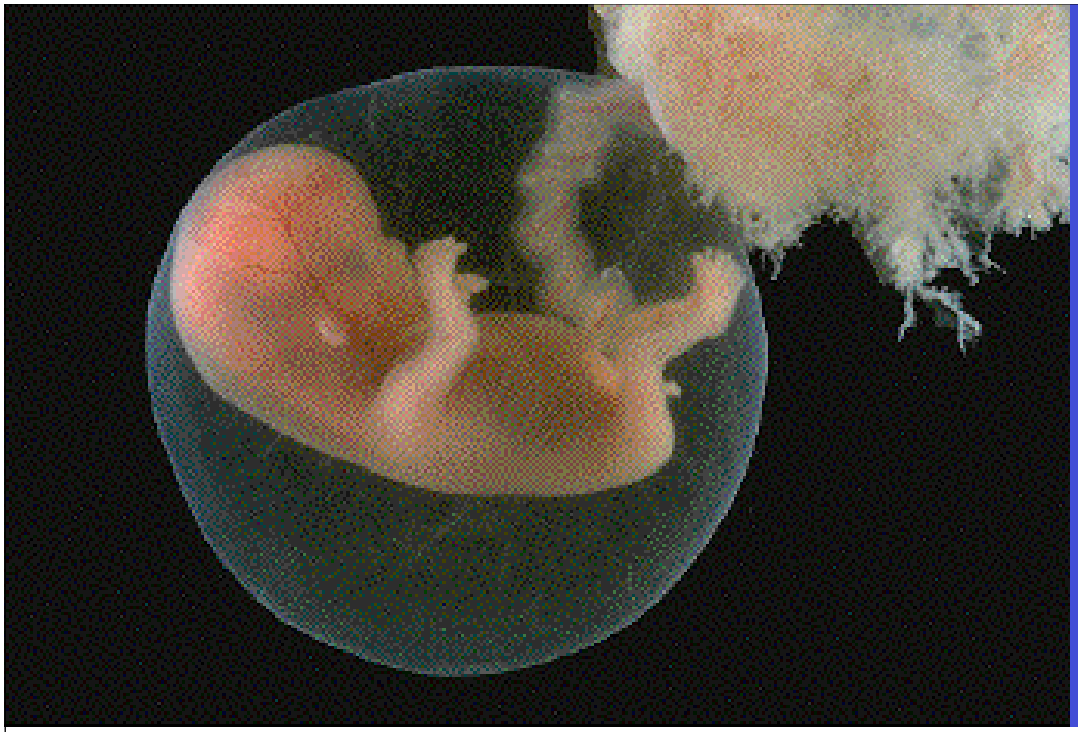

Who initiates parturition?

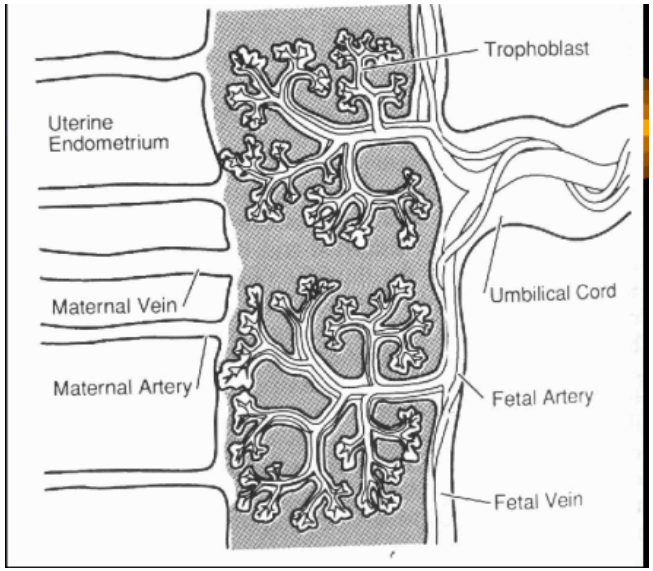

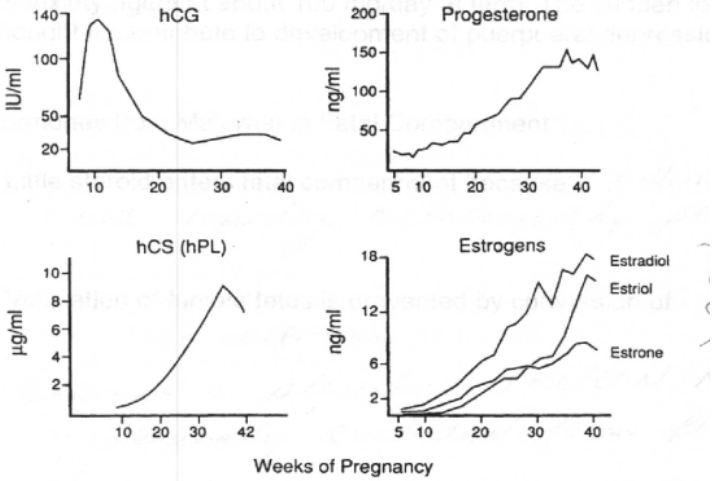

Figure 47-6. Changes in plasma levels of pregnancy hormones.

Generic Critical Precursors to a Bifurcation

Braxton hicks contractions

(Simple example of Catastrophe theory)

-Amplitude of fluctuations

-Response to external forcing

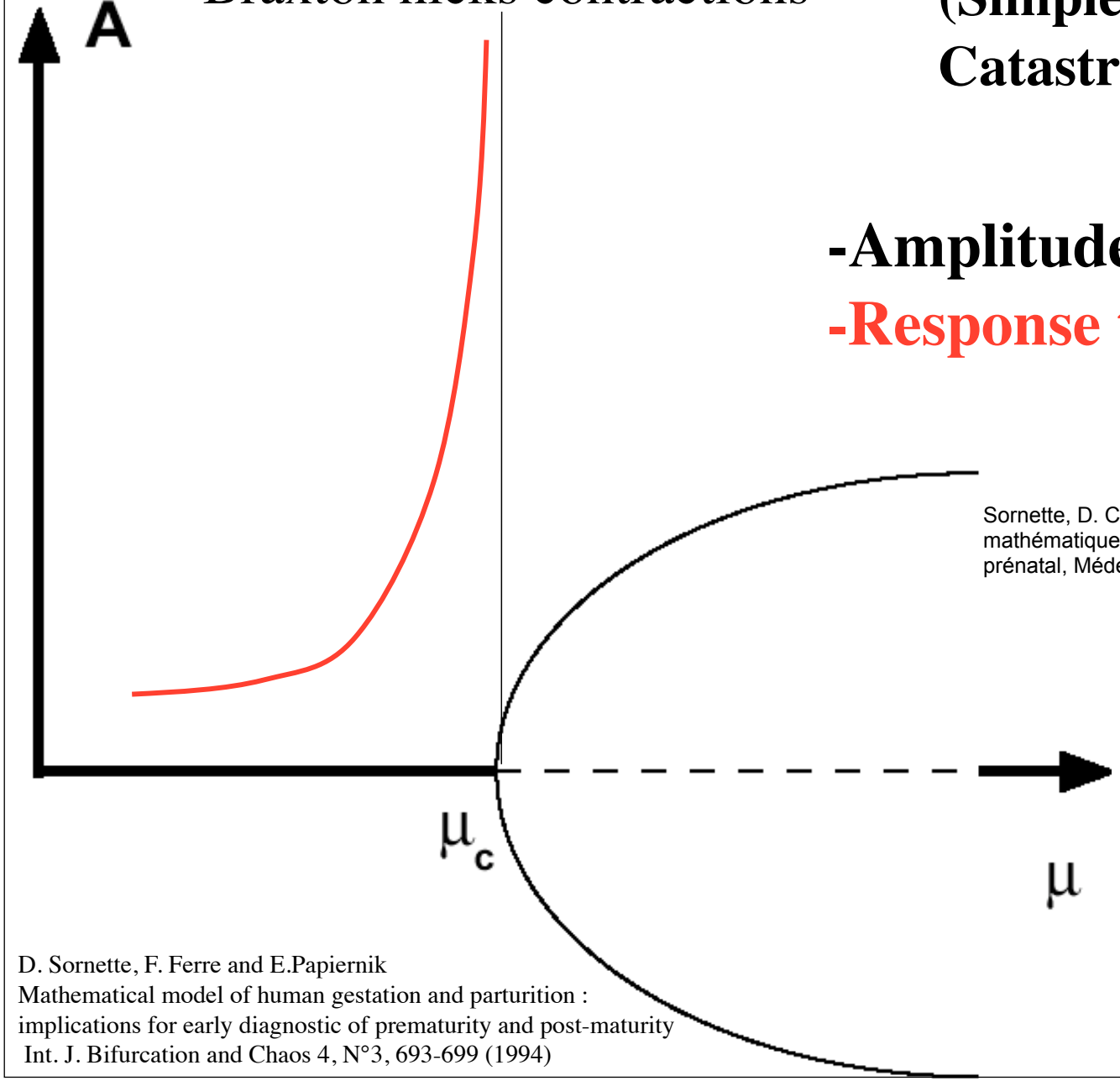

Sornette, D. Carbone, F.Ferre, C. Vauge and E.Papiernik, Modèle mathématique de la parturition humaine : implications pour le diagnostic prénatal, Médecine/Science 11, n°8, 1150-1153 (1995)

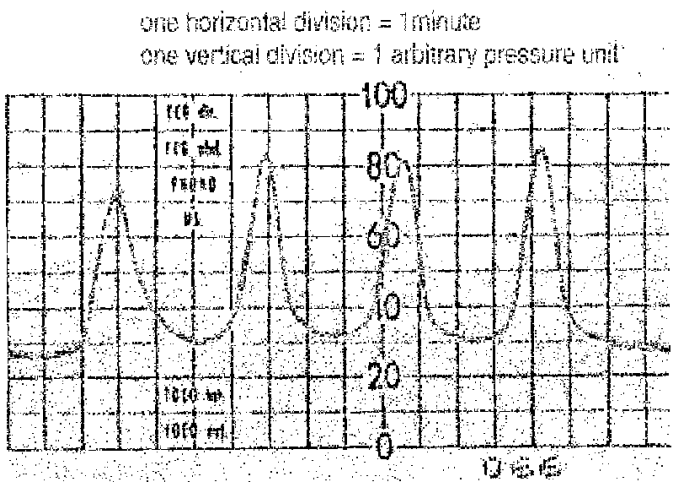

D. Sornette, F. Ferre and E.Papiernik
Mathematical model of human gestation and parturition : implications for early diagnostic of prematurity and post-maturity
Int. J. Bifurcation and Chaos 4, N°3, 693-699 (1994)

Critical Precursory Fluctuations

$$\frac{\mathrm{d}A}{\mathrm{d}t} = (\mu - \mu_\mathrm{c})A - \frac{A^3}{A_\mathrm{s}^2} + f(t)$$

Without NL term:

$$A(t) = \int_0^t \mathrm{e}^{-\delta(t-\tau)} f(\tau)\ \mathrm{d}\tau$$

$$\delta = \mu_c - \mu$$

$$\langle [A(t)]^2 \rangle = \int_0^t \mathrm{d}\tau \int_0^t \mathrm{d}\tau'\, \mathrm{e}^{-\delta(t-\tau)} \mathrm{e}^{-\delta(t-\tau')} \langle f(\tau) f(\tau') \rangle$$

$$= D \int_0^t \mathrm{e}^{-2\delta(t-\tau)}\ \mathrm{d}\tau \qquad \rightarrow$$

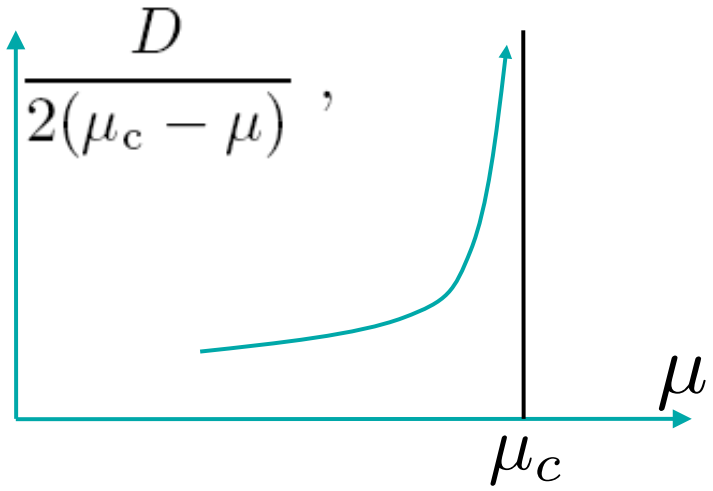

Strategy: look at the forest rather than at the tree

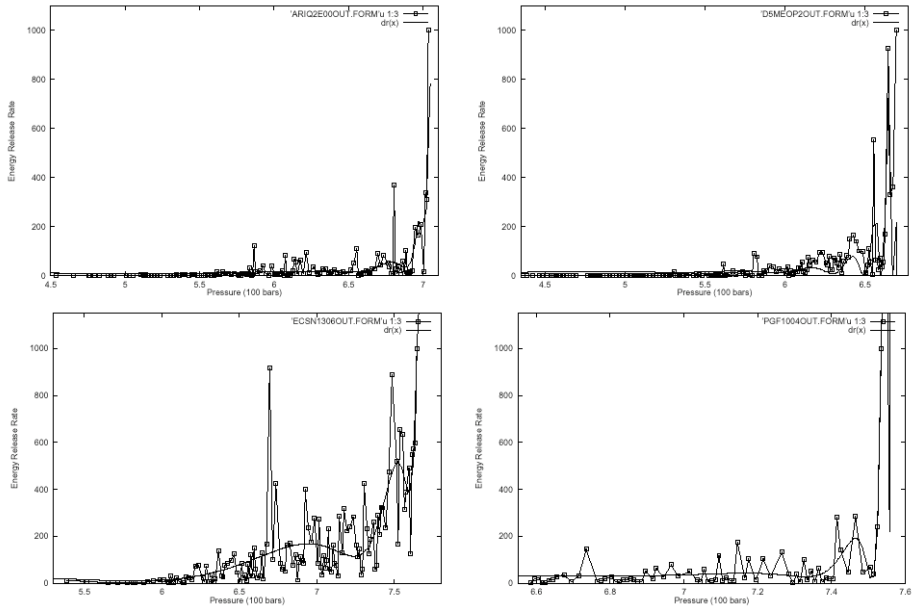

Our prediction system is now used in the industrial phase as the standard testing procedure.

EADS LAUNCH VEHICLES

J.-C. Anifrani, C. Le Floc'h, D. Sornette and B. Souillard
"Universal Log-periodic correction to renormalization group scaling for rupture stress prediction from acoustic emissions", J.Phys.I France 5, n°6, 631-638 (1995)

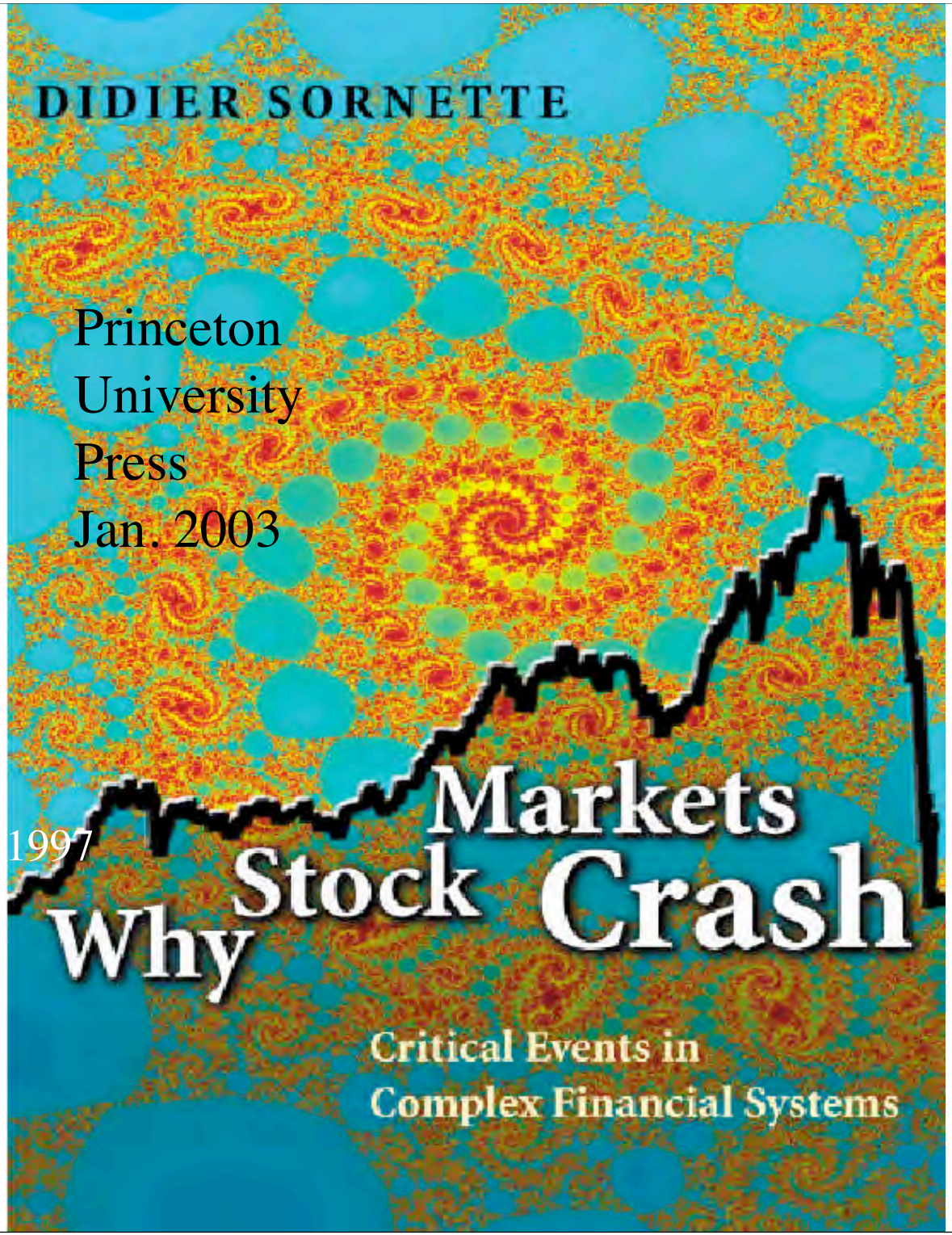
DIDIER SORNETTE
Princeton
University
Press
Jan. 2003
1997
Why Stock Markets Crash
Critical Events in
Complex Financial Systems

Various Bubbles and Crashes

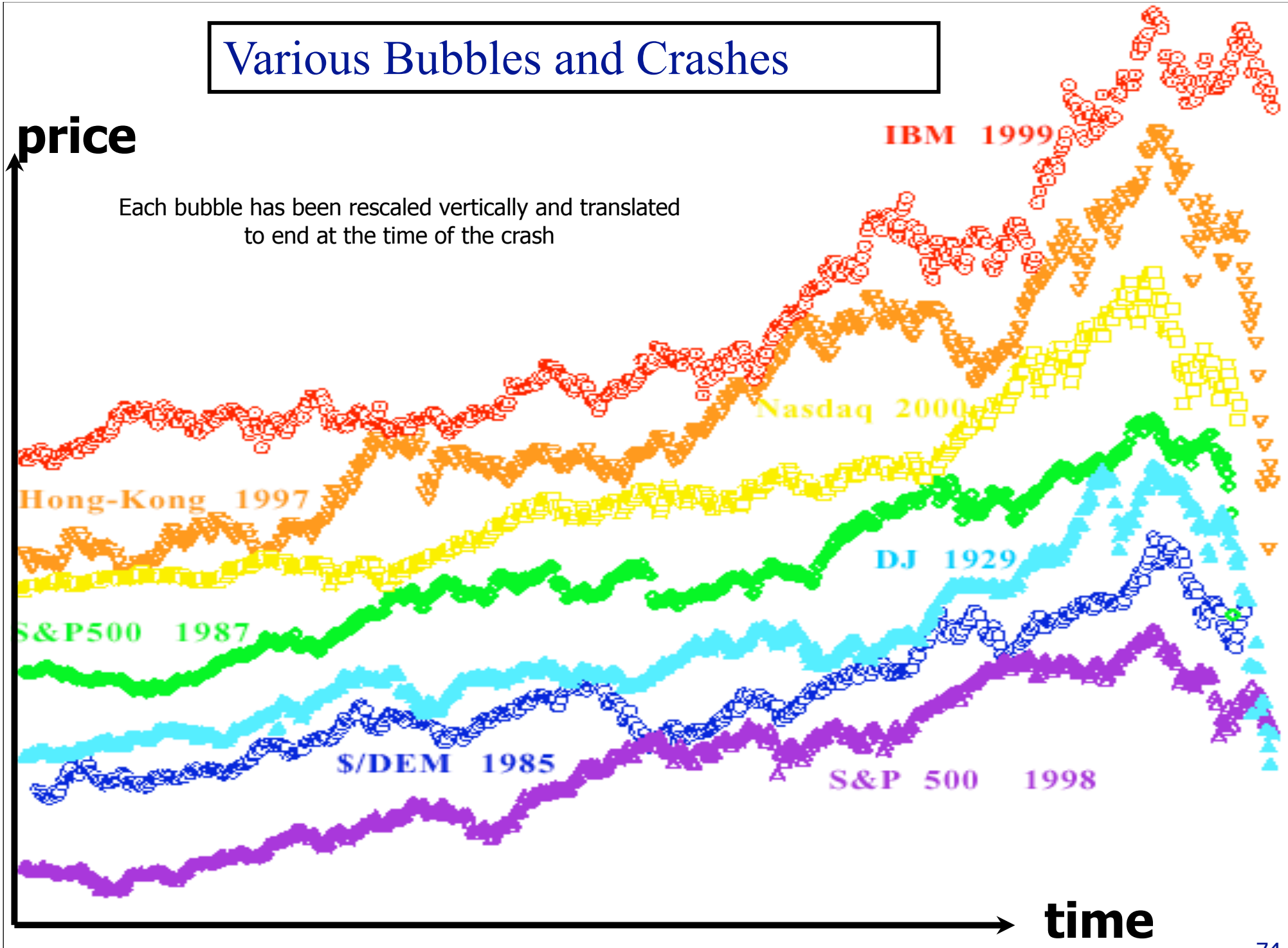

Real-estate in the UK

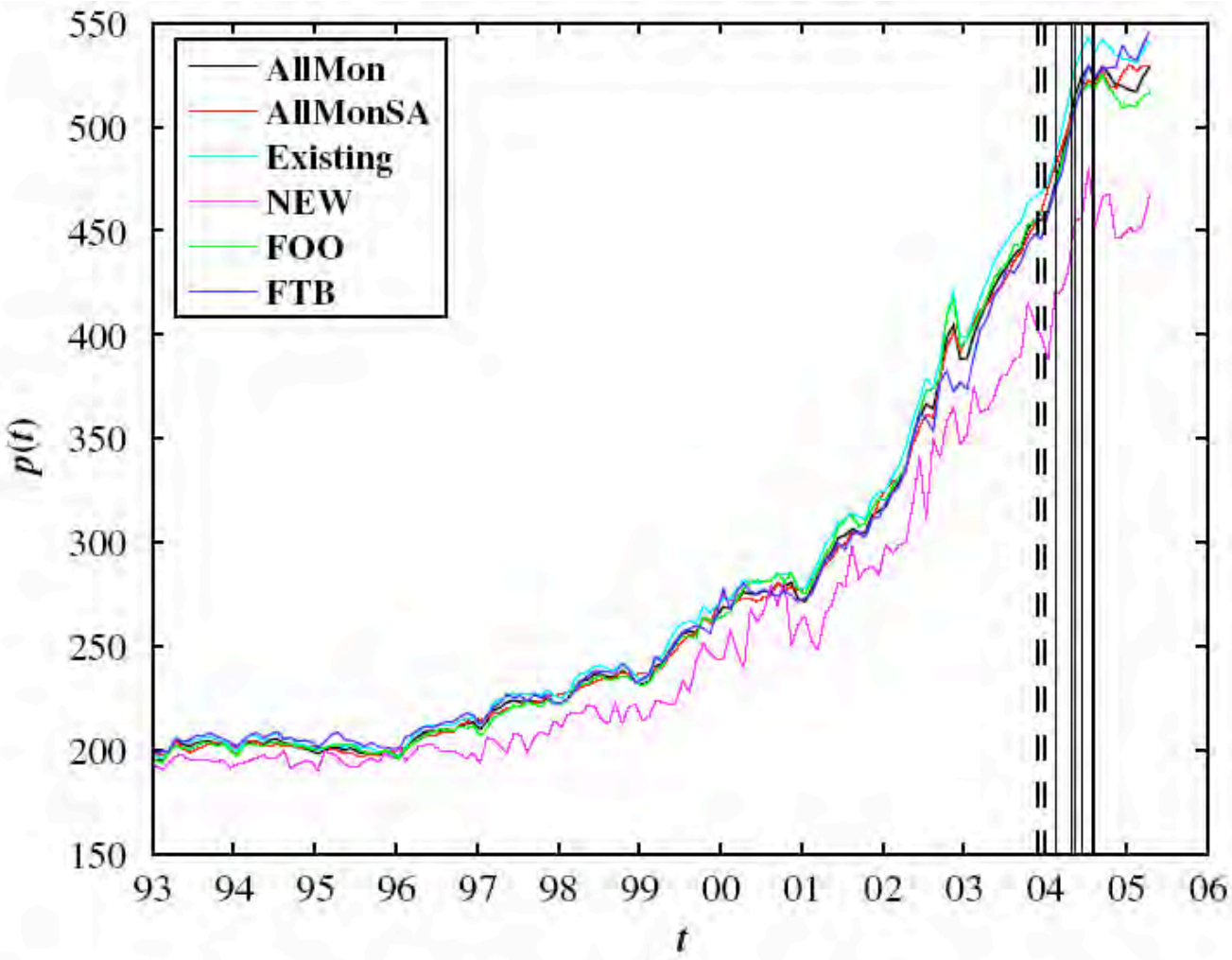

Fig. 1. (Color online) Plot of the UK Halifax house price indices from 1993 to April 2005 (the latest available quote at the time of writing). The two groups of vertical lines correspond to the two predicted turning points reported in Tables 2 and 3 of [1]: end of 2003 and mid-2004. The former (resp. later) was based on the use of formula (2) (resp. (3)). These predictions were performed in February 2003.

W.-X. Zhou, D. Sornette, 2000–2003 real estate bubble in the UK but not in the USA, Physica A 329 (2003) 249–263.

Real-estate in the USA

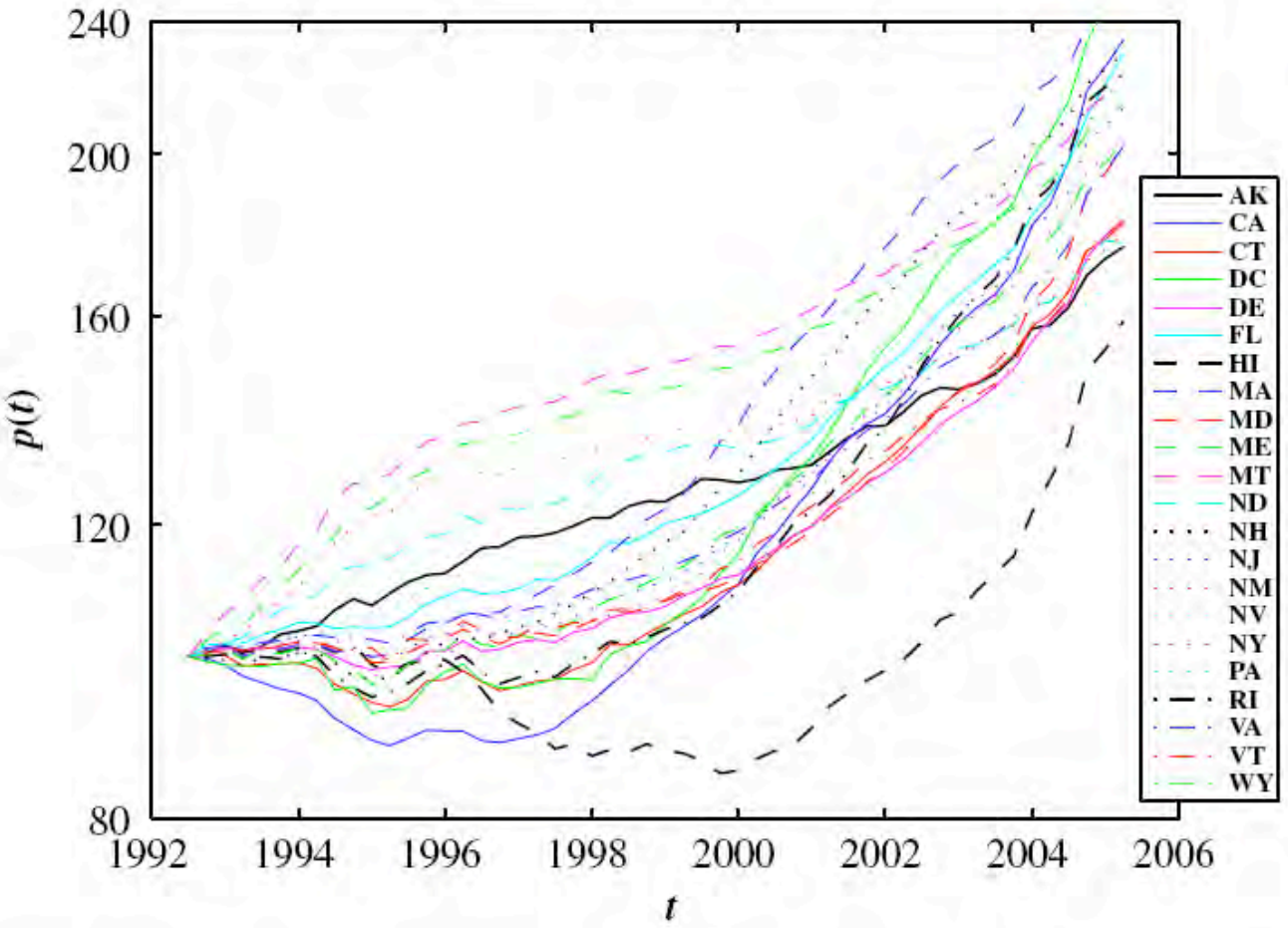

Fig. 5. (Color online) Quarterly average HPI in the 21 states and in the District of Columbia (DC) exhibiting a clear upward faster-than-exponential growth. For better representation, we have normalized the house price indices for the second quarter of 1992 to 100 in all 22 cases. The corresponding states are given in the legend.

W.-X. Zhou, D. Sornette / Physica A 361 (2006) 297–308

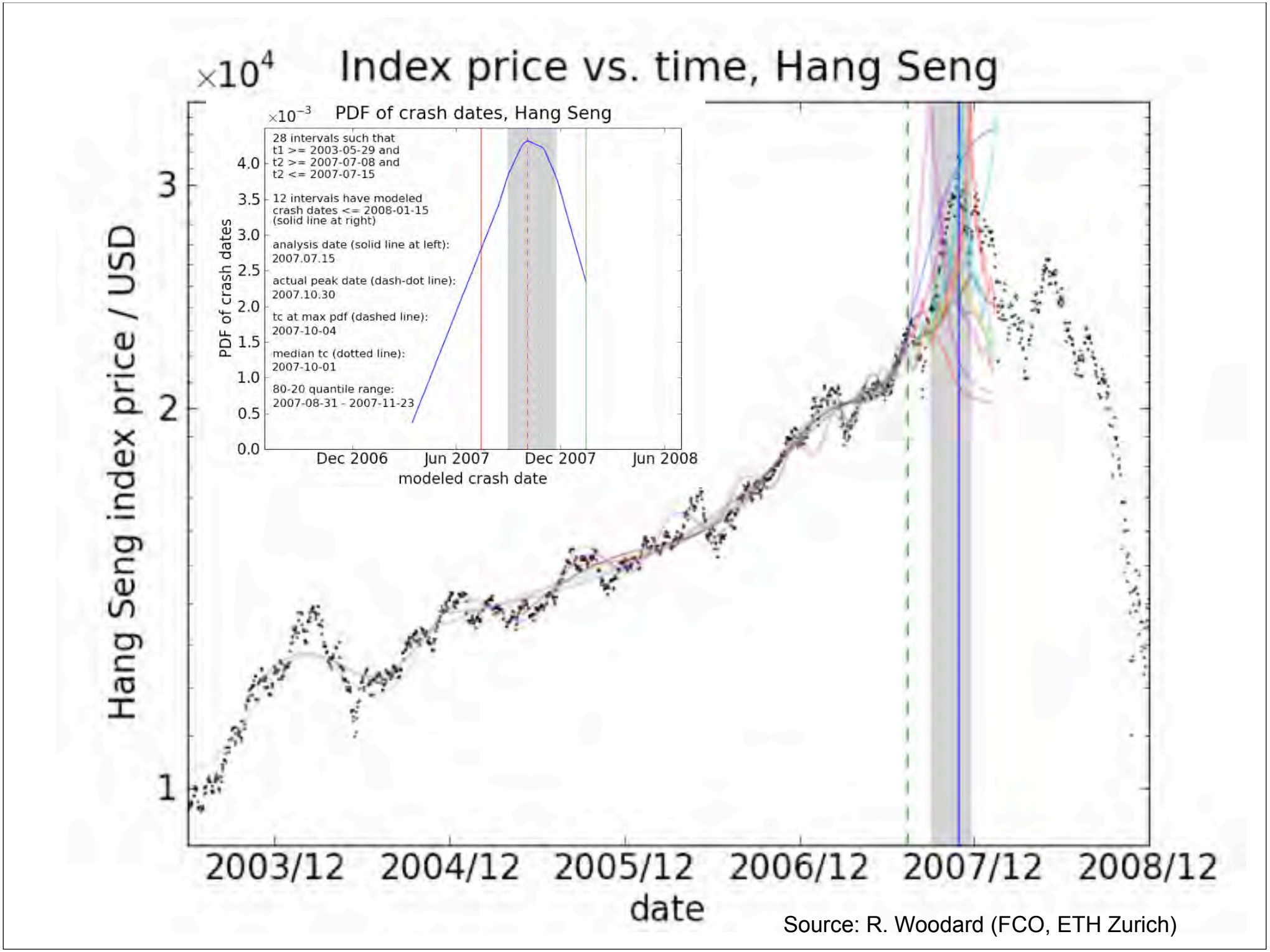

Source: R. Woodard (FCO, ETH Zurich)

2006-2008 Oil bubble

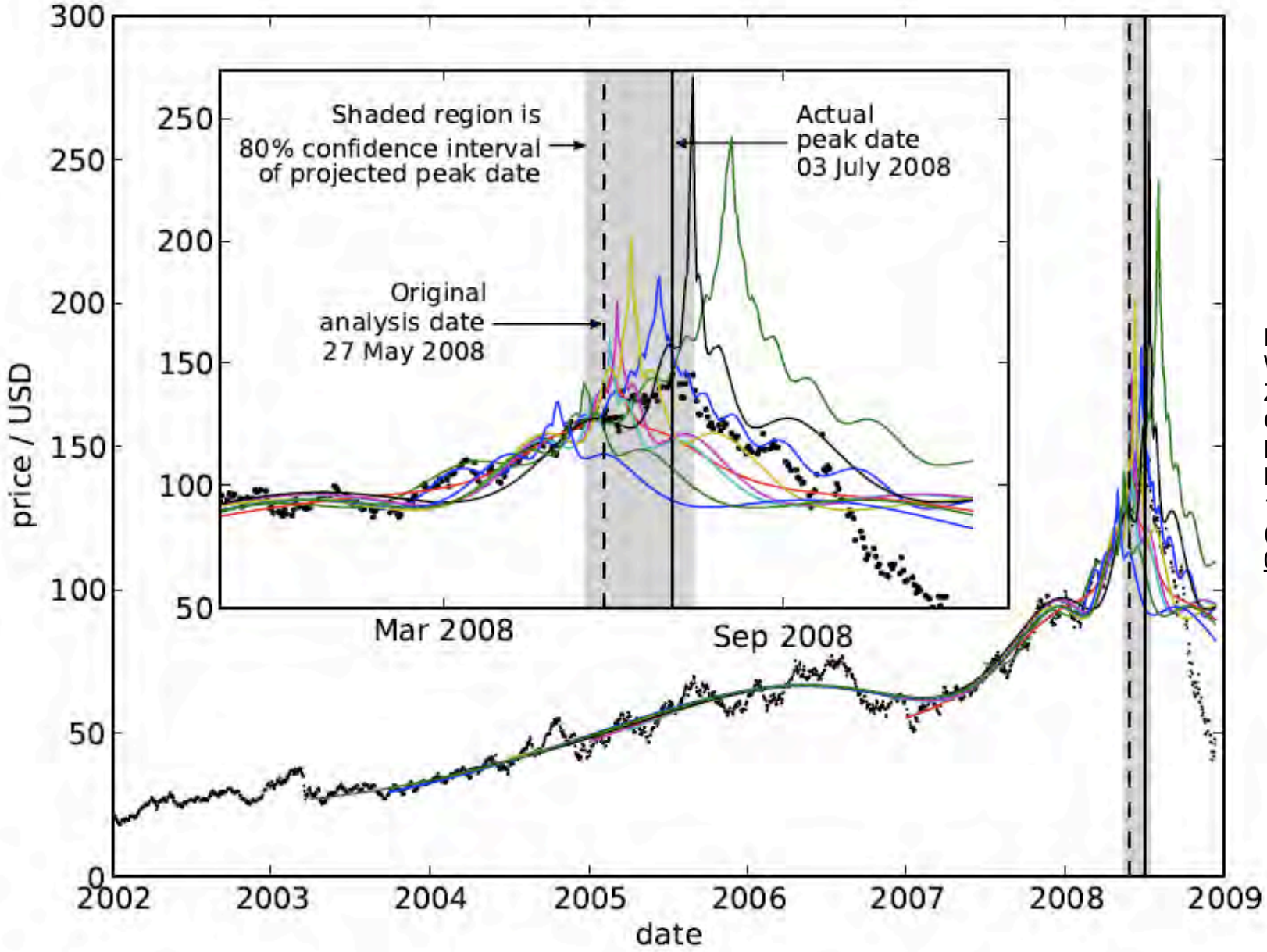

D. Sornette, R. Woodard and W.-X. Zhou, The 2006-2008 Oil Bubble and Beyond, Physica A 388, 1571-1576 (2009) (arXiv.org/abs/0806.1170)

Typical result of the calibration of the simple LPPL model to the oil price in US$ in shrinking windows with starting dates t_{start} moving up towards the common last date t_{last} = May 27, 2008.

Slowing down as an early warning signal for abrupt climate change

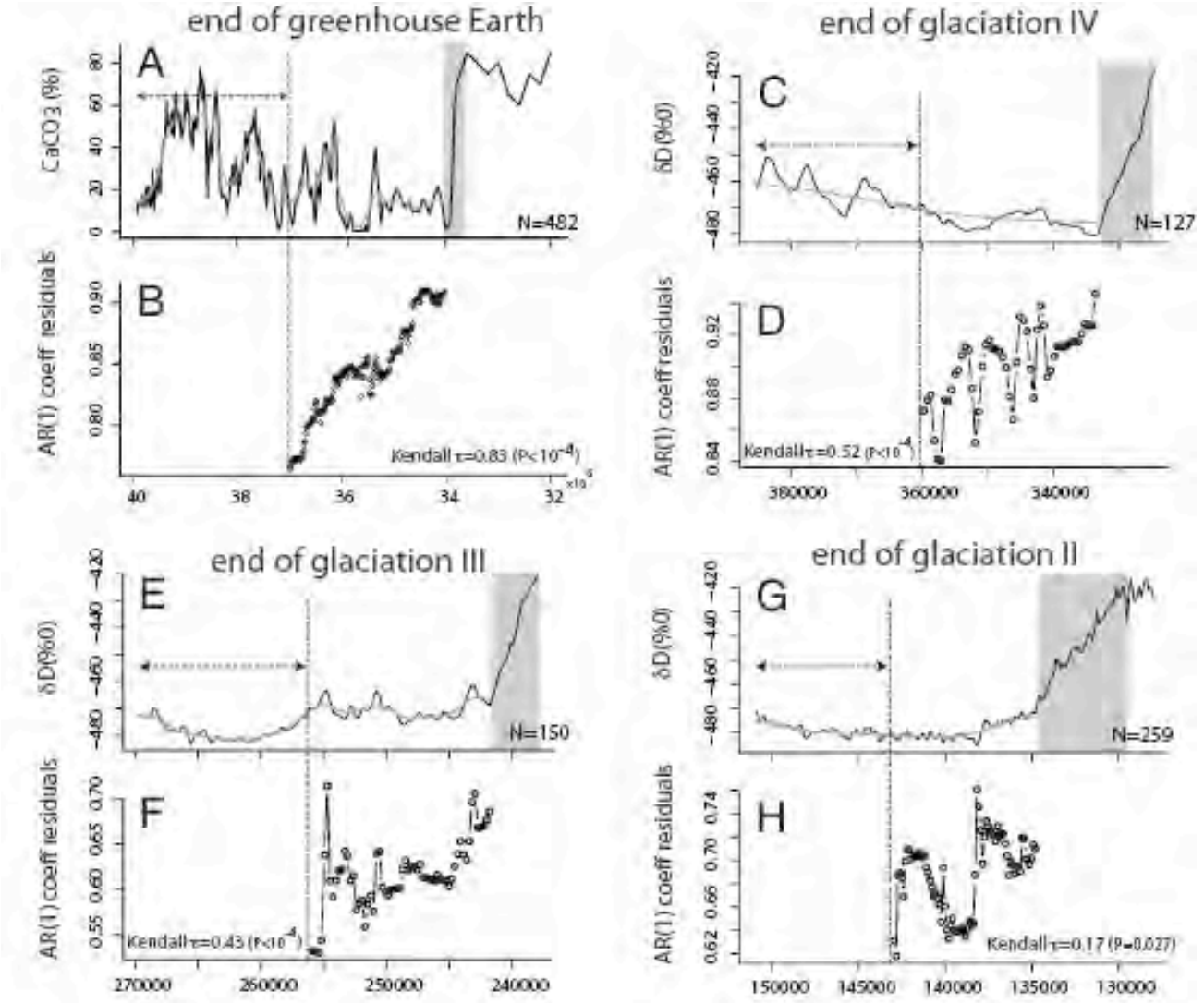

V. Dakos, M. Scheffer, E.H. van Nes, V. Brovkin, V. Petoukhov‡, and H. Held, Slowing down as an early warning signal for abrupt climate change, PNAS 105 (38), 14308-14312

Eight reconstructed time series of abrupt climate shifts in the past. (*A*) The end of the greenhouse Earth, (*M*) the end of the Younger Dryas, (*K*) the Bølling-Allero¨dtransition, (*O*) the desertification of North Africa, (*I*) theendof the last glaciation,and(*G*,*E*,and*F*) the ends of earlier glaciations. In all cases the dynamics of the system slow down before the transition, as revealed by an increasing trend in autocorrelation (*B*,*D*, *F*,*H*, *J*, *L*,*N*, and *P*). The gray bands identify transition phases. The arrows mark the width of the moving window used to compute slowness. The smooth gray line through the time series is the Gaussian kernel function used to filter out slow trends. Data in *A* come from tropical Pacific sediment core records, data in*M*are from the Cariaco basin sediment, data in *K* come from the Greenland GISP2 ice core, data in *O* from the sediment core ODP Hole 658C off the west coast of Africa, and data presented in *C*, *E*, *G*, and *I* are from the Antarctica Vostok ice core.

Slowing down as an early warning signal for abrupt climate change

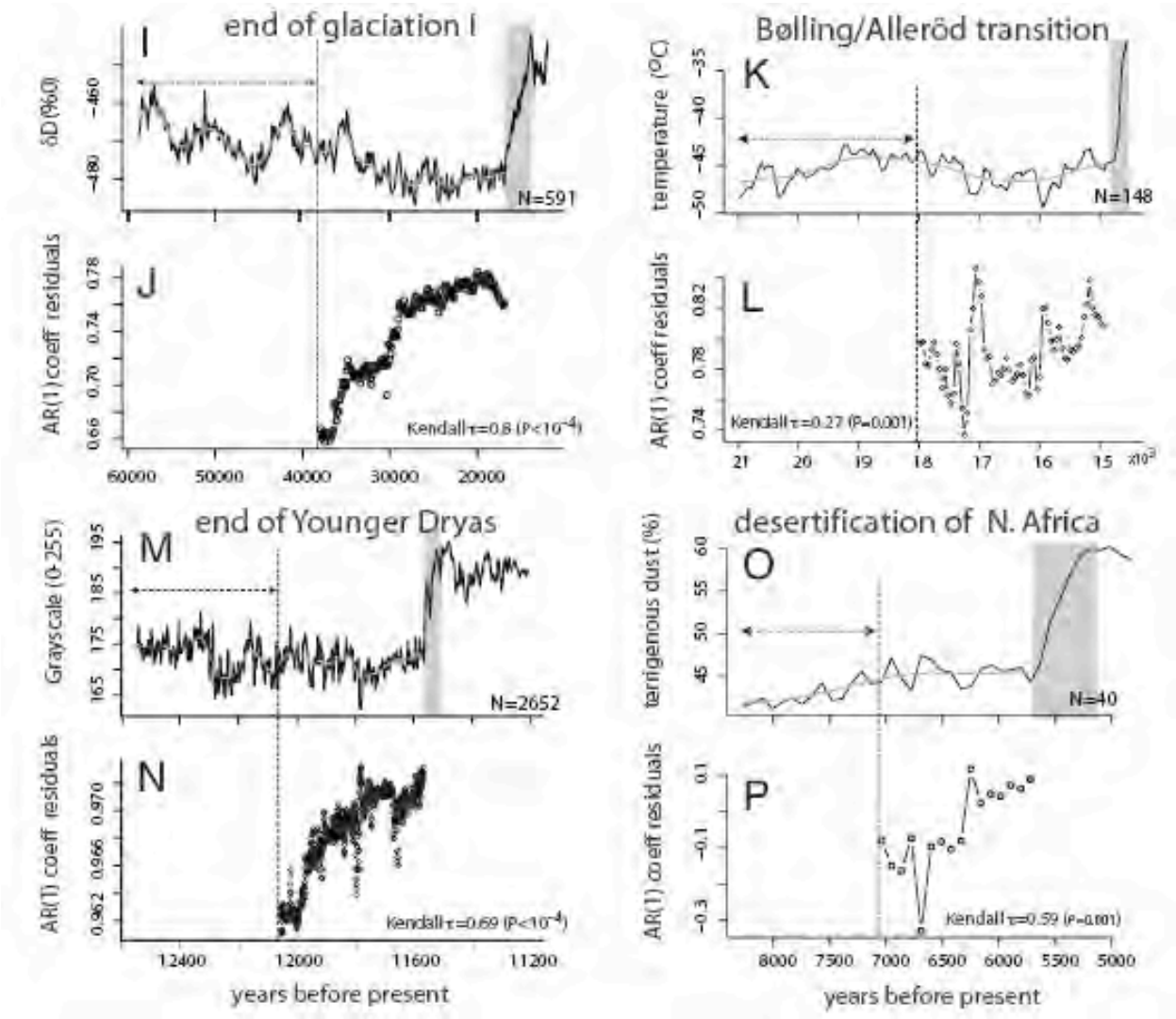

V. Dakos, M. Scheffer, E.H. van Nes, V. Brovkin, V. Petoukhov‡, and H. Held, Slowing down as an early warning signal for abrupt climate change, PNAS 105 (38), 14308-14312

Eight reconstructed time series of abrupt climate shifts in the past. (*A*) The end of the greenhouse Earth, (*M*) the end of the Younger Dryas, (*K*) the Bølling-Allero¨dtransition, (*O*) the desertification of North Africa, (*I*) theendof the last glaciation,and(*G*,*E*,and*F*) the ends of earlier glaciations. In all cases the dynamics of the system slow down before the transition, as revealed by an increasing trend in autocorrelation (*B*,*D*, *F*,*H*, *J*, *L*,*N*, and *P*). The gray bands identify transition phases. The arrows mark the width of the moving window used to compute slowness. The smooth gray line through the time series is the Gaussian kernel function used to filter out slow trends. Data in *A* come from tropical Pacific sediment core records, data in*M*are from the Cariaco basin sediment, data in *K* come from the Greenland GISP2 ice core, data in *O* from the sediment core ODP Hole 658C off the west coast of Africa, and data presented in *C*, *E*, *G*, and *I* are from the Antarctica Vostok ice core.

Mechanism for and Detection of Pockets of Predictability in Complex Adaptive Systems

Predictability of Large Future Changes in a Competitive Evolving Population

Lampert, Howison and Johnson, PRL 88, 017902 (2002)

Third-party game calibration on a black-box game

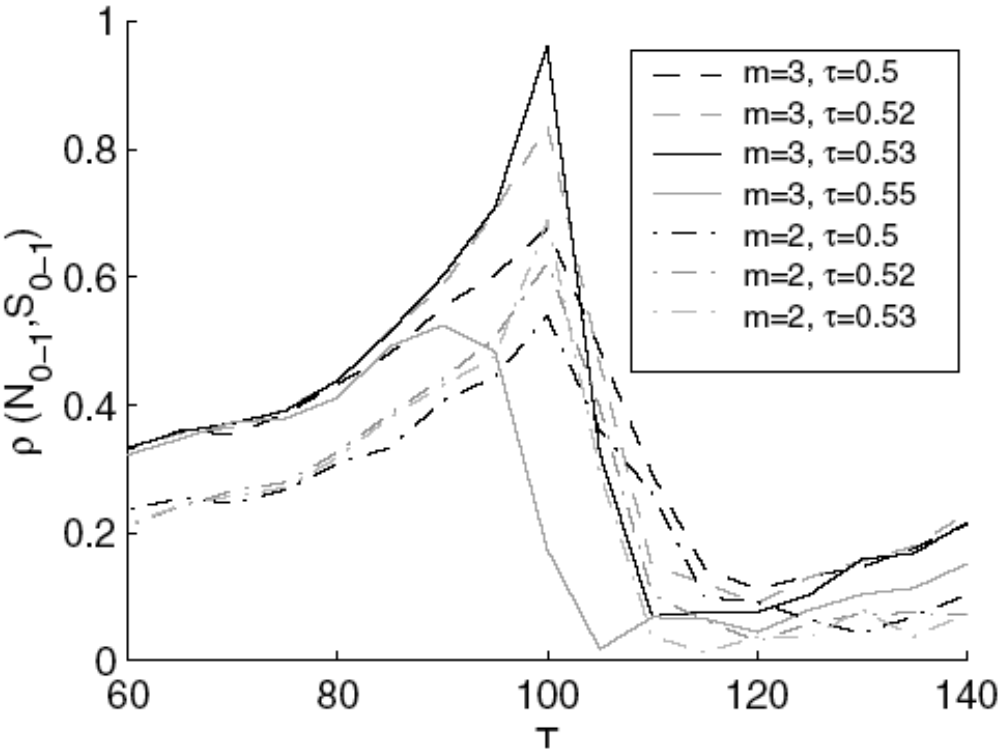

FIG. 1. Estimation of the parameter set for the black-box game. The correlation between N_{0-1} and S_{0-1} is calculated over 200 time steps for an ensemble of candidate third-party games. The third-party game that achieves the highest correlation is the one with the same parameters as the black-box game.

Crash prediction

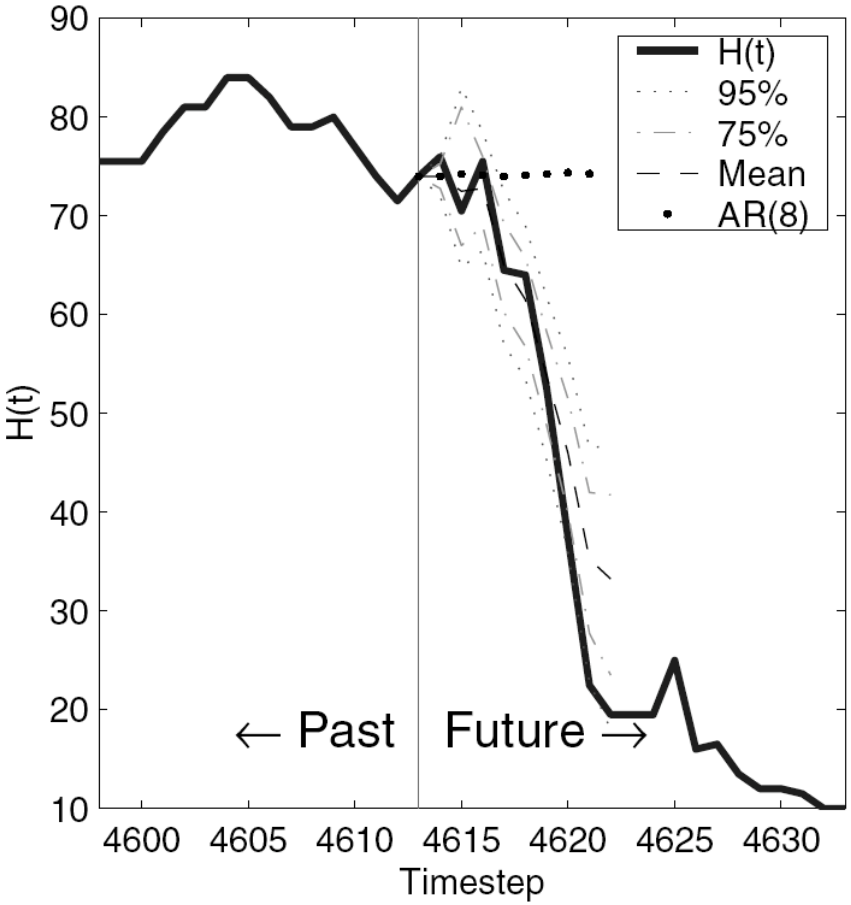

FIG. 3. Comparison between the forecast density function and the realized time series $H(t)$ for a typical large movement. The large, well-defined movement is correctly predicted. An AR(8)-based prediction has been included for comparison.

Mechanism for and Detection of Pockets of Predictability in Complex Adaptive Systems

If decoupled strategies dominate => predictability
since decision independent of next outcome(s)

Decomposition of total action:

$$A^{\mu_m(t)} \equiv A^{\mu_m(t)}_{\text{coupled}} + A^{\mu_m(t)}_{\text{decoupled}} \qquad (3)$$

Condition of certain predictability

$$|A^{\mu_m(t)}_{\text{decoupled}}(t+n+1)| > N/2$$

For N=25 and N=102, very small probability for these pockets of predictability to occur by chance (assuming decoupling between agents)

$$\text{Pr}_{\text{pred}} < 7 \cdot 10^{-4} \text{ and } \text{Pr}_{\text{pred}} < 2.5 \cdot 10^{-15}$$

Mechanism for and Detection of Pockets of Predictability in Complex Adaptive Systems

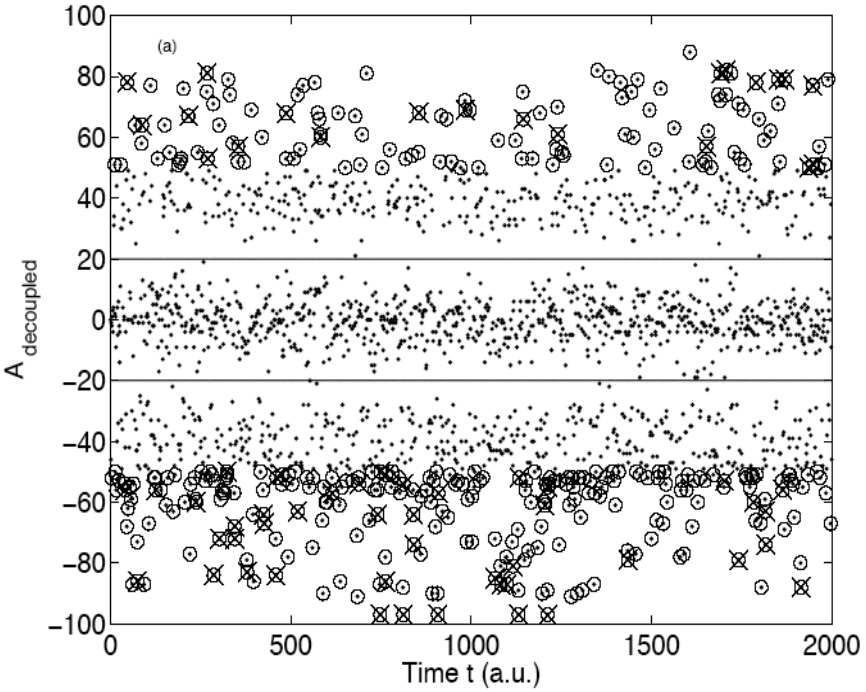

FIG. 1: $A_{\text{decoupled}}$ defined in (3) as a function of time for the MG with $N = 101, s = 12, m = 3$. Circles indicate one-step prediction days, crosses are the subset of days starting a run of two or more consecutive one-step prediction days.

$\lvert A\rvert$	0	0.5	1	1.5	2	2.5	3	3.5	4	4.5
%	53	61	67	65	82	70	67	67	100	100
Nb	62	49	39	23	17	10	6	3	2	1

TABLE I: Out-of-sample success rate % (second row) using different thresholds for the predicted global decoupled action (first row) of the third-party $-games calibrated to the Nasdaq Composite index. Nb (third row) is the number of days from $t = 62$ to 123 which have their predicted global decoupled action $\lvert A_{\text{decoupled}}\rvert$ larger than the value indicated in the first row.

J.V. Andersen and D. Sornette, Europhys. Lett., 70 (5), 697-703 (2005)

A Mechanism for Pockets of Predictability in Complex Adaptive Systems

Predictability of large future changes in major financial indices

D. Sornette and W.-X. Zhou

International Journal of Forecasting 22, 153-168 (2006)

Sparse-data pattern recognition method

Physics of the Earth and Planetary Interiors, 11 (1976) 227–283

PATTERN RECOGNITION APPLIED TO EARTHQUAKE EPICENTERS IN CALIFORNIA

I.M. GELFAND [1], Sh.A. GUBERMAN [1], V.I. KEILIS-BOROK [2], L. KNOPOFF [3], F. PRESS [4], E.Ya. RANZMAN [5], I.M. ROTWAIN [6] and A.M. SADOVSKY [2]

[1] *Institute of Applied Mathematics, Academy of Sciences, Moscow (U.S.S.R.)*
[2] *Institute of Physics of the Earth, Academy of Sciences, Moscow (U.S.S.R.)*
[3] *Institute of Geophysics, University of California, Los Angeles, Calif. (U.S.A.)*
[4] *Department of Earth and Planetary Sciences, Massachusetts Institute of Technology, Cambridge, Mass. (U.S.A.)*
[5] *Institute of Geography, Academy of Sciences, Moscow (U.S.S.R.)*
[6] *Laboratory of Mathematical Methods in Biology, Moscow University, Moscow (U.S.S.R.)*

Trait: array of answers to set of questions

Feature: a treat which is frequent in class I and unfrequent in class II

Alarm index(t): moving average of number of features at time t

Short-term earthquake prediction

Research

- A novel methodology: Reverse Tracing of Precursors (RTP), is developed for short-term (months in advance) earthquake prediction
- The RTP methodology uses increase of earthquake correlation range as a short-term premonitory signal
- An experiment in advance prediction has been launched in four seismically active regions around the World; first results are encouraging

A case history:

Advance prediction of San Simeon (M6.5, Dec. 22, 2003)

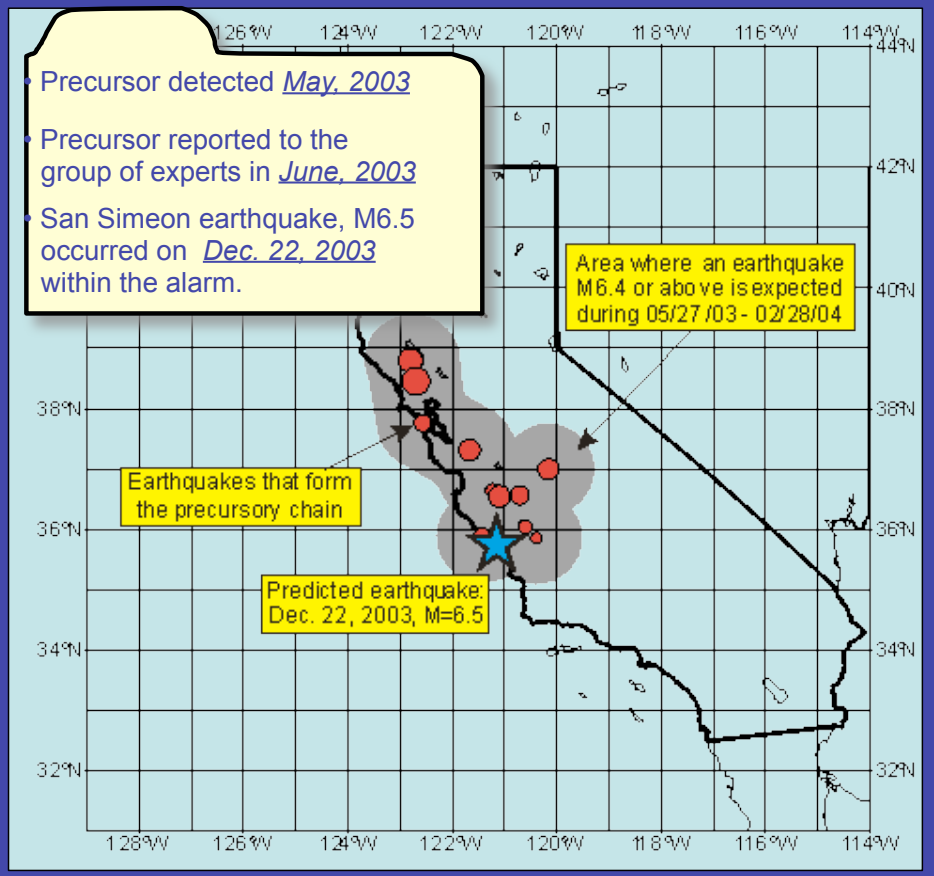

Broader Impact

- Potential applications to other geological, geotechical disasters. Collaboration with experts in geodynamics, complex systems, pattern recognition, and disaster management from US, Russia, Japan, France, Italy and UN

Keilis-Borok's group

Determination of relevant "traits" that allow us to distinguish targets from non targets in the Learning process

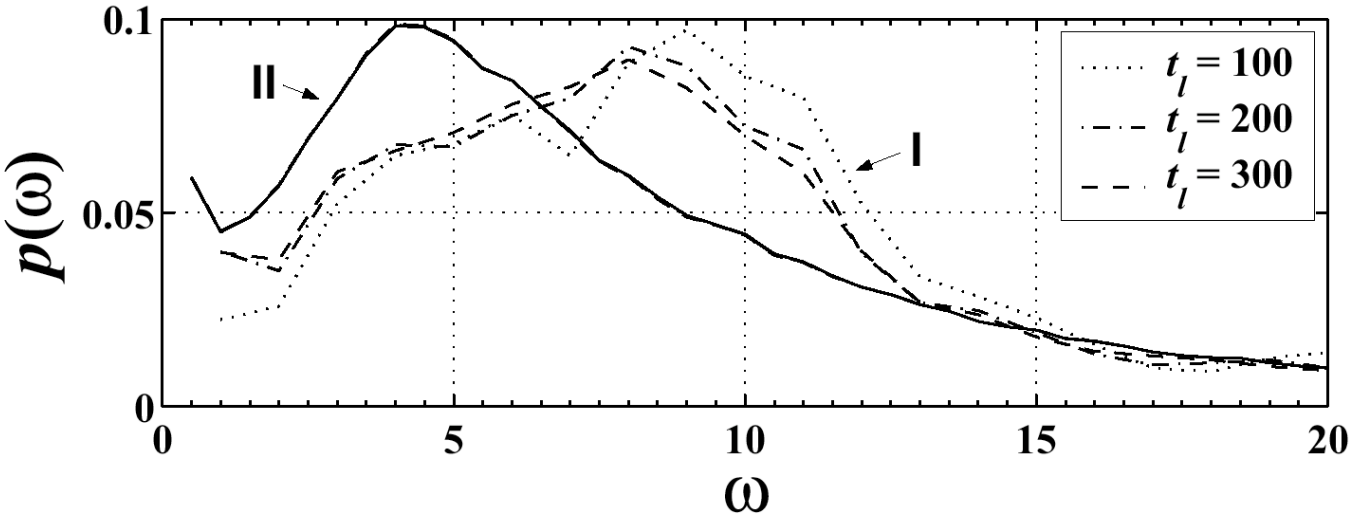

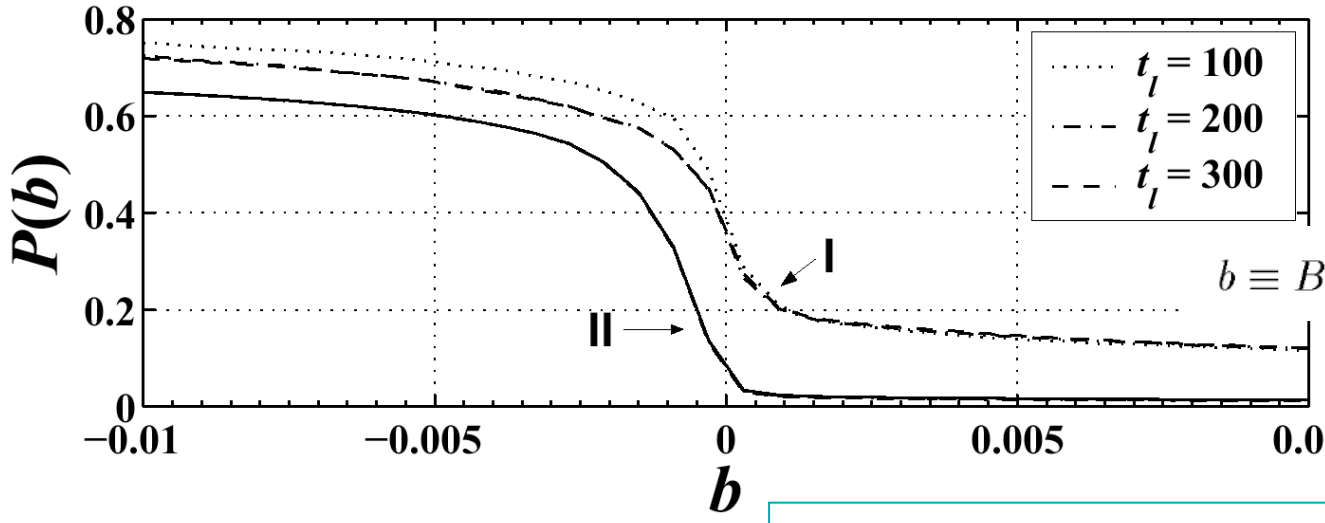

$$h(t) \geq 0,$$

$$b \equiv Bm - |C|\sqrt{m^2 + \omega^2} \geq 0$$

Parameter for positivity of crash hazard rate

Figure 1: Density distribution $p(\omega|\text{I or II})$ of the DSI parameter ω obtained from (1) and complementary cumulative distribution $P(b|\text{I or II})$ of the constraint parameter b obtained from (2) for the objects in classes I (dotted, dashed, and dotted-dashed) and II (continuous) for three different values of t_l.

Multi-scale approach to critical times

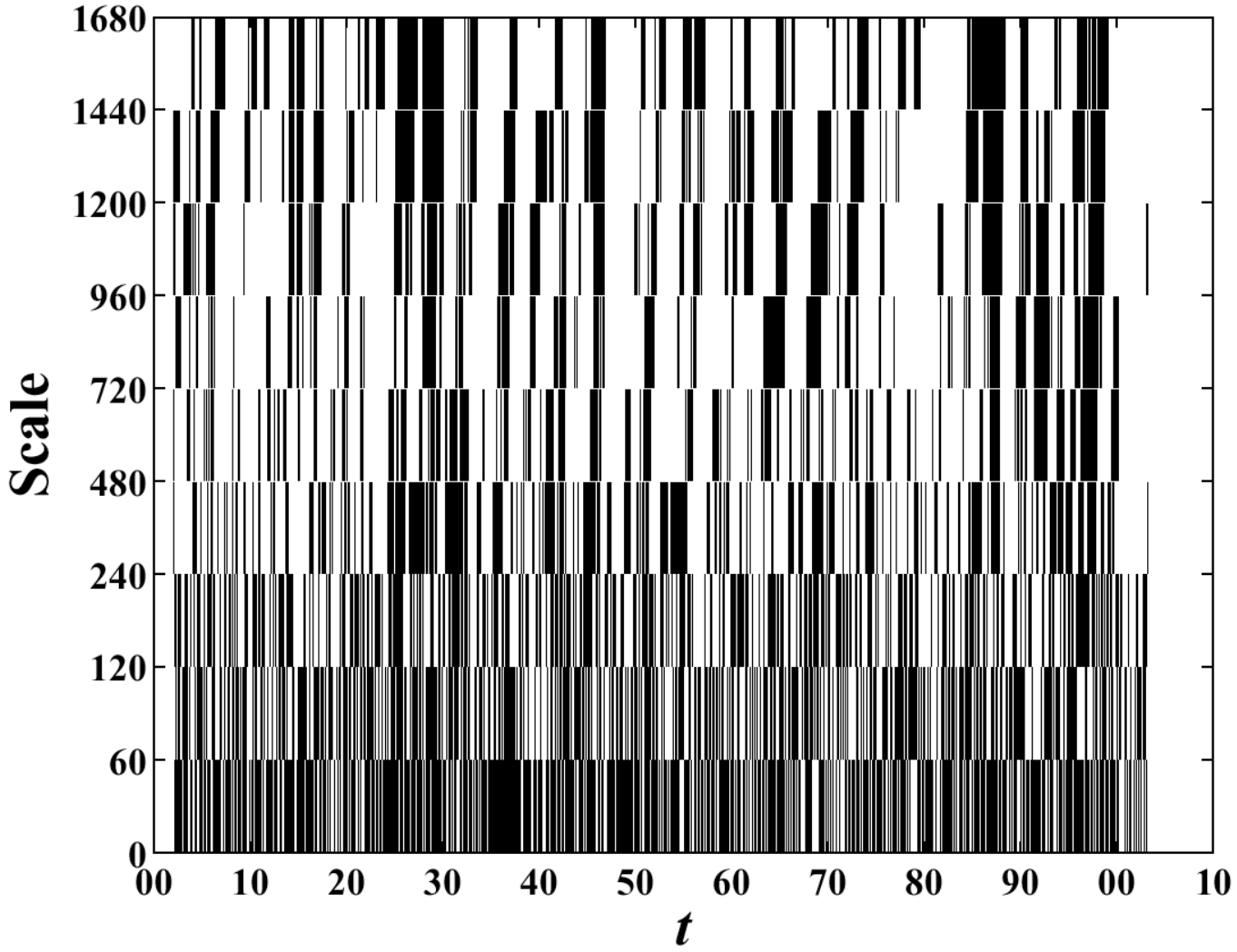

Figure 2: Alarm times t (or dangerous objects) obtained by the multiscale analysis. The alarms satisfy $b \geq 0$, $6 \leq \omega \leq 13$ and $0.1 \leq m \leq 0.9$ simultaneously. The ordinate is the investigation "scale" in trading day unit. The results are robust with reasonable changes of these bounds.

Multiscale Pattern Recognition Method

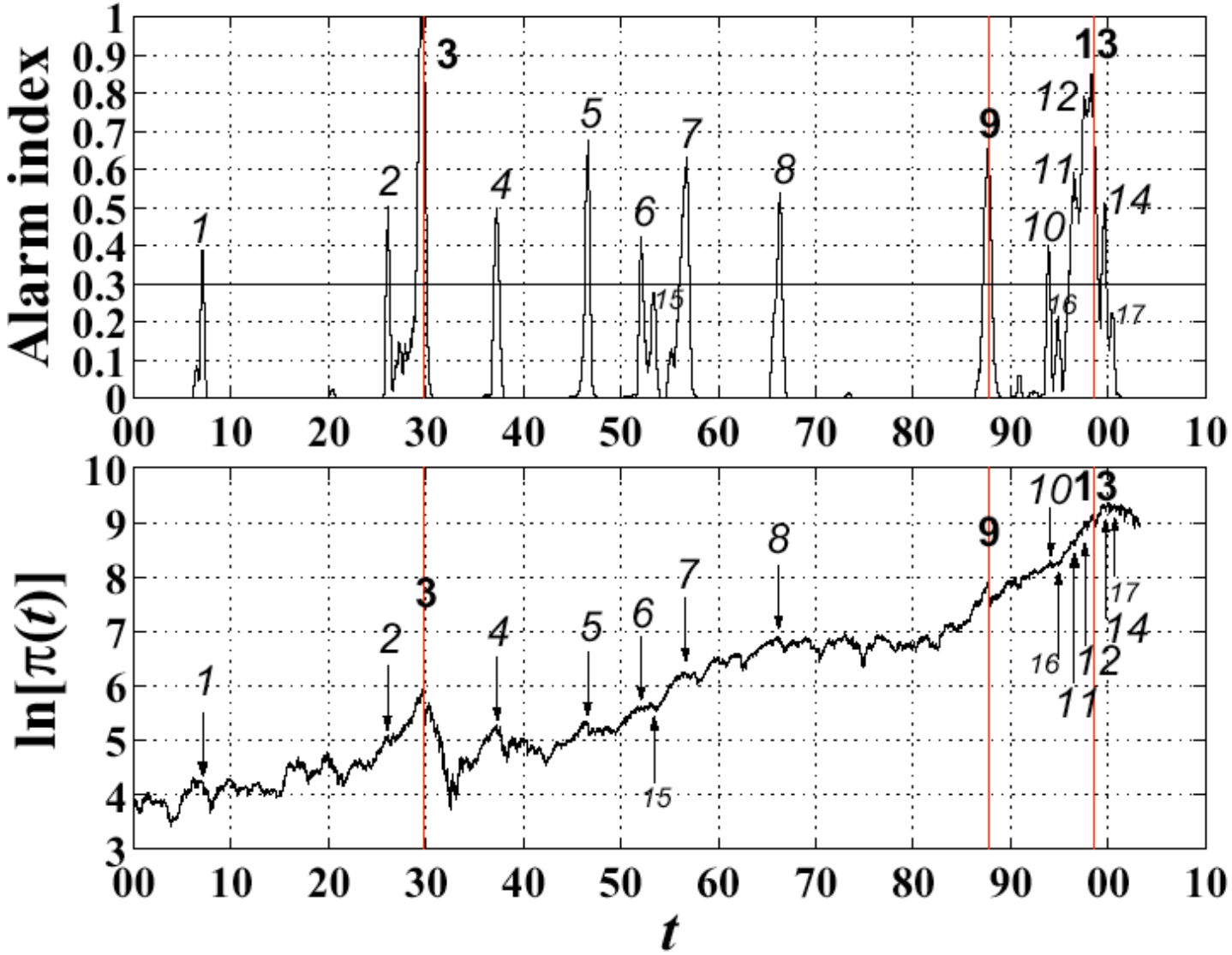

D. Sornette and W.-X. Zhou, Predictability of Large Future Changes in Complex Systems, (http://arXiv.org/abs/cond-mat/0304601)

Extension to a multi-scale LPPL analysis with Gelfand's method of pattern recognition to predict

Figure 3: (Color online) Alarm index $AI(t)$ (upper panel) and the DJIA index from 1900 to 2003 (lower panel). The peaks of the alarm index occur at times indicated by arrows in the bottom panel.

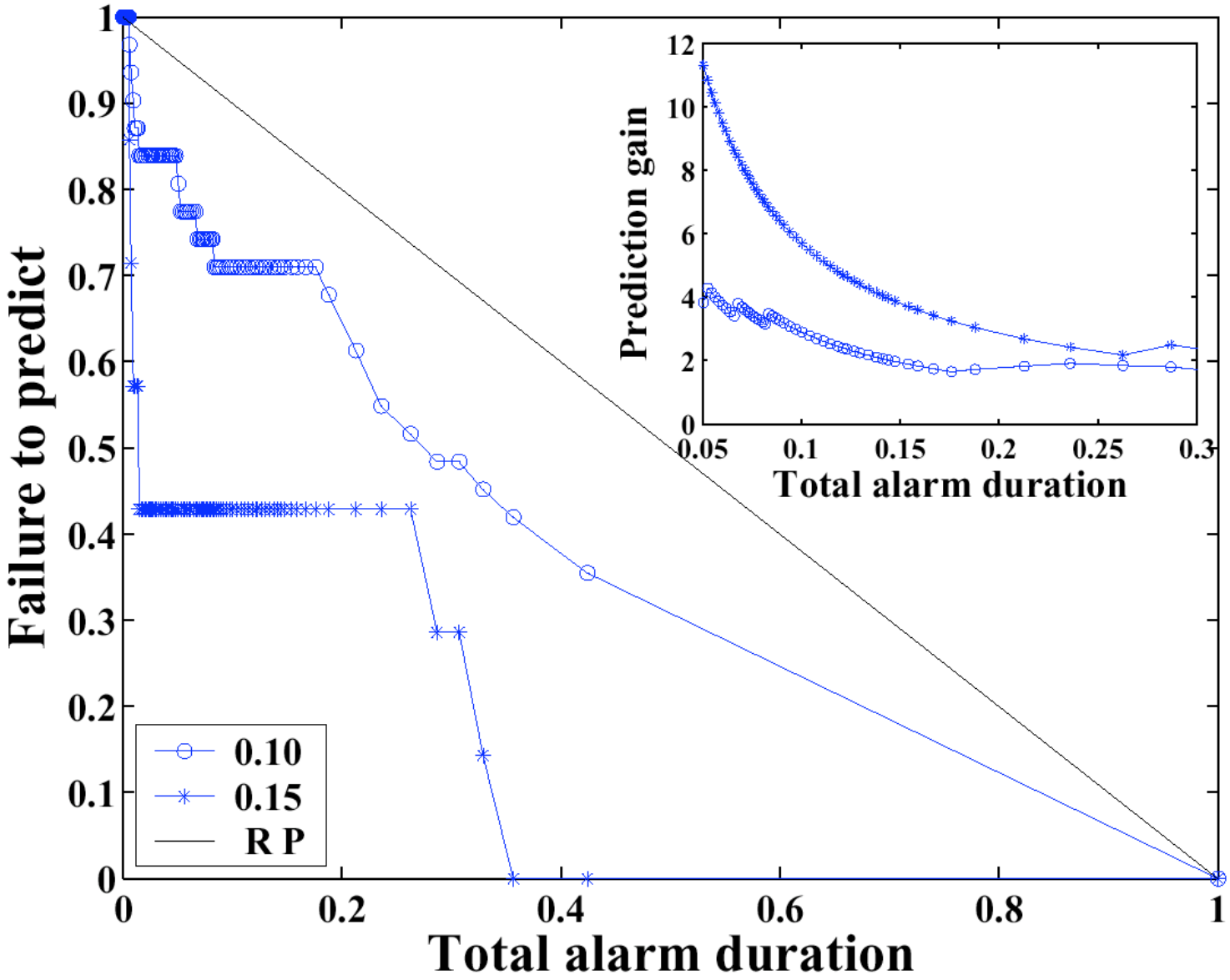

We obtain very significant prediction gains

Figure 5: Error diagram for our predictions for two definitions of targets to be predicted $r_0 = 0.1$ and $r_0 = 0.15$ obtained for the DJIA. The anti-diagonal line corresponds to the random prediction result. The inset shows the prediction gain.

Shuttle Flight 51-L (Challenger) 1986

Feynman's Appendix to the Rogers Commission Report on the Space Shuttle Challenger Accident

It appears that there are enormous differences of opinion as to the probability of a failure with loss of vehicle and of human life. The estimates range from roughly 1 in 100 to 1 in 100,000. The higher figures come from the working engineers, and the very low figures from management. What are the causes and consequences of this lack of agreement? Since 1 part in 100,000 would imply that one could put a Shuttle up each day for 300 years expecting to lose only one, we could properly ask "What is the cause of management's fantastic faith in the machinery?

On January 28, 1986 seven crew members died when the space shuttle Challenger exploded just over a minute after take-off. The Report of the Presidential Commission on the Space Shuttle Challenger Incident (1986) concluded that neither NASA nor Thiokol, the seal designer, “responded adequately to internal warnings about the faulty seal design. . . . A well structured and managed system emphasizing safety would have flagged the rising doubts about the Solid Rocket Booster joint seal.”

Challenger disaster

Technical cause:

- failure of a pressure seal (“O-ring”) in the aft field joint of the right solid rocket motor
- Solid rocket motor assembled from four cylindrical sections, 25 feet long, 12 feet diameter, containing 100 tons of fuel
- 2 O-rings seal gaps in the joints caused by pressure at ignition

Factors:

- temperature: cold reduces resiliency of the O-ring
- chance of O-ring failure increased by test procedures causing blow holes in the putty used to pack the joint

But this was just the point failure…

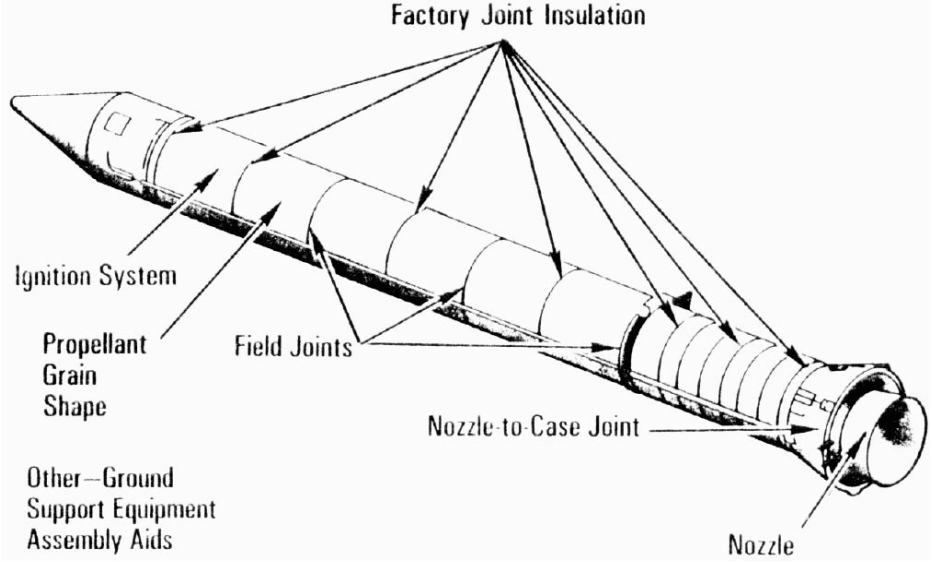

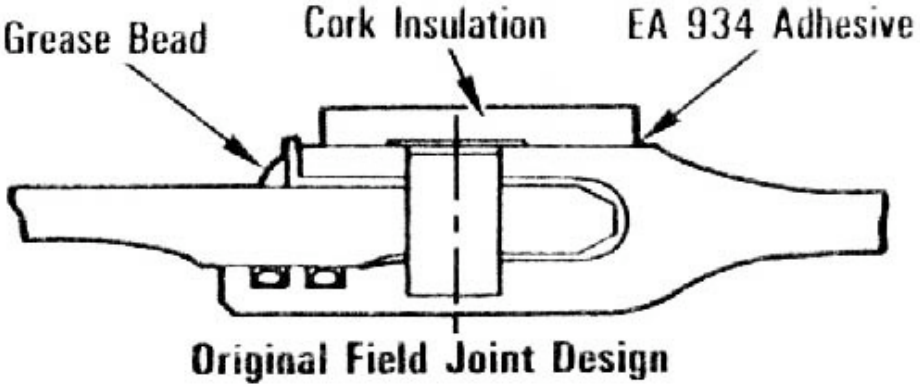

Finding patterns to predict RISKS

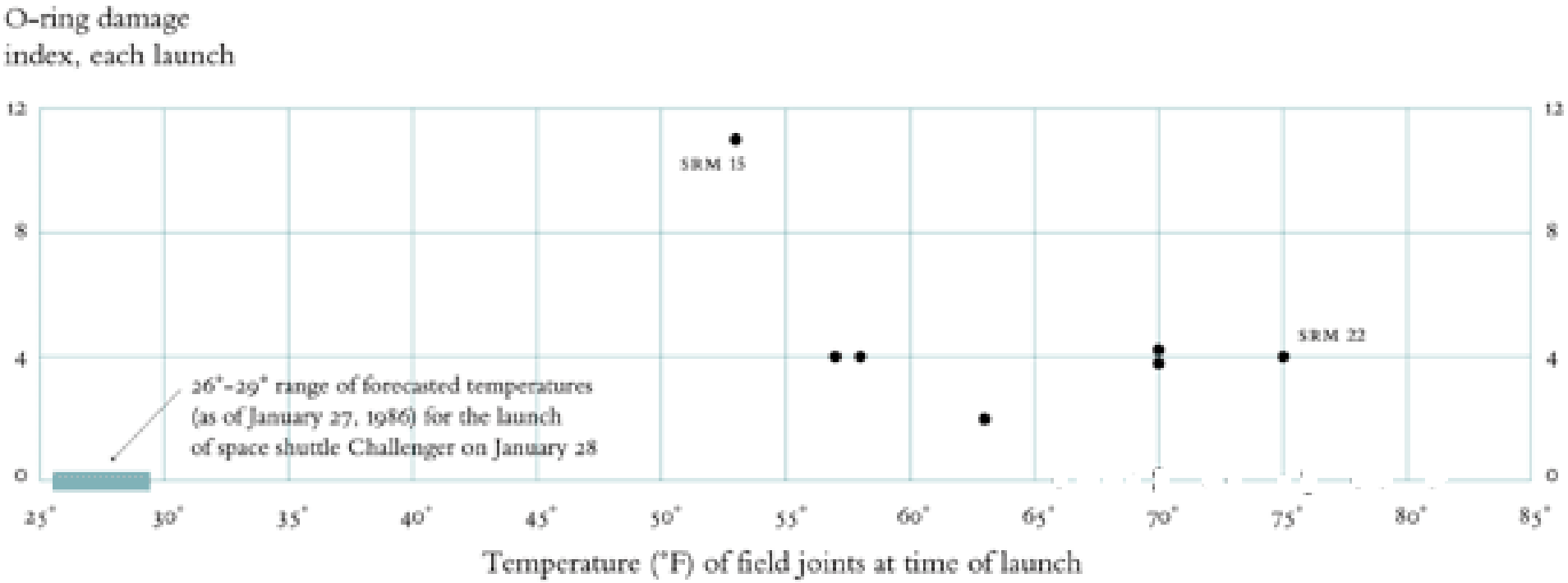

EDWARD R. TUFTE

VISUAL AND STATISTICAL THINKING:

DISPLAYS OF EVIDENCE FOR MAKING DECISIONS

Finding patterns to predict RISKS

"The dog that did not bark" (Sherlock Holmes)

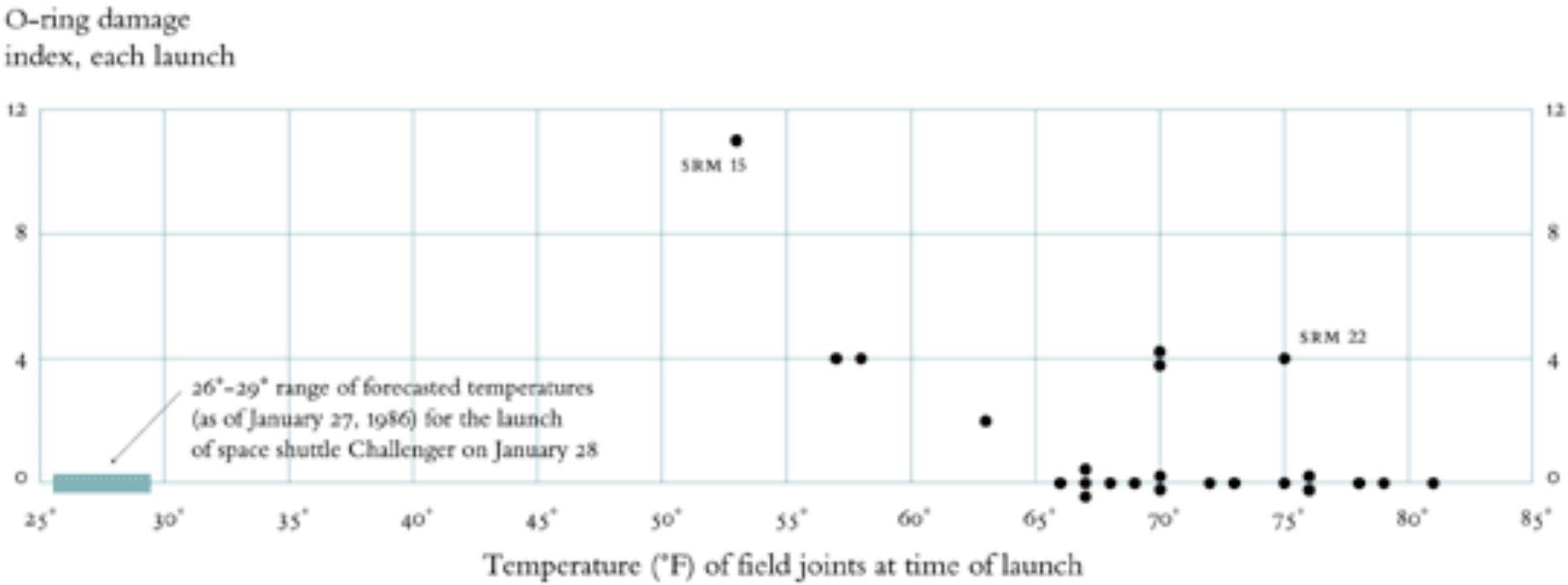

EDWARD R. TUFTE

VISUAL AND STATISTICAL THINKING:

DISPLAYS OF EVIDENCE FOR MAKING DECISIONS

A Formalized Iterative Approach to Verification and Validation (V&V), with Examples

Didier Sornette†

Swiss Federal Institute of Technology (ETH Zurich)

Department of Management, Technology and Economics (D-MTEC)

† formerly at UCLA – Institute for Geophysics and Planetary Physics (IGPP)

Anthony B. Davis

Los Alamos National Laboratory

Space & Remote Sensing Group (ISR-2)

James R. Kamm

Los Alamos National Laboratory

Methods & Verification Team (X-1-MV)

D. Sornette, A. B. Davis, K. Ide, K. R. Vixie, V. Pisarenko, and J. R. Kamm, Algorithm for Model Validation: Theory and Applications, Proc. Nat. Acad. Sci. USA 104 (16), 6562-6567 (2007)

Summary

- **A four-step approach for a quantitative validation step:**
  1. **Start with a prior "potential trust" of a model's value: V_{prior} .**
  2. **Conduct an experiment, use the model, compare results.**
  3. **Grade the comparison between data y_{obs} and model M.**
  4. **Update posterior "trust":** $V_{\text{posterior}} \big/ V_{\text{prior}} = F[p(M \mid y_{\text{obs}}),\ q\ ;\ c_{\text{novel}}]$
     - **The multiplier F must satisfy certain (plausible) constraints.**
- **Iterate the validation process:**

$$V^{(1)}_{\text{prior}} \to V^{(1)}_{\text{posterior}} = V^{(2)}_{\text{prior}} \to V^{(2)}_{\text{posterior}} = V^{(3)}_{\text{prior}} \to \ \ldots \ \to V^{(n)}_{\text{posterior}}$$

- **4 simplified examples—using discrete values of p/q and c_{novel}— illustrated the nature of this process.**
  - **Olami-Feder-Christensen model of seismicity**
  - **Compressible CFD code for Richtmyer-Meshkov instability (induced mixing and shock tests)**
  - **Multifractal random walk as a model of financial returns**
  - **Anomalous diffusion as a model for solar reflectivity in cloudy atmosphere**

D. Sornette, A. B. Davis, K. Ide, K. R. Vixie, V. Pisarenko, and J. R. Kamm, Algorithm for Model Validation: Theory and Applications, Proc. Nat. Acad. Sci. USA 104 (16), 6562-6567 (2007)

A Formalized Iterative Approach to Verification and Validation (V&V), with Examples

Validation as a Constructive Iterative Process

n	test description	c_{novel}	p/q	$V^{(n)}_{before} = V^{(n-1)}_{after}$	$F(\ldots)$	$V^{(n)}_{after}$
1	Pauli exclusion principle	100	∞	1	2.9	2.9
2	EPR paradox	100	∞	2.9	2.9	8.41
3	Aharonov-Bohm effect	100	∞	8.41	2.9	24.4
4	Josephson effect	100	∞	24.4	2.9	70.7
5	Bose-Einstein condensation	100	∞	70.7	2.9	205
6	Is there a paradox-free nonlinear QM theory?	100	∞	205	2.9	595
7	NBS (Boulder): nonlinear corrections to QM < 10^{-21}	10	10	595	2.4	1428

D. Sornette, A. B. Davis, K. Ide, K. R. Vixie, V. Pisarenko, and J. R. Kamm, Algorithm for Model Validation: Theory and Applications, Proc. Nat. Acad. Sci. USA 104 (16), 6562-6567 (2007)

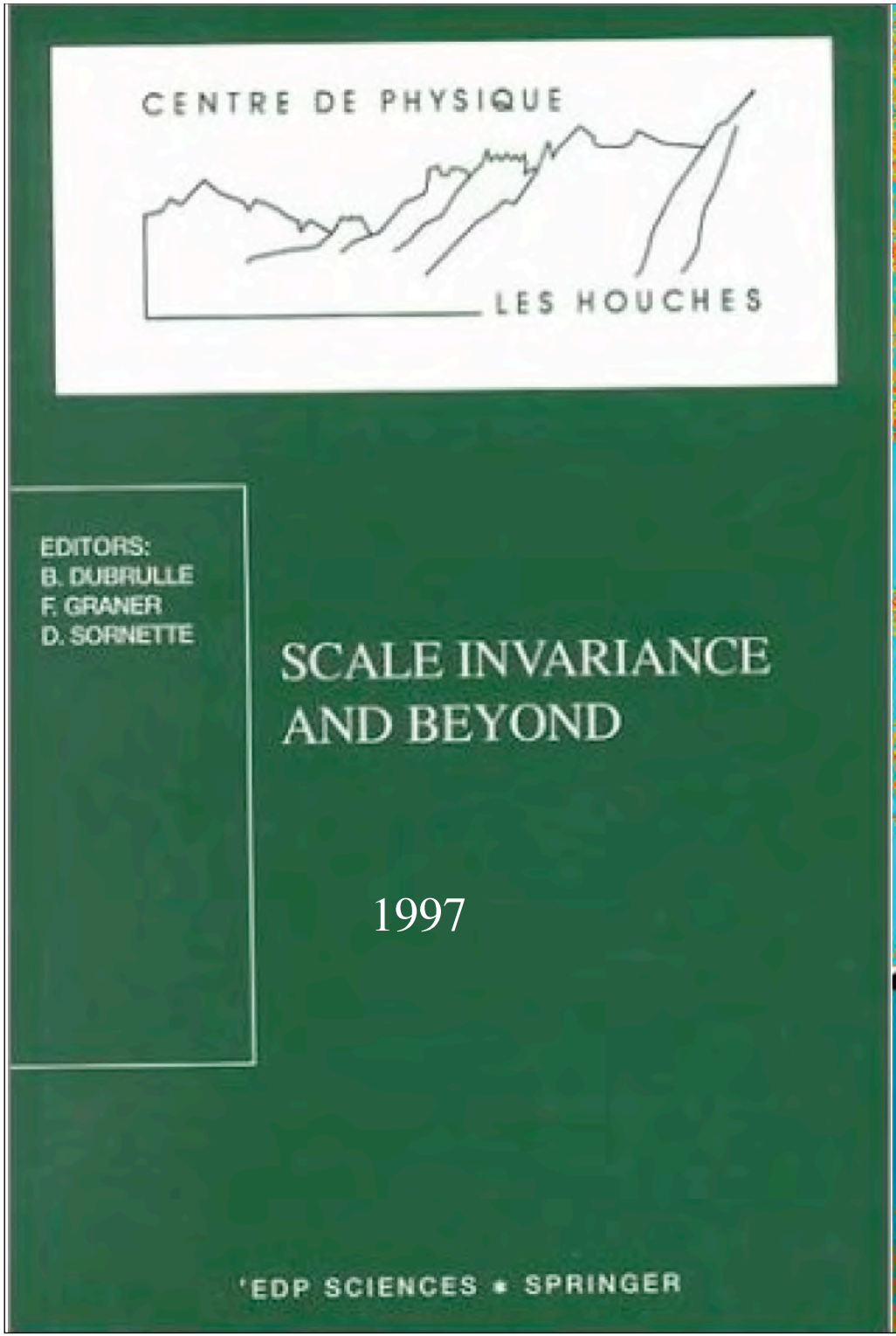
CENTRE DE PHYSIQUE
LES HOUCHES
EDITORS:
B. DUBRULLE
F. GRANER
D. SORNETTE
SCALE INVARIANCE
AND BEYOND
1997
EDP SCIENCES • SPRINGER

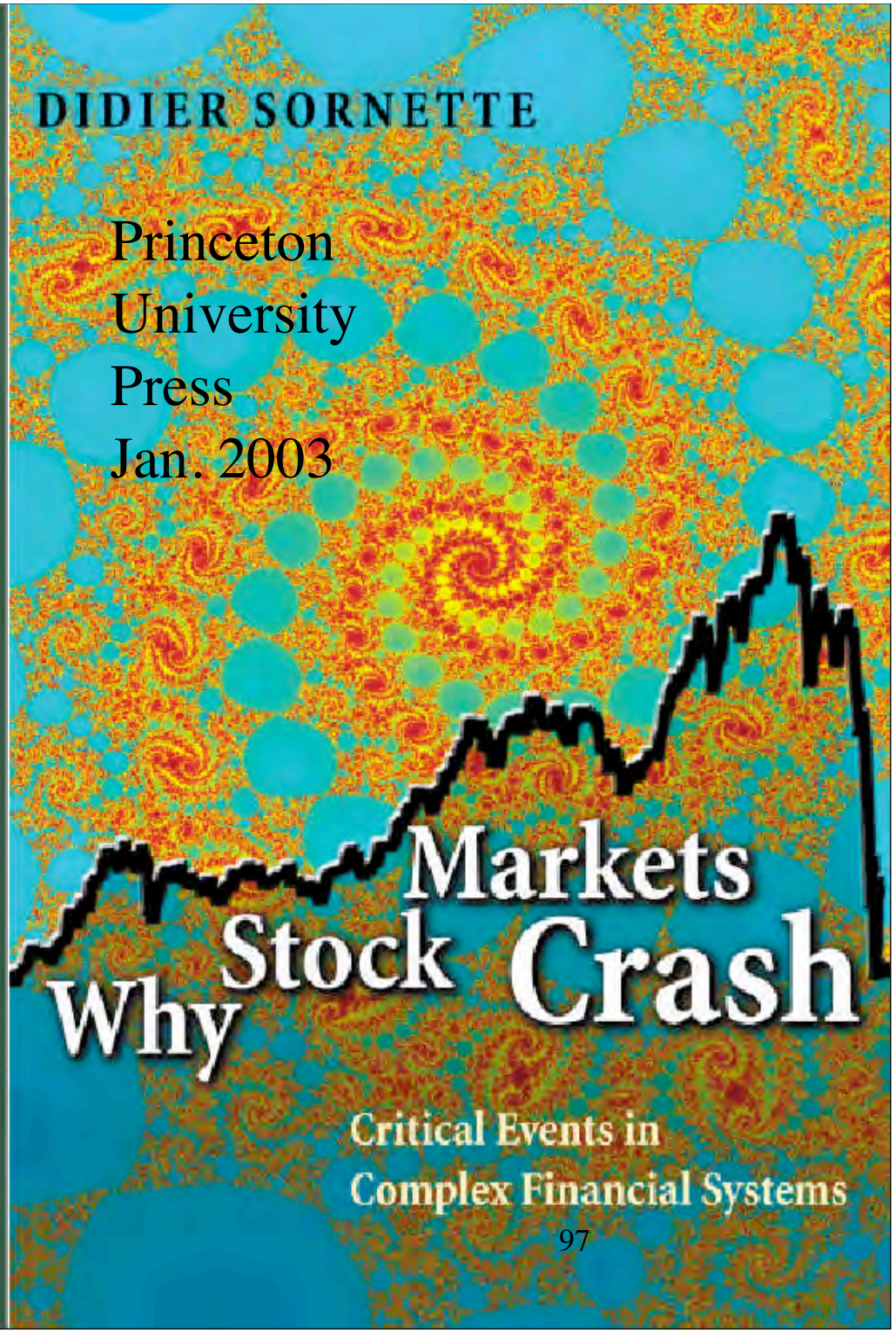
DIDIER SORNETTE
Princeton
University
Press
Jan. 2003
Why Stock Markets Crash
Critical Events in
Complex Financial Systems

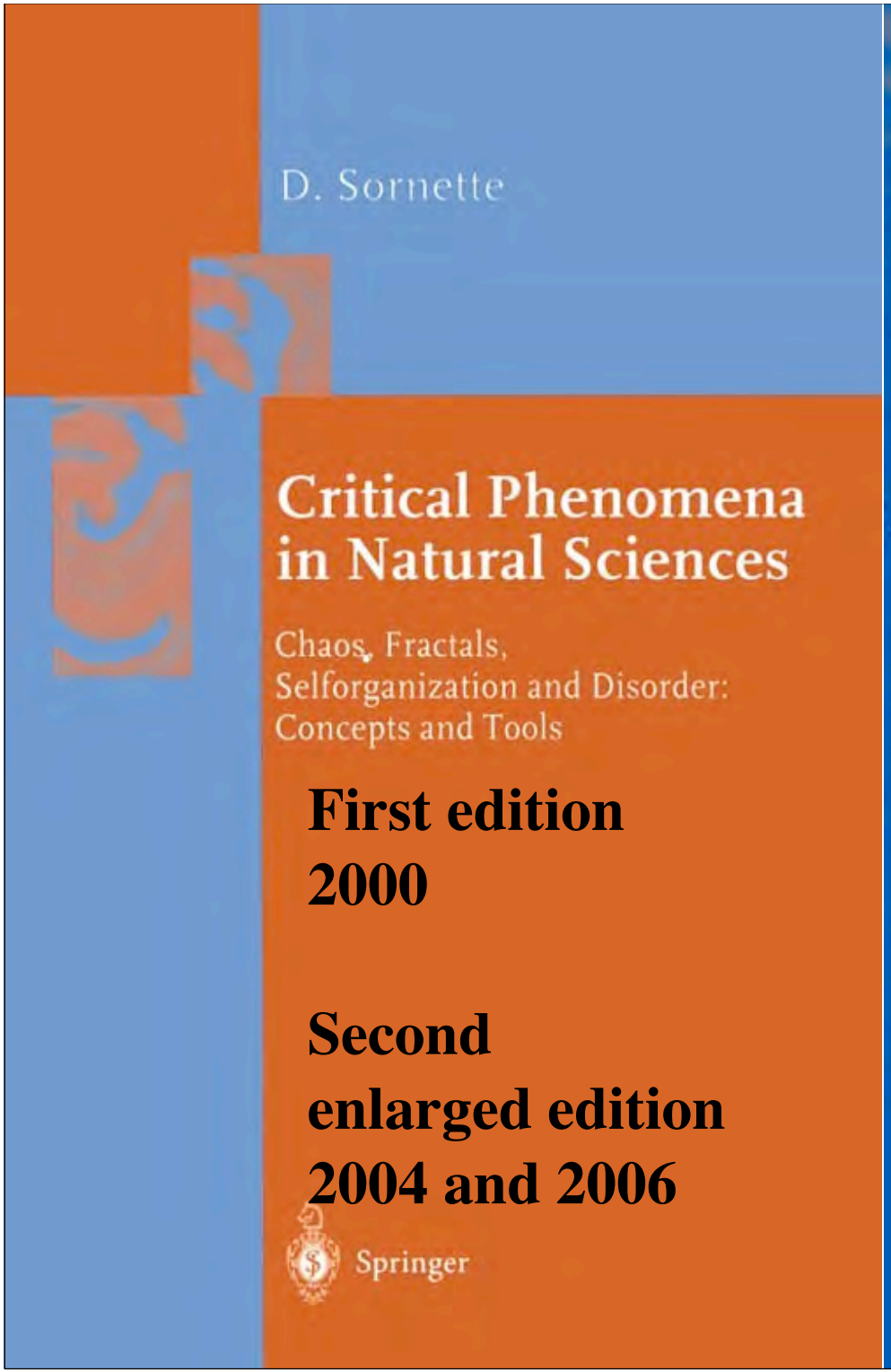
D. Sornette
Critical Phenomena in Natural Sciences
Chaos, Fractals, Selforganization and Disorder: Concepts and Tools
First edition 2000
Second enlarged edition 2004 and 2006
Springer

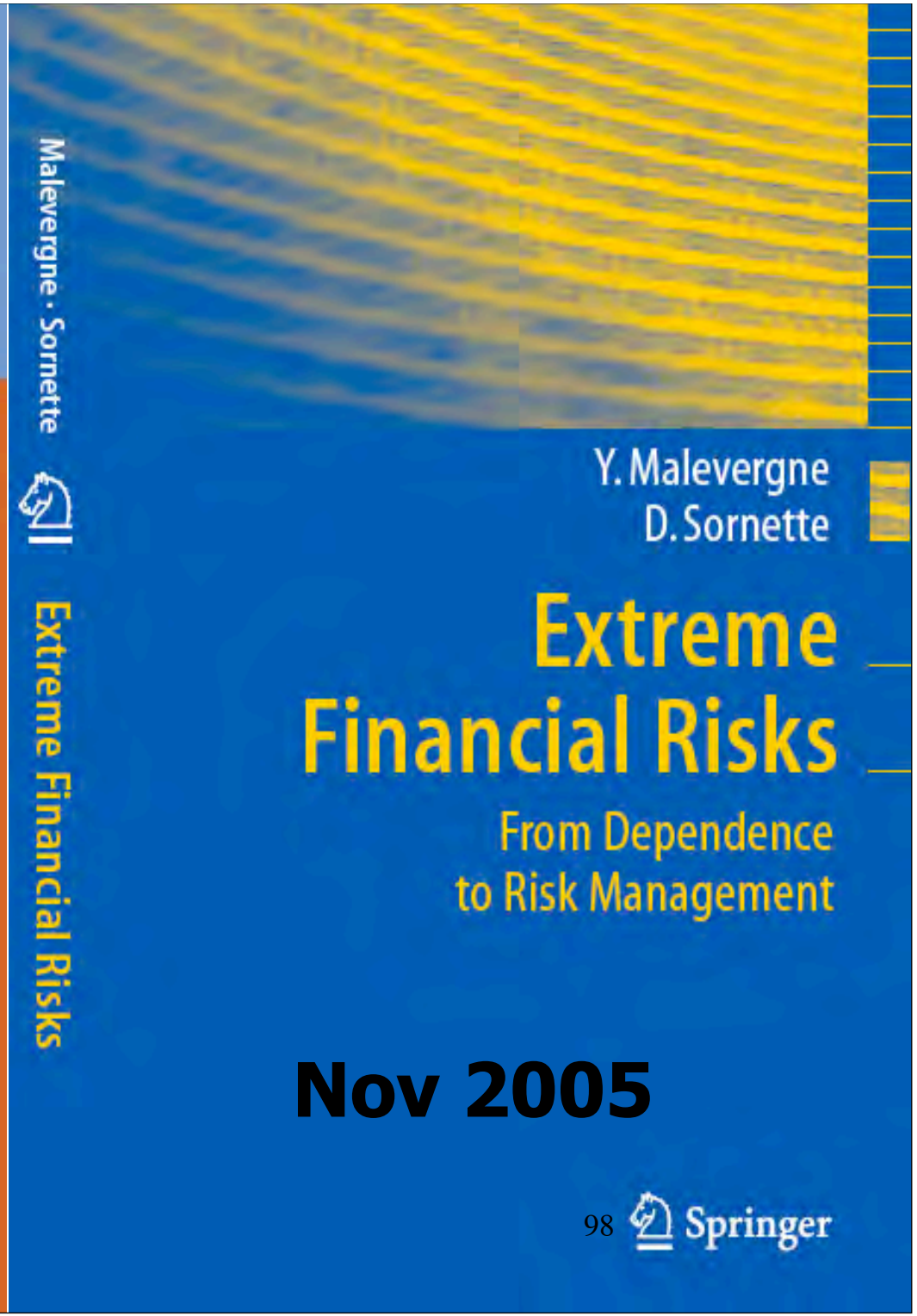
Malevergne · Sornette
Extreme Financial Risks
Y. Malevergne
D. Sornette
Extreme Financial Risks
From Dependence to Risk Management
Nov 2005
98
Springer

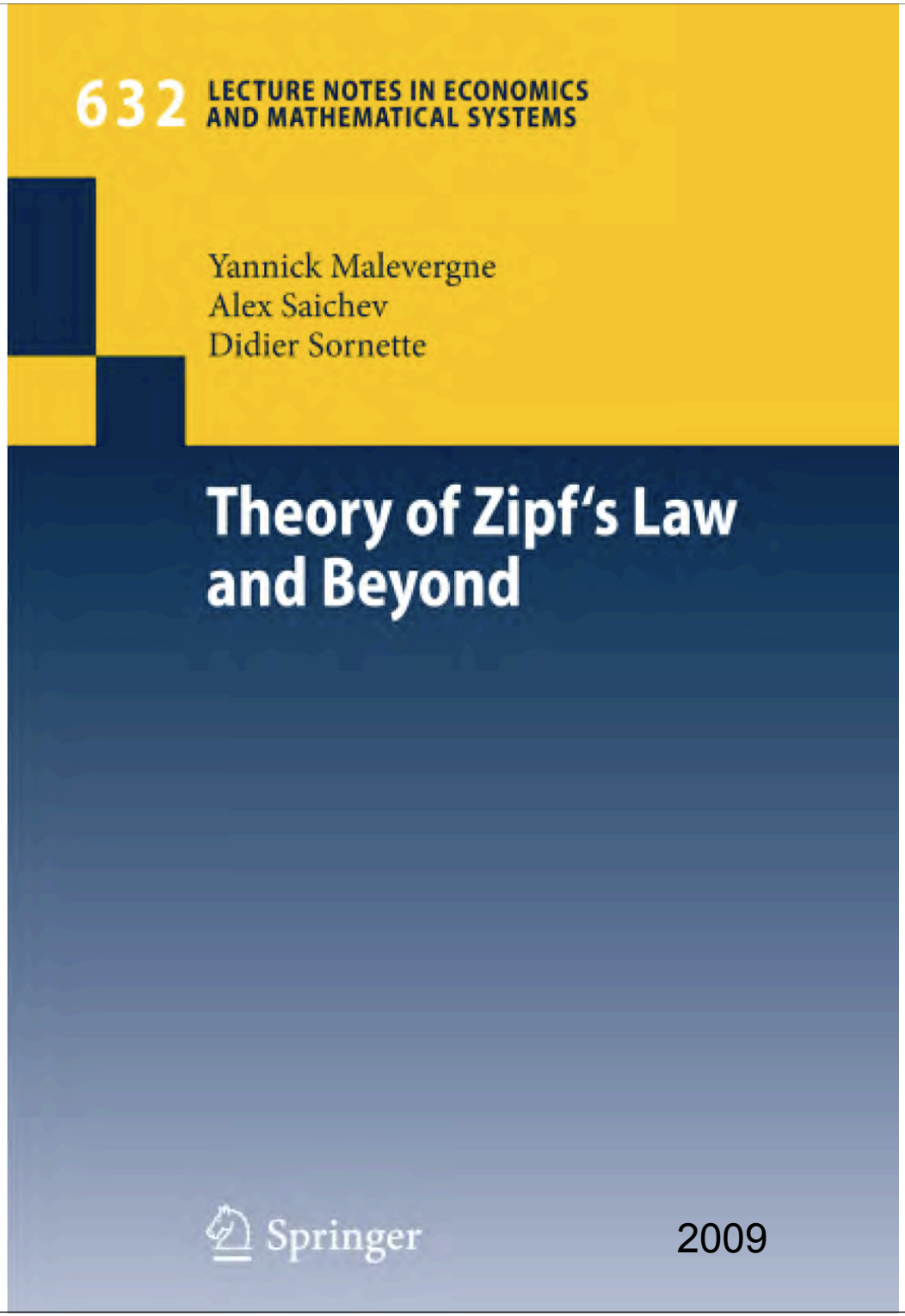
632 LECTURE NOTES IN ECONOMICS AND MATHEMATICAL SYSTEMS
Yannick Malevergne
Alex Saichev
Didier Sornette
Theory of Zipf's Law and Beyond
Springer
2009